

Function of Interferon Inducible Transmembrane Proteins (IFITMs) in the White Pekin
Duck

by

Graham Allan Duncan Blyth

A thesis submitted in partial fulfillment of the requirements for the degree of

Master of Science

in

Physiology, Cell and Developmental Biology

Department of Biological Sciences
University of Alberta

© Graham Allan Duncan Blyth, 2015

Abstract

Interferon Inducible Transmembrane Proteins (IFITMs) can restrict the entry of a wide range of viruses. IFITM3 localizes to endosomes and can potently restrict the replication of the influenza A virus (IAV), and several other viruses that also enter host cells through the endocytic pathway. Given the major contribution of mammalian IFITM3 to restriction of IAV I investigated whether IFITMs were involved in protection in ducks, the natural host of influenza. Ducks and wild waterfowl are the environmental reservoir of all avian influenza viruses, and often display little to no disease symptoms after infection. I identified and sequenced duck *IFITM1*, *IFITM2*, *IFITM3* and *IFITM5*. Using qPCR I demonstrated upregulation of these genes in lung tissue in response to highly pathogenic IAV infection 400-fold, 30-fold, 30-fold and 5-fold, respectively. I cloned and expressed each IFITM in chicken DF-1 cells and showed duck IFITM1 was expressed at the cell surface, while IFITM3 localizes to LAMP1 containing compartments. DF-1 cells stably expressing duck IFITM3 restrict replication of H1N1, H6N2 and H1N9 IAV strains, but not vesicular stomatitis virus. I generated chimeric and mutant IFITM3 proteins and show duck IFITM3 does not require its N-terminal domain for endosomal localization or antiviral function, however, this N-terminal end confers endosomal localization and antiviral function on IFITM1. In contrast to mammalian IFITM3, the conserved YXXØ endocytosis signal sequence in the N-terminal domain of duck IFITM3 is not the sole contributor to correct endosomal localization. Despite significant structural and amino acid divergence duck IFITM3 is functional against AIV.

Acknowledgements

I would like to thank my supervisor, Dr. Kathy Magor for providing an excellent work environment, and providing me with all of the tools necessary to succeed. I am thankful for the encouragement, support, direction, and guidance that you have given me throughout my degree. You have provided me with an opportunity to be a part of an excellent lab, develop professionally, and perhaps most importantly you have provided me with an environment to learn. I am grateful for all of the opportunities you have provided to me.

Thank you to my committee members, Dr. James Stafford and Dr. Maya Shmulevitz for your time, constructive feedback, guidance and suggestions.

I would like to acknowledge all of the members of the Kathy Magor lab for helping me in one way or another. Hillary for completing the previous study that allowed me to have a fantastic project to work on. Domingo, for your hard work, expertise, and patience in helping me learn numerous techniques. Aly for your help and humour. Dave, Luke, and Danyel for the great friendship, expertise, and assistance. Ximena and Laura for all of the technical skills and laughs. Thank you to Dustin, for the scientific discussion, an ear to complain to, coffees, lunches, and friendship.

Thank you to my funding sources. I was financially supported by the Department of Biological Sciences, GSA, FGSR, and a QEII scholarship in completion of this degree.

Finally, I would like to thank my family. To my parents, for always supporting me and providing me with the encouragement that I needed. You have always shown pride in me, and offered extra motivation to become as successful and hard working as both of you are. Thank you. To my partner Blair, for giving me support, encouragement, advice, friendship, and an escape from the stress.

Table of Contents

Chapter 1. Introduction	1
1.1 Influenza A virus.....	1
1.2 Ducks and influenza A viruses	4
1.3 Innate immune sensing of influenza viruses in duck	11
1.4 Interferon inducible transmembrane proteins	15
1.4.1 IFITM topology	16
1.4.2 Non-Immune functions of IFITMs	17
1.4.3 Immune functions of IFITMs.....	18
1.4.4 IFITM3 and influenza A virus	21
1.4.5 Cellular localization of IFITMs	22
1.4.6 Mechanisms of IFITMs.....	24
1.5 Experimental aims and results summary	26
1.5.1 Experimental aims	27
Chapter 2. Materials and Methods	32
2.1 Identification, sequencing and analysis of duck IFITMs	32
2.2 Generation of expression constructs	33
2.3 Duck infections and RNA extraction	33
2.4 Quantification of IFITM expression by real-time PCR	34
2.5 Generation of chimeric proteins and point mutants	34
2.6 Cell culture, transfections and generation of stable cell lines expressing IFITM...	35
2.7 Western blots	36
2.8 Cell culture and virus infections	36

2.9 Fluorescent microscopy analysis of viral infection	37
2.10 Flow cytometric analysis of viral infection	37
2.11 Plaque assays	38
2.12 Cellular localization of IFITMs by confocal microscopy.....	38
Chapter 3. Results	45
3.1 Characterization of the duck IFITM repertoire.....	45
3.2 Duck IFITMs are upregulated in response to influenza A virus infection	46
3.3 Duck IFITM3 restricts influenza A viruses	48
3.4 Duck IFITMs localize to distinct cellular compartments	50
3.5 Duck IFITM3 inhibits influenza, but does not inhibit vesicular stomatitis virus ...	50
3.6 The N-terminal domain of dIFITM3 is not essential for antiviral activity or endosomal localization.....	52
3.7 N-terminal YXX θ endocytic signal sequence of dIFITM3 is not essential for correct cellular localization.....	53
Chapter 4. Discussion	70
4.1 Ducks possess a conserved IFITM locus	70
4.2 Duck IFITM3 localizes to endosomes, the entry site of IAV	72
4.3 Duck IFITM3 has conserved antiviral function against IAV	73
4.4 N-terminal domain of duck IFITM3 partially regulates cellular localization.....	78
4.5 Post-translational modifications of IFITMs.....	81
4.6 Future directions	83
4.7 Conclusions.....	86
References.....	90

List of Figures

Figure 1. Proposed topology of IFITMs	30
Figure 2. Cellular localization of IFITMs.....	31
Figure 3. Vector map of pcDNA3.1/Hygro+ with duck IFITM and N-terminal V5 epitope tagged duck IFITM inserts.....	44
Figure 4. Organization of IFITM locus in duck, chicken, human and mouse	55
Figure 5. Amino acid alignment of duck, chicken, human, and mouse IFITMs	56
Figure 6. The N-terminal repetitive region of IFITM1 is present in two individual ducks	57
Figure 7. Duck IFITMs are upregulated in lung tissue in response to highly pathogenic IAV infection	58
Figure 8. Duck IFITM1 is upregulated in intestinal tissue in response to low pathogenic IAV infection	59
Figure 9. Duck IFITM qPCR probe and primers are specific to their respective IFITMs	60
Figure 10. Duck IFITM3 restricts replication of low pathogenic IAV.....	61
Figure 11. Non-epitope tagged duck IFITM3 restricts replication of low pathogenic IAV	62
Figure 12. Optimization of transfection of duck IFITMs into DF-1 chicken fibroblast cells	63
Figure 13. Optimization of IAV infection in DF-1 chicken fibroblast cells.....	64

Figure 14. Duck IFITMs localize to different cellular compartments	65
Figure 15. Generation of DF-1 cells stably overexpressing duck IFITM1	66
Figure 16. Duck IFITM3 restricts low pathogenic IAV, but not VSV	67
Figure 17. The N-terminal domain of dIFITM3 is not necessary for antiviral activity	68
Figure 18. The N-terminal YXX θ endocytic signal sequence of dIFITM3 is not necessary for endosomal localization or antiviral activity	69
Figure 19. Multiple residues important for antiviral function are conserved in duck IFITM3	87
Figure 20. Summary of duck IFITM localization and function	88
Figure 21. Duck IFITM3 likely undergoes post-translational modification.....	89

List of Tables

Table 1. Primer sequences for amplification of duck IFITMs.....	40
Table 2. Primer sequences for sequencing of duck IFITMs	41
Table 3. Primer and probe sequences for qPCR analysis of duck IFITM gene expression	42
Table 4. Primer sequences for generation of chimeric IFITM and mutant dIFITM3 proteins.....	43

Abbreviations

ATHL1	Acid trehalase-like 1
B4GALNT4	Beta-1,4-N-acetyl-galactosaminyl transferase 4
BC500	A/mallard/BC500/05 (H5N2)
CARD	Caspase recruitment domain
CD	Cluster of differentiation
EID	Egg infectious dose
GAPDH	Glyceraldehyde-3-phosphate dehydrogenase
HA	Hemmagglutinin
IAV	Influenza A virus
IFIT	Interferon-induced protein with tetratricopeptide repeats
IFITM	Interferon-inducible transmembrane protein
IFN	Interferon
Ig	Immunoglobulin
IKK	I κ B kinase family
IFNAR	The interferon- α/β receptor
IRAK	interleukin-1 receptor-associated kinase
IRF	Interferon regulatory factor
ISG	Interferon stimulated gene
I κ B	Inhibitor of NF- κ B
JAK	Janus kinase
M1/2	Matrix protein
MAVS	Mitochondrial antiviral signaling protein

MDA5	Melanoma Differentiation-Associated protein 5
Mx	Myxovirus resistance gene
MyD88	Myeloid differentiation primary response 88
NA	Neuraminidase
NEMO	NF-kappa-B essential modulator
NEP	Nuclear export protein
NF-κB	Nuclear factor kappa-light-chain-enhancer of activated B-cells
NP	Nucleoprotein
NS1/2	Nonstructural protein 1/2
OASL	2'-5'-oligoadenylate synthetase-like
OSBP	Oxysterol-binding protein
PA	Polymerase acidic protein
PB1/2	Polymerase basic protein
pDC	Plasmacytoid dendritic cell
PKR	Protein kinase R
RACE	Rapid amplification of cDNA ends
RIG-I	Retinoic Acid Inducible Gene-I
RLR	RIG-I like receptor
STAT	Signal transducer and activator of transcription
TIR	Toll/Interleukin-1 receptor
TLR	Toll-like receptor
TRAF	Tumor necrosis factor receptor associated factor family
TRIM	Tripartite-motif family

TYK2	Tyrosine kinase 2
VAPA	Vesicle-membrane-protein-associated protein A
VN1203	A/Vietnam/1203/04 (H5N1)
rVSV-GFP	Recombinant vesicular stomatitis virus- green fluorescent protein

Chapter 1. Introduction

1.1 Influenza A virus

The influenza A virus (IAV) is a member of the orthomyxovirus family (Reviewed by Bouvier and Palese, 2008). IAV has a segmented single stranded RNA genome with eight segments (Palese and Schulman, 1976) that collectively encode at least ten proteins, and sometimes as many as seven accessory proteins . Segment one, two, three, and five encode PB2, PB1, PA, (Palese et al., 1977) and NP, (Ritchey et al., 1976) respectively, while segments four and six encode HA and NA respectively (Palese and Schulman, 1976). Segment seven encodes the M1 and M2 proteins (Allen et al., 1980), while segment eight encodes NS1 and NEP (NS2) (Lamb et al., 1980). The seven accessory proteins identified are PB1-F2 (Chen et al., 2001), PB1-N40 (Wise et al., 2009), PA-X (Jagger et al., 2012), PA-N155 , PA-N182 (Muramoto et al., 2013), M42 (Wise et al., 2012), and NS3 (Selman et al., 2012), and are encoded either by use of alternate start codons, or alternate splicing (Reviewed by Vasin et al., 2014). The functional roles of each accessory protein are not fully understood, and represent an area of current research.

IAV virions are roughly 80-120nm in size (Fujiyoshi et al., 1994), and can range from spherical to filamentous in shape (Choppin et al., 1960). The two major surface proteins on the viral envelope, HA and NA, are involved in viral entry and release respectively (Laver and Valentine, 1969). An additional membrane protein, M2, is an ion channel (Pinto et al., 1992) that is involved in viral uncoating (Wharton et al., 1994). The

structural M1 protein lies on the inner leaflet of the viral membrane, and appears to influence virion structure (Bourmakina and García-Sastre, 2003; Burleigh et al., 2005), as well as linking viral nucleoproteins to the virion during assembly (Noton et al., 2007). Internal to the matrix are the viral nucleoproteins, as well as one additional viral protein, NEP (NS2). The viral RNA segments are associated with NP, and the viral polymerase, which consists of PB1, PB2, and PA.

IAV HA protein binds cell surface sialic acid residues to facilitate entry (reviewed by Skehel and Wiley, 2000). Avian influenza strains preferentially bind to sialic acid residues with α 2,3 linkages, whereas human strains preferentially bind α 2,6 linkages (Connor et al., 1994). Upon binding to host cell sialic acid residues, the virion is internalized via both clathrin-dependent (Matlin et al., 1981) and clathrin-independent (Sieczkarski and Whittaker, 2002) endocytosis. Upon entering low pH endosomal compartments, the viral HA protein undergoes significant conformational changes leading to the fusion of viral and host cell membranes (reviewed by Cross et al., 2009). The trimeric HA protein extends outward, inserting the fusogen peptide into the host cell membrane (Tsurudome et al., 1992). HA then pulls the viral and host membranes into close proximity and forms small proteinaceous pores in the host membrane, initiating the formation of a hemifusion intermediate, before full fusion occurs (Bonnafous and Stegmann, 2000).

The M2 ion channel allows an influx of protons that leads to release of the ribonucleoproteins from the viral matrix (Wharton et al., 1994). The viral nucleoproteins

are shuttled to the nucleus through nuclear localization signals in viral proteins (Neill and Jaskunas, 1995). The viral polymerase complex synthesizes both viral mRNA for protein synthesis and RNA for packaging into infectious virions. The PA and PB2 proteins take 5' caps from host pre-mRNAs to initiate viral mRNA synthesis in a process known as "cap snatching" (Dias et al., 2009; Fechter et al., 2003). Viral RNA is exported from the nucleus through interactions with M1 and NEP (Akarsu et al., 2003; Martin & Helenius, 1991). Assembly of infectious virions occurs at the cell surface. Budding is initiated through accumulation of M1 protein, and its association with the plasma membrane and ribonucleoproteins (Noton et al., 2007). Release is mediated through NP, which cleaves sialic acid from the host cell surface, releasing infectious virions (Colman et al., 1983; Palese et al., 1974). During infection, translation of the viral NS1 protein also occurs. NS1 is a major interferon antagonist, and efficiently shuts down the host cell production of type-I IFN (Egorov et al., 1998; García-Sastre et al., 1998).

There is great variation in the two major surface proteins of IAV. Eighteen HA and eleven NA subtypes exist (reviewed by Yoon et al., 2014). The genetic makeup and diversity of IAV can change based primarily on two mechanisms. Genetic drift can occur which introduces mutations due to the error prone viral RNA polymerase (Parvin et al., 1986). Genetic drift occurs in response to pressure from the host immune response. Mutations will accumulate in the major antigenic sites of HA and NA proteins, the two major surface proteins of IAV, as the virus mutates to evade immune detection. Genetic shift may occur when two or more different IAV strains infect the same cell. Genetic shift results in the reassortment of IAV RNA segments in progeny virions, and the generation

of novel IAV strains. In the absence of selection pressure against reassorted viruses, progeny virus produced by coinfection can be products of reassortment over 80% of the time *in vitro* and *in vivo* (Marshall et al., 2013). Reassortment of RNA segments occurs resulting in a virus that contains a new set of gene segments. Generation of novel strains through antigenic shift and antigenic drift results in viruses in which hosts have either reduced or no immunological memory. Human IAV pandemics in 1957 and 1968 occurred following reassortment of human and avian viruses that introduced novel strains into the human population (Scholtissek et al., 1978).

Thus, IAV represent a significant pathogen for several reasons. The large number of subtypes of IAV provides potential candidates for introduction of novel strains into a host population in which no immunological memory exists. In addition, RNA viruses have the highest mutation rate of known pathogens, and genetic drift can occur to evade host immune responses. The segmented nature of IAV genome allows for genetic shift to occur, potentially generating novel strains. In addition, IAV circulate globally using their natural reservoir species, ducks and wild waterfowl. Consequently, unlike human restricted pathogens like smallpox and polio, eradication of IAV is not possible due to their persistence in the reservoir species.

1.2 Ducks and influenza A viruses

Ducks and wild waterfowl are the reservoir species for IAV. The reservoir species and virus have coevolved and exhibit a typical example of a reservoir host and pathogen relationship. While the host has evolved mechanisms to limit the damaging effects of

influenza infection, the virus has evolved mechanisms to both limit the mortality of the natural reservoir, and limit damaging effects of the host's immune response (reviewed by Webster and Bean, 1992). The result is a relationship where IAV can replicate to high levels within the reservoir host without causing disease symptoms. Replication of IAV typically occurs within the intestinal tissue of ducks, where high quantities of the virus can be shed into the environment (Webster et al., 1978). Experimentally infected ducks can shed up to $10^{8.7}$ EID₅₀ of virus per gram of feces into the environment, and shedding can occur for up to three weeks (Hinshaw et al., 1980). Transmission to susceptible ducks occurs typically from contaminated pond water, as infective virus can be isolated from unconcentrated pond water. IAV are more commonly isolated from dabbling and diving ducks, suggesting aquatic lifestyles are important for the maintenance of IAV (Munster et al., 2007).

IAV are classified based on their HA and NA proteins. HA and NA subtypes can be distinguished serologically, and antibodies from one subtype will not cross-react with antibodies of another subtype. Presently, H1-H16 and N1-N9 subtypes have been identified in wild waterfowl, with two recently identified HA and NA subtypes identified in bats (Tong et al., 2013). While sixteen HA and nine NA subtypes circulate within the wild waterfowl population, only certain subtypes are endemic in other species (reviewed by Yoon et al., 2014). H1-H3 and N1-N2 subtypes are able to circulate within the human population, with H1N1 and H3N2 subtypes currently circulating. In swine the H1 and H3 subtypes are endemic, while H7N7 subtypes previously circulated in equine populations (Webster, 1993), and have since been replaced by H3 subtypes (Daly et al., 1996).

Additionally, IAV may cross the species barrier from the reservoir species causing sporadic infections in other avian or mammalian species. While IAV typically do not display disease symptoms in the natural reservoir species, infection in other species including humans, swine, chicken, and turkey can result in significant morbidity and mortality.

In North America, approximately 20% of wild migratory ducks are positive for influenza infection in staging areas in Canada prior to migration (Hinshaw et al., 1980). In wintering areas, the prevalence can drop to below 2% (Stallknecht et al., 1990) and upon their return to northern locations after migration prevalence can be as low as 0.25% (Webster and Bean, 1992), indicating that populations can maintain influenza viruses throughout their migration. Following migration, introduction of large numbers of susceptible juveniles into the population raises the prevalence. More recently, a study of the prevalence of IAV in wild bird populations in North America from April 2006 to March 2011 showed a mean prevalence of 11.4%, with the highest prevalence in dabbling ducks of 15.8% (Bevins et al., 2014). It is also suggested that influenza A viruses can remain stable in pond water and ice over winter. Influenza viruses can remain stable and infective in 17°C water for 207 days, and for longer at 4°C (Stallknecht et al., 1990). It is noted that temperature, pH, and salinity of the water can greatly influence the stability of IAV virions.

It is observed that ducks display a relatively weak immunological memory to IAV infection (reviewed by Magor, 2011). Replication of IAV in the intestinal tract of ducks

does not lead to a good antibody response, despite efficient viral replication (Kida et al., 1980). Additionally, ducks express a truncated form of IgY antibodies (analogous to mammalian IgG) that lacks the Fc region (Magor et al., 1992). These truncated antibodies likely cannot contribute to several important immune processes including opsonization, antibody dependent cellular cytotoxicity, or antigen internalization, which is required for effective presentation of antigen to CD4⁺ T-cells (War et al., 1995). Despite this, younger ducks are more susceptible to infection, implying that ducks are able to generate immunological memory against IAV, although it may be a comparatively weak immune response (Jourdain et al., 2010). These results suggest that ducks do not produce a strong memory response to low pathogenic IAV infection, which may contribute to the propagation and maintenance of IAV in the natural host.

Migratory ducks have the capacity to transmit influenza viruses to other species, where the rates of morbidity and mortality can be high (Alexander et al., 1986; reviewed by Kim & Negovetich, 2009). Highly pathogenic IAV can emerge that can have close to 100% lethality in chickens, but remain asymptomatic in ducks (Alexander et al., 1986; Cooley et al., 1989; Shortridge et al., 1998). Highly pathogenic IAV are classified on two criteria. They exhibit at least 75% mortality in 4 to 8 week old chickens, or have an intravenous pathogenicity index (IVPI) of 1.2 (World Organization for Animal Health, 2014). The second criteria is based on the sequence of the HA gene. Sequencing of the HA gene must show it is either of the H5 or H7 subtype, with a polybasic cleavage site present within the viral HA sequence.

Highly pathogenic IAV strains are infamous for their ability to cause systemic infections with high rates of mortality. While there are several differences between low pathogenic and highly pathogenic IAV strains, the major determinant of pathogenicity is the sequence of the IAV HA protein (Horimoto and Kawaoka, 1994; Perdue et al., 1997; Senne et al., 1996). In order for IAV to be infectious, HA must first be cleaved into functional HA1 and HA2 subunits, which exposes the fusion peptide. In low pathogenic IAV strains the cleavage site typically contains only one basic residue, and the cleavage is mediated by trypsin-like enzymes found in the respiratory or intestinal tract (Klenk et al., 1975). Introduction of multiple basic residues into this site increases its sensitivity to proteolytic cleavage. Polybasic cleavage sites can be cleaved by multiple cellular proteases such as furin-like proteases that are much more ubiquitous (Horimoto and Kawaoka, 1995; Rott et al., 1995). Consequently, the replication of low pathogenic IAV is restricted to tissues where trypsin-like proteases are present whereas highly pathogenic strains are able to cause systemic infections.

Emergence of highly pathogenic strains occurs when low pathogenic IAV replicates within poultry where the virus can mutate into highly pathogenic strains. It was initially believed that highly pathogenic strains are not found within the natural host. However, highly pathogenic IAV strains have since been isolated from wild waterfowl confirming their existence in the wild population (Chen et al., 2005; Chen et al., 2006). These infections have been linked to the recent spread of H5N1 highly pathogenic IAV across Asia and into Europe (Sturm-Ramirez et al., 2005; Webster et al., 2006). It has been experimentally shown that highly pathogenic H5N1 can be transmitted from an

infected mallard to a contact mallard in penned conditions (Sturm-Ramirez et al., 2004). While mutation of low pathogenic strains into highly pathogenic strains outside of the natural host is the major mechanism of the emergence of highly pathogenic IAV, ducks can be asymptotically infected, and as such they are thought of as the “Trojan Horse” of highly pathogenic strains (reviewed by Kim & Negovetich, 2009). Further surveillance will help our understanding of highly pathogenic IAV in wild populations, and the contribution of these populations to the spread of highly pathogenic strains.

Since 2002, highly pathogenic IAV have emerged that have the ability to cause significant disease symptoms and death in wild waterfowl populations (Ellis et al., 2004; Sturm-Ramirez et al., 2004). The emergence of such viruses suggests that the equilibrium between reservoir species and pathogen has been disrupted, and when this occurs significant disease can occur in the natural host. Evidence suggests that successive passage of these highly pathogenic strains in ducks may result in reduced pathogenicity in ducks but maintained pathogenicity in chickens, indicating a possible return to equilibrium with the reservoir species (Hulse-Post et al., 2005). Despite the relatively recent cases of morbidity and mortality, ducks remain the reservoir species of influenza viruses, and contribute to the spread of both low pathogenic and highly pathogenic IAV.

Agricultural practices that allow the interaction of wild duck populations with domestic duck and poultry populations, such as backyard farming or the grazing system typically employed in southeast Asia, are a major risk factor for the introduction of IAV from wild populations into domestic populations (reviewed by Songserm et al., 2006).

Live markets are key areas where mixing of various domestic species from different regions occurs. Transmission of highly pathogenic strains between poultry flocks has devastating consequences. The high mortality rates of highly pathogenic strains in gallinaceous birds can quickly wipe out entire flocks, and culling of infected flocks is commonly practiced to stop the spread of the virus. In addition, sporadic transmission to humans may occur where mortality rates are approximately 60%. To date, there have been 784 reported human cases, 429 of which resulted in death. Highly pathogenic IAV strains represent not only a threat to human health, but also to the significant economic losses associated with outbreaks in the poultry industry.

The mechanisms that allow ducks to facilitate the replication of IAV, and avoid disease from highly pathogenic strains is due to an interaction of multiple viral and host factors. The rapid lethality in chickens caused by highly pathogenic IAV infections, and the apparent absence of disease symptoms in ducks suggests chicken innate immune mechanisms are unable to control viral replication, whereas duck mechanisms are successful. On the other hand, inappropriate immune responses can lead to a cytokine storm and immunopathology in lung tissue, and contribute to influenza associated disease (reviewed by Damjanovi et al., 2012). Characterization of innate immune genes of ducks, particularly the genes that are involved in the innate immune sensing and downstream effector components may give insight into the relationship between IAV and the innate immune response of ducks.

1.3 Innate immune sensing of influenza viruses in duck

The innate immune response is the first line of defense against invading viral pathogens. The rapid detection and subsequent activation of immune effectors is essential in any successful innate immune response. A particularly important part of the antiviral innate immune response is the production of type-I interferon (IFN). Type-I IFN, comprised of IFN α and IFN β , work in a paracrine and autocrine fashion to upregulate hundreds of interferon stimulated genes (ISGs) in the induction of an antiviral state. Ducks are able to sense the presence of IAV through intracellular Toll-like receptors (TLRs) and retinoic acid inducible gene I-like receptors (RLRs). Engagement of both TLR7 and RLRs with their respective ligands results in initiation of signaling pathways that ultimately produce type-I IFN. TLR7 is able to sense the presence of viral ssRNA in endosomes (Lund et al., 2004). The cytosolic RLR receptors Retinoic Acid-Inducible Gene I (RIG-I) and Melanoma Differentiation-Associate Gene 5 (MDA5) both detect viral RNA, albeit with different specificities (Yoneyama et al., 2004, 2005). RIG-I binds to smaller 5' triphosphorylated single stranded RNA (approximately 300 base pairs) (Hornung et al., 2010; Pichlmair et al., 2006), whereas MDA5 binds longer (approximately 1000bp) of double stranded RNA (Kato et al., 2008). During IAV infection, RIG-I contributes more to the production of type-I IFN, although MDA5 does contribute (Kato et al., 2006). Ducks possess both a functional RIG-I (Barber et al., 2010) and MDA5 (Wei et al., 2014) whereas chickens sense IAV infection through MDA5 (Liniger et al., 2012).

The induction of type-I IFN is achieved through the transcription factors NF- κ B, IRF3, and IRF7. The signaling pathways downstream of both TLR7 and RIG-I/MDA5 are reviewed by Brubaker et al., (2015) and Jensen and Thomsen, (2012). In chickens and ducks there has been no IFR3 gene identified (reviewed by Magor et al., 2013). It is hypothesized that although chicken and duck lack IFR3, signaling for the production of type-I IFN is compensated for by the redundant IRF7. Engagement of TLR7 with ssRNA in the endosome initiates signaling through its TIR domain, and recruits the adaptor protein Myeloid Differentiation Primary Response 88 (MyD88) (Honda et al., 2005). MyD88 forms a complex with IRAK1, IRAK4, TRAF6, and IKK α (Lin et al., 2010; Motshwene et al., 2009). This complex then phosphorylates IFR7 through IRAK1 or IKK α , which causes translocation of IRF7 to the nucleus and promotion of the expression of type-I IFN (Diebol et al., 2004). TLR7 is predominantly expressed in plasmacytoid dendritic cells (pDCs). pDCs are known as professional IFN producing cells. They sense the presence of RNA viruses mainly through TLR7, and produce large quantities of type-I IFN (Diebold et al., 2004). TLR7 consequently represents a major contributor to the overall antiviral innate immune response.

RIG-I and MDA5 both sense the presence of cytosolic viral RNA, and converge on the same signaling pathway in the production of type-I IFN (reviewed by Reikine et al., 2014). Upon binding 5' triphosphorylated RNA, RIG-I CARD domains are activated by ubiquitination by TRIM25 (Gack et al., 2007). Duck RIG-I also requires ubiquitination by TRIM25 for activation (Miranzo-Navarro and Magor, 2014). Ubiquitinated RIG-I then translocates to the mitochondria, where it interacts with MAVS

(Kawai et al., 2005). Activated RIG-I acts as a template for the oligomerization of MAVS filaments at the mitochondria, generating long filaments (Wu et al., 2014). MDA5 also interacts with MAVS at the mitochondria, and the downstream signaling of RIG-I and MDA5 converge at this point. Complexes of ubiquitinated RIG-I and MAVS act as a scaffold to further activate downstream signaling events (Liu et al., 2013). Signaling through TRAF6 leads to the activation of IKK- α , IKK- β and IKK- γ (NEMO). This complex phosphorylates the inhibitor of NF- κ B (I κ B), which leads to subsequent ubiquitination and degradation. NF- κ B then translocates to the nucleus to upregulate the expression of type-I IFN. Signaling can also proceed through TRAF3 (Tang and Wang, 2009). TRAF3 can activate TBK-1 and IKK- ϵ , which can directly phosphorylate and activate IRF-3 (presumably IRF-7 in avian species).

Type-I IFN bind to the IFNAR to initiate the signaling the leads to the upregulation ISGs (reviewed by Stark and Darnell, 2012). After engagement of the IFNAR, TYK2 and JAK kinases are activated, which subsequently phosphorylate STAT1 and STAT2 (Müller et al., 1993). STAT1 and STAT2 then heterodimerize and bind IRF9 and translocate to the nucleus. This complex can bind to ISREs and cause the upregulation of ISGs. The upregulation of hundreds of ISGs leads to a cellular “antiviral state” and results in resistance to a wide range of viral pathogens.

TLR7 is present and functional in ducks, whereas the TLR8 gene has been disrupted (MacDonald et al., 2008). This disruption is also observed in chickens (Philbin et al., 2005). Chickens also lack the important innate immune receptor RIG-I (Barber et

al., 2010). Overexpression of duck RIG-I in DF-1 chicken fibroblast cells increases their ability to upregulate IFN- β and multiple ISGs after infection with IAV. This is also associated with an ability to decrease IAV replication *in vitro*. Although chickens lack RIG-I, they are able to partially compensate with detection through MDA5 (Liniger et al., 2012). The apparent lack of RIG-I in chickens is likely a contributing factor to the increased susceptibility of chickens to highly pathogenic IAV infections. This increased susceptibility cannot be explained by the absence of RIG-I alone. However, the ability of ducks to sense the presence of IAV, produce type-I IFN, and the subsequent upregulation of hundreds of ISGs will be of great importance in the avoidance of disease symptoms from highly pathogenic IAV.

Ducks display a strong innate immune response after infection with highly pathogenic IAV. A suppressive subtractive hybridization screen identified several genes that are upregulated in duck lung tissue after infection with highly pathogenic H5N1 including MHC-I, IRF-1 and multiple ISGs including OASL, ISG12, IFIT5, and IFITM1 (Vanderven et al., 2012). Analysis of the duck transcriptome revealed transcripts of many innate genes increased in lung tissue after infection with two different H5N1 highly pathogenic IAV strains including the innate immune receptors RIG-I and TLR3, -4, and -7, several cytokines and chemokines, and three ISGs belonging to the same family, IFITM3, -5, and -10 (Huang et al., 2013).

Several ISGs with known antiviral function include TRIM5 α , ISG15, IFITs, OAS, PKR, VIPERIN, and tetherin (reviewed by Schneider et al., 2014; Schoggins, 2014).

Their antiviral activities are mediated through diverse functions such as inhibition of viral entry, inhibition of protein synthesis, sequestration of viral RNA, degradation of host and viral mRNA, mutation of viral genomes, and inhibition of virion release. The Interferon-Inducible Transmembrane Proteins (IFITMs) are a recently characterized gene family of ISGs that inhibit viral entry and are particularly important in the outcome of IAV infections (reviewed by Bailey et al., 2014). Importantly, IFITMs have been identified as genes that are upregulated in duck lung tissue in response to highly pathogenic H5N1 IAV infection (Huang et al., 2013; Vanderven et al., 2012). The IFITM gene family, and their function in the innate immune response against IAV will be discussed below.

1.4 Interferon inducible transmembrane proteins

IFITMs were originally identified in a screen of genes upregulated by type-I IFN (Friedman et al., 1984). The human genes were first annotated as 9-27 (IFITM1), 1-8D (IFITM2), and 1-8U (IFITM3) (Lewin et al., 1991). The human IFITM family contains IFITM1, IFITM2, IFITM3, IFITM5 and IFITM10 while the mouse IFITM family contains two additional genes, IFITM6 and IFITM7. IFITMs can be divided into three specific clades based on their function and sequence (Zhang et al., 2012). Immune-related IFITMs include IFITM1, IFITM2, and IFITM3. They restrict viral replication through inhibition of viral entry (Feeley et al., 2011). IFITM5 makes up the second clade. In mammals, its expression is not inducible by type-I IFN and is restricted to osteoblasts where it is involved in bone mineralization (Hanagata et al., 2011; Lazarus et al., 2013; Moffatt et al., 2008). IFITM10 makes up the remaining clade, is located at a different genetic locus than the immune related IFITMs and IFITM5, and has unknown function.

All IFITMs contain one hydrophobic intramembrane domain linked to a second hydrophobic intramembrane/intermembrane domain, with highly variable N- and C-termini. IFITMs all contain a conserved CD225 domain, which consists of the first intramembrane domain and linker region. IFITMs are part of a larger group of proteins called dispanins (Almén et al., 2012). There are fourteen human members of the dispanin family, however outside of the IFITM genes the function of other dispanins is poorly characterized. Dispanins have been identified in brown algae and a range of bacterial species, suggesting an ancient origin.

1.4.1 IFITM topology

It is agreed that the region spanning the two hydrophobic regions is cytosolic, but the orientation of the N- and C-termini are disputed, with multiple proposed topologies (Fig. 1). Initial reports detected the presence of epitope tags on both the N- and C-termini in the extracellular space (Brass et al., 2009), and revealed the N-terminal domain of IFITMs is likely cytosolic (Smith et al., 2006). The N-terminal domain of IFITM3 is both phosphorylated (Jia et al., 2012) and ubiquitinated (Yount et al., 2012), and requires access to cytosolic enzymes for these modifications to occur. In addition, there is a noted lack of glycosylation of the N-terminal domain of IFITM3, further suggesting a cytosolic orientation (Yount et al., 2012). Evidence exists for both the N- and C-termini of the proteins facing the cytosol with two intramembrane domains. The addition of a prenylation motif to the C-terminus of IFITM3 suggests it is located within the cytosol (Yount et al., 2012). However, these experiments were performed with IFITM3 that

contained mutated cysteine residues and an artificial N-terminal myristoylation motif. An additional model of IFITM3 topology has also been proposed with a cytosolic N-terminal domain, one intramembrane domain, and a transmembrane domain leading to a luminal C-terminal tail (Bailey et al., 2013). The C-terminal domain of IFITM3 can be cleaved, presumably by endosomal proteases. This makes the use of a C-terminal epitope tag for analysis difficult. This topology has also been proposed for IFITM1 (Weston et al., 2014). There is also evidence to suggest that IFITMs can exist in different topologies in different cell types, albeit with major and minor contributors to the overall topology (Bailey et al., 2013). Paralogous IFITMs may also exist in different topologies as significant sequence differences exist.

1.4.2 Non-Immune functions of IFITMs

Although IFITMs were initially identified as ISGs, their function remained unresolved for many years. The role of IFITMs in murine germ cell homing was investigated as one of the initial functions of IFITMs. IFITM3 was identified as a specific marker of primordial germ cells (PGCs) (Tanaka and Matsui, 2002). IFITM1 and IFITM3 expression in developing embryos has marked effects on PGC homing. IFITM1 is expressed in the endoderm where it apparently acted as a repulsive signal, whereas IFITM3 expression in PGCs leads to proper cell homing (Tanaka et al., 2005). Furthermore, expression of IFITM3 in somatic cells can alter cell homing during embryonic development to resemble that of PGCs. However, these observations are disputed. Generation of mice lacking either the entire IFITM locus, or IFITM3 alone

develop normally, and display no obvious phenotype, suggesting IFITMs are not essential for proper germ cell homing and development (Lange et al., 2008).

The expression of mammalian IFITM5 has previously been shown to be limited to bone tissue, where it is involved in bone mineralization (Moffatt et al., 2008). Defective IFITM5 is associated with Osteogenesis Imperfecta Type V (Lazarus et al., 2013). Although IFITM5 itself is not stimulated by type-I IFN, there is a single report of IFITM5 function in the stimulation of expression of several other ISGs, suggesting a potential for immune function *in vitro* (Hanagata & Li, 2011). In addition, zebrafish IFITM5 expression is absent from bone, and is expressed in muscle, brain and liver tissue while chicken IFITM5 is highly expressed in liver, muscle, and spleen tissue suggesting a different function than mammalian IFITM5 (Hickford et al., 2012).

1.4.3 Immune functions of IFITMs

IFITM1 is capable of interacting with components of the B-cell receptor complex, and co-immunoprecipitates with TAPA-1, CD19, and CD21 (Bradbury et al., 1992; Matsumoto et al., 1993). Additionally, antibodies that bind IFITM1 promotes cell adhesion and aggregation in leukemic B- and T-cells, and inhibit proliferation of B lymphocytes (Chen et al., 1984; Evans et al., 1990). It is unclear if these findings are physiologically relevant. There has been no ligand for IFITMs identified, and the increased adhesion and inhibition of proliferation is likely an artifact of binding with an antibody.

While there was an early report of the inhibition of VSV replication by IFITM1 (Alber and Staeheli, 1996), the important antiviral function of IFITMs was discovered in an siRNA screen of host genes that affected the replication of IAV (Brass et al., 2009). Overexpression of IFITM1, IFITM2, and IFITM3 all reduced the percentage of IAV infected cells *in vitro*. Since their role in restriction of IAV was demonstrated, numerous reports focused on studying the range of viruses that are susceptible to restriction by IFITMs. IFITMs restrict the replication of several enveloped viruses including Flaviviruses (West Nile virus and dengue virus) (Brass et al., 2009; Jiang et al., 2010; John et al., 2013), SARS corona virus (Huang et al., 2011), filoviruses (Ebola virus and Marburg virus) (Huang et al., 2011), bunyaviruses (rift valley fever virus, Andes virus, Haantan virus, and LaCrosse virus) (Mudhasani et al., 2013), VSV (Alber & Staeheli, 1996; Weidner et al., 2010), HIV-I (Lu et al., 2011), RSV (Everitt et al., 2013), and HCV (Wilkins et al., 2013). Reinfection with dengue virus can often be more severe due to antibody-dependent enhancement of infection. However, IFITM3 is able to restrict this antibody-dependent enhancement of infection (Chan et al., 2012). Interestingly, IFITM3 is able to inhibit the replication of reovirus, a non-enveloped virus (Anafu et al., 2013).

Additionally, resident memory cells generated after IAV infection are able to avoid infection from a second IAV infection through maintained IFITM3 expression, while their counterparts lacking IFITM3 expression were lost suggesting IFITM3 can play an important role in the survival of memory immune cells (Wakim et al., 2013). Furthermore, basal expression of IFITMs in the absence of type-I IFN confer intrinsic protection against viral infection (Brass et al., 2009). Collectively, these results suggest

that IFITMs are major components of the innate immune response, and inhibit the replication of a broad range of viral pathogens.

While IFITMs are all able to restrict a broad range of viruses, each IFITM has an ability to best restrict a certain range of viral pathogens. IFITM3 has the ability to restrict the replication of IAV, and flaviviruses to a greater extent than IFITM1 and IFITM2 (Brass et al., 2009; Huang et al., 2011; Jiang et al., 2010). IFITM1 appears to restrict the replication of filoviruses and SARS-coronavirus better than IFITM2 and IFITM3, although IFITM3 can also be most efficient at restricting these viruses depending on cell type (Huang et al., 2011). IFITM2 and IFITM3, but not IFITM1 can efficiently restrict rift valley fever virus (Mudhasani et al., 2013). Interestingly, while IFITM1 is unable to restrict rift valley fever virus, it is able to restrict most other bunyaviruses. There is convincing evidence IFITMs are able to restrict HIV-1, despite reports of HIV-I resistance to the effects of IFITMs (Jia et al., 2012; Lu et al., 2011; Schoggins et al., 2011). IFITM1 appears to better restrict HIV-1 than IFITM2 or IFITM3.

Several viruses, including arenaviruses (Brass et al., 2009; Chan et al., 2012) and multiple DNA viruses including human papilloma virus, cytomegalovirus and adenovirus (Warren et al., 2014) are resistant to IFITM restriction. Some viral pathogens, such as human corona virus OC43 and HPV16 use IFITMs to promote their own infection (Warren et al., 2014; Zhao et al., 2014). The mechanisms on how IFITMs mediate the promotion of certain viruses, and how certain viruses evade restriction by IFITMs is unknown. There are no obvious differences between IFITM sensitive and resistant

viruses. Common pathways are often used to infect host cells such as clathrin mediated endocytosis, although some arenaviruses use a clathrin and caveolin independent mechanism for entry (Rojek and Kunz, 2008). In addition, IFITMs are unable to restrict the replication of numerous non-viral pathogens. IFITM3^{-/-} mice are not more susceptible to infection with *Mycobacterium tuberculosis*, *Citrobacter rodentium*, *Salmonella typhimurium*, and *Plasmodium berghei* than wild-type control mice, suggesting their effects are restricted to viral pathogens (Everitt et al., 2013).

1.4.4 IFITM3 and influenza A virus

Although IFITM1, IFITM2, and IFITM3 are all able to reduce the percentage of IAV infected cells, IFITM3 is the most potent restrictor of IAV. IFITM3 alone is responsible for between 40-70% of the antiviral activity of type-I IFN against IAV *in vitro* (Brass et al., 2009). Upon infection with low pathogenic IAV, IFITM3^{-/-} mice developed fulminant pneumonia and morbidity and mortality similar to infections with highly pathogenic IAV, whereas wild type mice recovered from infection and displayed no mortality (Everitt et al., 2012). In addition, there was no observable difference between the susceptibility of mice lacking the entire IFITM locus and IFITM3^{-/-} mice to IAV infection, indicating that IFITM3 alone is responsible for the majority of IFITM mediated restriction of IAV (Bailey et al., 2012). It is important to note that IFITMdel and IFITM3^{-/-} mice also have a disrupted *Mx1* and *Mx2* genes, as many inbred strains of mice have this disruption. Mice expressing *Mx1* are resistant to IAV infection, and use of *Mx1* deficient mice can often change the interpretation of experimental results (Ikasaki and Pillai, 2014; Koerner et al., 2007). Therefore, the lack of ability of these mice to

respond to IAV infection is due to loss of both Mx1 and IFITM3, although these results do suggest IFITM3 is a major contributor to the innate immune response against IAV infection.

A SNP of IFITM3 exists in the human population that introduces a splice acceptor site into the coding region of IFITM3 (Everitt et al., 2012). The introduced splice acceptor site in the rs12252C-allele of IFITM3 creates the use of an internal methionine residue as a start codon, and the expression of a truncated protein missing the first 21 amino acids of the protein. Previous reports identify an enrichment of this rs12252-C allele of IFITM3 in patients hospitalized with seasonal or pandemic influenza infections, and in severe influenza infections in Han Chinese patients (Everitt et al., 2012; Zhang et al., 2013). The rs12252-C allele of IFITM3 was shown to be non-functional *in vitro*. Collectively, these results demonstrate that IFITM3 can potently restrict IAV *in vitro*, and are indispensable *in vivo* for an effective innate immune response against IAV infections.

1.4.5 Cellular localization of IFITMs

The apparent ability of IFITMs to differentially restrict different ranges of viruses has been linked to their cellular localization. Early studies on the cellular localization of IFITMs produced conflicting results. Initial reports detected IFITM3 at the cell surface, using flow cytometry (Tanaka et al., 2005). Further analysis revealed IFITM2 and IFITM3 colocalized with internal vesicles containing the late endosomal markers LAMP2 and CD63 (Feeley et al., 2011; Huang et al., 2011), while IFITM1 resides mainly at the cell surface (Xu et al., 2009). IFITMs therefore are able to restrict the entry of certain

ranges of viruses depending on their cellular localization. IFITM1 apparently is better able to restrict viruses that enter host cells at the cell surface, or in early endosomes, whereas IFITM2 and IFITM3 are better suited to restrict viruses that enter host cells in early and late endosomes (Fig. 2). The observed overlap of viruses restricted by both IFITM2 and IFITM3 likely results from the partial overlap of endocytic compartments that both of these proteins reside in, although IFITM2 localization is less clearly defined (Lu et al., 2011; Mudhasani et al., 2013).

The N-terminal domains of IFITM2 and IFITM3 both contain a YXX θ endocytic signal sequence that is important for endosomal localization, where X is any amino acid and θ is a large hydrophobic residue. The rs-12252C allele of IFITM3 that is missing the first 21 amino acids is apparently unable to restrict the replication of IAV *in vitro* (Everitt et al., 2012). Further studies revealed that deletion of the first 21 amino acids of IFITM3 resulted in accumulation of the protein at the cell surface, and led to the identification of the YXX θ endocytic signal sequence (Jia et al., 2012, 2014) Mutation of the critical tyrosine residue within this sequence is sufficient to disrupt its function as an endocytic signal sequence, and cause mislocalization of IFITM3 away from endosomes to the cell surface. Both the deletion of the first 21 amino acids and mutation of the critical tyrosine motif are associated with a loss of ability to restrict the entry of IAV and VSV. A chimeric IFITM protein expressing the N-terminal domain of IFITM3 and the CD225 domain of IFITM1 resulted in a cellular staining pattern similar to IFITM3, suggesting the N-terminal domain of IFITM3 is sufficient for cellular localization (John et al., 2013). In addition, the N-terminal YXX θ sequence of IFITM3 is able to cause internalization of

CD4 (Chesarino et al., 2014). These results suggest that the N-terminal YXX θ motif is the major contributor to the endosomal localization of IFITM3, and is sufficient to cause endosomal localization on its own.

Recently, the importance of this YXX θ endoytic signal sequence in the cellular localization of IFITM3 has been challenged. Neither deletion of the first 21 amino acids or mutation of the critical tyrosine within the YXX θ signal sequence resulted in decreased antiviral function against IAV (Williams et al., 2014). There was a noted shift in the cellular localization of the mutated IFITM3 proteins, but not dramatic relocalization of the proteins to the cell surface previously described. The authors suggest that certain epitope tags can affect both antiviral function and cellular localization. Additionally, early work demonstrated chimeric IFITM1 expressing the N-terminal domain of IFITM3 was still localized to the cell surface (Tanaka et al., 2005). Collectively, these results suggest that the N-terminal domain of IFITM3 may not be essential for endosomal localization.

1.4.6 Mechanisms of IFITMs

IFITMs prevent the entry of virions into host cells, and prevent the delivery of viral genetic material and proteins into the cytoplasm (Feeley et al., 2011). The mechanism of how IFITMs inhibit viral entry remains unresolved, with numerous potential mechanisms proposed. The mechanism must include a disruption of a pathway used for entry by the diverse array of viruses that are inhibited by IFITMs. IFITM sensitive viruses use different receptors for attachment and entry, excluding mechanisms

that suggest a disruption of the interaction of specific viral attachment proteins and cellular receptors. As such, IFITMs do not inhibit the binding of viruses with host cells, and do not cause a downregulation of cellular receptors, or interfere with virion access to endocytic compartments (Brass et al., 2009; Huang et al., 2011). The mechanisms also must not be exclusive to enveloped viruses, as IFITM3 is capable of restricting the non-enveloped reovirus (Anafu et al., 2013).

IFITMs inhibit the entry of viruses by blocking the fusion of viral and host membranes (Desai et al., 2014; Feeley et al., 2011; Li et al., 2013). Cell-cell fusion assays suggest that IFITMs restrict the hemifusion event between viral and host membranes (Li et al., 2013). This restriction was shown with all three types of viral fusogens, demonstrating their broad-spectrum abilities. However, a direct virus-cell fusion assay suggests that IFITMs restrict pore formation after hemifusion in order to restrict viral and host membrane fusion (Desai et al., 2014). IFITMs have been hypothesized to introduce spontaneous positive curvature in the outer membrane of host endosomes, and reduce membrane fluidity as a means to restrict membrane fusion (Li et al., 2013; Lin et al., 2013). Additionally, IFITMs interact with Vesicle-membrane-protein-associated protein A (VAPA), preventing its association with oxysterol-binding protein (OSBP), leading to a disruption in cholesterol homeostasis (Amini-Bavil-Olyaei et al., 2014). This disruption of cholesterol homeostasis is proposed to be a mechanism in which IFITMs disrupt membrane fusion events, although there are reports of cholesterol independent viral restriction (Desai et al., 2014; Wrensch et al., 2014).

Overexpression of IFITMs often results in expanded endocytic compartments (Feeley et al., 2011; Huang et al., 2011). Interestingly, IFITMs do not appear to perturb virion trafficking and entry into endocytic compartments, or drastically alter pH or proteolytic activity of endosomal proteases (Anafu et al., 2013; Feeley et al., 2011; Huang et al., 2011). Although there is a report of interaction between IFITM3 and the vacuolar ATPase, perhaps disrupting its function and decreasing endosomal acidification (Wee et al., 2012). Additionally, IFITMs can influence clathrin organization, and absence of IFITMs can result in a decreased capacity for endocytosis (Wee et al., 2012). The exact mechanism of how IFITMs are able to restrict viral entry is not elucidated, and could include a combination of the mechanisms above. It is agreed upon that IFITMs prevent viral entry into host cells, and cause shuttling of entering virions into lysosomal compartments where they are ultimately degraded.

1.5 Experimental aims and results summary

It has been shown that ducks display a strong innate immune response after infection with highly pathogenic IAV (Barber et al., 2010; Vanderven et al., 2012), however, the host factors involved in protection are unknown. Previous studies have focused on identification of genes that are upregulated in ducks after infection, and studies examining the functional roles of these identified genes are lacking. Previously, a screen of genes enriched in duck lung tissue after infection with highly pathogenic IAV led to the identification of an IFITM gene (Vanderven et al., 2012). In addition, expression levels of IFITM3, -5, and -10 all increased in analysis of duck lung transcriptome after infection with two different highly pathogenic H5N1 influenza A

virus strains (Huang et al., 2013). The recently characterized chicken IFITM locus identified four IFITM genes, IFITM1, -2, -3, and -5, with IFITM3 able to restrict IAV *in vitro* (Smith et al., 2013). Information on the functionality of other avian IFITMs is lacking. Of particular interest is whether IFITMs function in the duck, or whether influenza evades this restriction in its natural host. Although IFITMs represent a small fraction of the genes that are upregulated in duck lung tissue in response to highly pathogenic IAV, their functional role is interesting.

Here, I characterize the IFITM gene family in the genome sequence of White Pekin ducks. I show ducks contain an intact IFITM locus, containing IFITM1, IFITM2, IFITM3 and IFITM5, and demonstrate their upregulation in lung tissue in response to highly pathogenic influenza A virus infection. Additionally, I show duck IFITM1 is modestly upregulated in intestinal tissue in response to low pathogenic IAV infection. I show dIFITM3 is a potent restrictor of IAV replication in avian cells, identifying duck IFITM3 as an important mediator of the duck innate immune response against IAV. In addition, I demonstrate that the N-terminal YXX θ endocytic signal sequence of dIFITM3 is not essential for endosomal localization or antiviral function, suggesting avian IFITM3 may function differently than mammalian IFITMs.

1.5.1 Experimental aims

Aim 1. Identification of the duck IFITM repertoire.

The duck IFITM locus was examined, and each IFITM gene was sequenced. Comparison of amino acid sequences and gene synteny was used to annotate each duck

IFITM gene. Each duck IFITM gene was cloned into a mammalian expression vector, both with and without an N-terminal V5 epitope tag to further characterize IFITM function.

Aim 2. Examination of duck IFITM expression in response to low pathogenic and highly pathogenic IAV.

IFITMs were originally identified in a screen of genes that are upregulated by type-I IFN (Friedman et al., 1984). qPCR was used to determine if duck IFITMs are upregulated in lung tissue in response to low pathogenic and highly pathogenic IAV infection. Expression in response to infection with low pathogenic IAV was also examined in intestinal tissue.

Aim 3. Characterization of the antiviral properties of duck IFITMs.

Duck IFITM antiviral activity was characterized *in vitro*. Each duck IFITM was cloned into the mammalian expression vector pcDNA3.1/Hygro. Duck IFITMs were overexpressed in DF-1 chicken fibroblast cells, and stably expressing clones were generated. DF-1 cells transiently or stably expressing duck IFITMs were challenged with H6N2, H11N9, and PR8 (H1N1) low pathogenic IAV, and VSV. The percentage of infected cells was determined using fluorescent microscopy and flow cytometry. The cellular localization of each duck IFITM was determined using confocal microscopy.

Aim 4. Identify critical regions and residues important for duck IFITM3 function.

Mammalian IFITM3 contains critical residues in the N-terminal domain that are critical for endosomal localization, and antiviral function. In order to determine if duck IFITM3 functions similarly to mammalian IFITM3, chimeric mutants were generated of duck IFITM1 and IFITM3 that swap the N-terminal domains. In addition, point mutants of duck IFITM3 were generated disrupting the N-terminal YXX θ endocytic signal sequence, and three other potential tyrosine based endocytic signal sequences. DF-1 cells stably expressing each mutant protein were generated, and antiviral function and cellular localization examined.

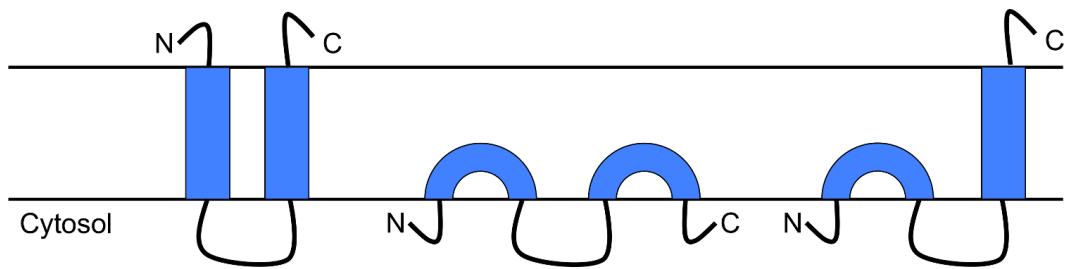


Figure 1. Proposed topology of IFITMs. IFITMs all have a common structure with two membrane spanning domains with a cytosolic loop region. IFITMs are predicted to exist in three topologies with either two intermembrane domains, two intramembrane domains, or one intra- and one intermembrane domain.

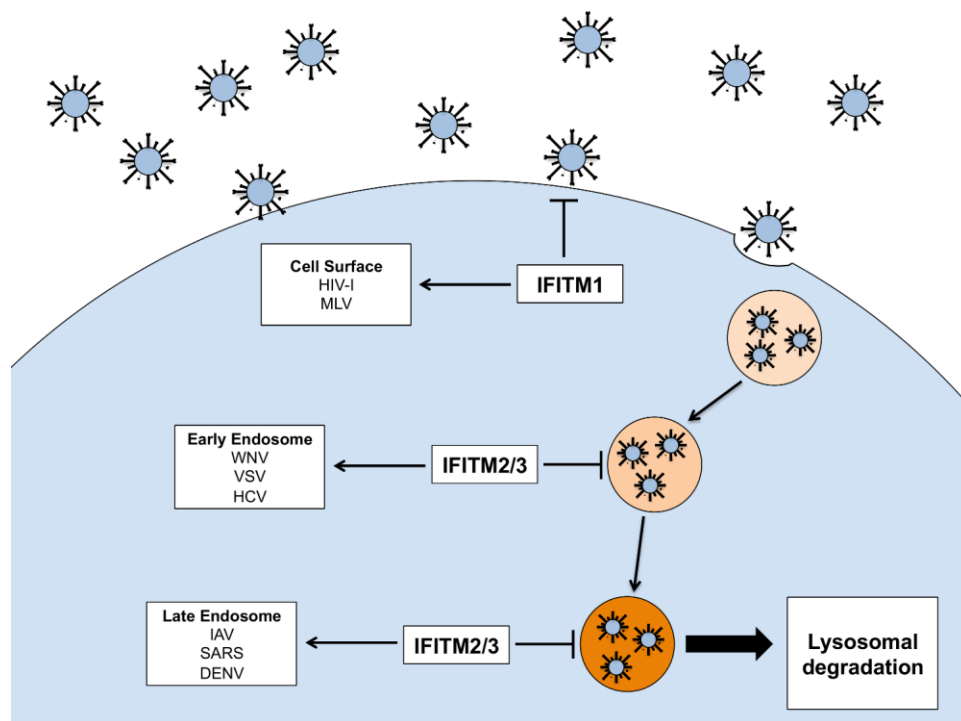


Figure 2. Cellular localization of IFITMs. IFITMs are expressed in distinct cellular compartments. Their ability to restrict the entry of viral pathogens is based on their cellular localization. IFITM1 is expressed at the cell surface, whereas IFITM2 and 3 are expressed in endocytic compartments.

Chapter 2. Materials and Methods

2.1 Identification, sequencing and analysis of duck IFITMs

Partial sequences of duck IFITM1, IFITM2, IFITM3, and IFITM5 were obtained through analysis of scaffold 2493 of the duck genome (ENSEMBL, BGI_duck_1.0). Genes flanking the IFITM locus, *B4GALNT4* and *ATHL1*, were identified and the genomic region in between analyzed. To obtain exon 1 sequences 5' RACE was used for IFITM3 (Clontech), and RNA transcriptome sequences were used to obtain IFITM2. Full-length duck IFITM coding sequences were amplified from cDNA from duck lung tissue with Phusion High-Fidelity DNA Polymerase (New England Biolabs) using primers that incorporate NheI and NotI restriction enzyme sites (Table 1). PCR products were gel extracted using the QIAquick Gel Extraction Kit (Qiagen) and subsequently A-tailed using Taq polymerase. A-tailed PCR products were cloned into pCR2.1-TOPO (Invitrogen). All plasmids were transformed into *Escherichia coli* DH5 α . Individual clones of each transformation were used for plasmid isolation using the Qiagen Miniprep Kit (Qiagen). All clones were sequenced in the forward and reverse direction using BigDye Terminator v3.1 (Applied Biosystems) using vector specific primers (Table 2). Sequences were analyzed using ContigExpress (Invitrogen). Sequence alignment of IFITMs was performed using T-COFFEE in JalView (Waterhouse, Procter, Martin, Clamp, & Barton, 2009). Maximum likelihood tree of IFITMs was generated using Phyml with 100 bootstrap replications (Dereeper et al., 2008).

2.2 Generation of expression constructs

Amplification and cloning of duck IFITMs into pCR2.1-TOPO was also performed with primers that incorporated an N-terminal V5 epitope tag and NheI and NotI cut sites. PCR products of epitope and non-epitope tagged duck IFITMs containing restriction sites and the mammalian expression vector pcDNA3.1/Hygro⁺ were digested with NheI and NotI (New England Biolabs). Digested insert and vector were ligated using T4 ligase (Invitrogen) (Fig. 3). Sequences of each clone were confirmed using vector specific primers (Table 2). High concentration plasmid preps were generated using the Qiagen Midiprep Kit (Qiagen).

2.3 Duck infections and RNA extraction

Previously, six week old White Pekin ducks were infected with PBS (mock), H5N2 A/mallard/BC500/05 (BC500), or H5N1 A/Vietnam/1203/04 (VN1203). 10^6 EID₅₀ of each virus were inoculated in nares, eyes, and trachea. One day, two days, and three days post infection ducks were sacrificed and tissues harvested. Total RNA was extracted using TRIzol (Invitrogen). Titres of oropharangeal swabs for VN1203 ranged from 10^2 to 10^4 and cloacal swabs for BC500 from 10^5 to 10^7 as reported previously (Vanderven et al., 2012). All animal infections and RNA extractions were performed in biosafety level 3 facilities at St. Jude Children's Research Hospital (Barber et al., 2010).

2.4 Quantification of IFITM expression by real-time PCR

1000 ng (for PCR amplification) or 500 ng (for qPCR) of total RNA was used for cDNA synthesis. RNA was DNaseI treated prior to cDNA synthesis (Invitrogen). oligo-dT primers were used to prime cDNA synthesis, and extension was performed using SuperscriptIII (Invitrogen). Quality of cDNA was confirmed with PCR amplification of a fragment of *GAPDH*. Primers and probes were generated (IDT Technologies) and validated for linear amplification of each duck IFITM in comparison to *GAPDH* endogenous control (Table 3). FastStart TaqMan master mix (Roche) and gene specific probe and primer mixes were used, and reactions were performed in a Prism 7500 Real Time PCR Machine (Applied Biosystems). All cDNA samples were assayed in triplicate. Changes in target gene expression are relative to a mock infected animal. Analysis was performed using relative quantification of gene expression ($\Delta\Delta CT$) using 7500 Fast System software v1.4 (Applied Biosystems).

2.5 Generation of chimeric proteins and point mutants

Chimeric proteins swapping the N-terminal domains of dIFITM1 and IFITM3 were generated by overlap extension PCR. Briefly, the N-terminal regions of dIFITM1 and dIFITM3 were amplified using the forward primers previously described, and reverse primers containing a 5' overhang that corresponds to the CD225 domain of either dIFITM1 or dIFITM3, O.E. IFITM1.rv.3CD225 and O.E. IFITM3.rv.1CD225 (Table 4). The CD225 and C-terminal tail was amplified for dIFITM1 and dIFITM3 using the reverse primers previously described and a forward primer containing a 5' overhang that corresponds to the N-terminal region of either dIFITM1 or dIFITM3,

O.E.IFITM1.fw.3NTD or O.E.IFITM3.fw.1NTD (Table 4). PCR products of the N-terminal of dIFITM1 and CD225 domain of dIFITM3 were combined, and PCR products of the N-terminal region of dIFITM3 and CD225 domain of dIFITM1 combined, and a final PCR was performed to create full length chimeric proteins using forward and reverse primers using the previous combined PCR products as template. Point mutants of dIFITM3 were generated by PCR using site directed mutagenesis (Table 4). Briefly, amplification of each mutant and vector was performed with the mutation incorporated into the primers, and template plasmid DNA was digested with DpnI to digest template methylated DNA (New England Bio Labs). For all mutants, individual clones were isolated, sequenced, and cloned into pcDNA3.1/Hygro+ as previously described.

2.6 Cell culture, transfections and generation of stable cell lines expressing IFITM

DF-1 cells, a spontaneously immortalized chicken fibroblast cell line, were cultured in Dulbecco's modified Eagles Medium (DMEM) (Life Technologies) supplemented with 10% fetal bovine serum (FBS) (Sigma) at 39°C and 5% CO₂. For transient transfections, cells were seeded overnight in 96-well plates (3×10^4 cells) and 24 hours later transfected with 0.2µg of plasmid DNA/well using 0.5µL of Lipofectamine 2000 (Invitrogen). Infections were performed 24 hours after transfection. Stably expressing DF-1 cells were generated by seeding cells overnight in 6-well plates (8×10^5 cells) and 24 hours later transfected with 1.25µg of linearized plasmid DNA/well using 3.75µL of Lipofectamine 2000 (Invitrogen). Plasmid DNA was linearized by digestion with BglIII (New England Biolabs). 48 hours after transfection, cells were put under selection using hygromycin (500 µg/mL) and surviving cells were expanded. After

approximately 10 days under selection, the concentration of hygromycin was lowered to a maintenance concentration (250 µg/mL). Individual clones were isolated by limiting dilution, and expression of duck IFITMs in individual clones screened by Western blot.

2.7 Western blots

Whole cell lysates of DF-1 cells were collected using Lysis Buffer (50 mM Tris-HCl (pH 7.2), 150 mM NaCl, 1% (v/v) Triton X-100) with cOmplete Mini, EDTA-free proteinase inhibitor (Roche Diagnostics). Cell lysates were boiled in 1X Laemmli buffer before separation by SDS-PAGE electrophoresis, and transfer to a nitrocellulose membrane. Membranes were blocked using 5% skim milk powder (w/v) in 1X PBS for one hour. Western blotting was performed using a primary mouse anti-V5 antibody at 1:5000 (Life Technologies) and subsequent blotting with a secondary goat anti-mouse-HRP at 1:5000 (BioRad). Proteins were visualized by chemiluminescence using the ECL kit (GE-Healthcare).

2.8 Cell culture and virus infections

A/chicken/California/431/00 (H6N2), A/duck/Memphis/546/1974 (H11N9) and A/Puerto Rico/8/1934 (H1N1) were all propagated in 10 day old embryonated chicken eggs. rVSV-GFP was propagated in BHK-21 cells. The titre of all stocks was determined by plaque assay on MDCK cells (IAV) or BHK-21 cells (rVSV-GFP). 24 hours after transfection or plating of stably expressing DF-1 cells, cells were challenged with either H6N2, H11N9, H1N1, or rVSV-GFP at the indicated multiplicity of infection. For influenza viruses, cells were cultured in DMEM supplemented with 0.3% BSA and L-

(tosylamido-2-phenyl) ethyl chloromethyl ketone–treated trypsin (Worthington Biochemical) (0.1 µg/mL). Cells were challenged with influenza A virus for 30 minutes, or rVSV-GFP for 1 hour before unbound virus was removed by removing media, and washing cells once with 1X PBS. Fresh media was added and cells were incubated for 6 hours (influenza virus) or 12 hours (rVSV-GFP) before fixing.

2.9 Fluorescent microscopy analysis of viral infection

Six hours after infection with influenza A virus cells were fixed in 1% formaldehyde and washed with 0.1% Triton X-100 for 10 minutes. Cells were washed three times with 1X PBS, and blocked for 1 hour with 4% BSA. The cells were then stained with anti-nucleoprotein-FITC (Argene) for 1 hour, followed by staining with Hoechst 33342 (Life Technologies). Images were taken with the Operetta High Content Imaging System (Perkin Elmer) to determine the percentage of infected cells.

2.10 Flow cytometric analysis of viral infection

Six hours after infection with influenza A virus, and twelve hours after infection with rVSV-GFP infected DF-1 cells were harvested using 0.25% Trypsin-EDTA (Invitrogen), and fixed in 1% paraformaldehyde. A longer time point was used for rVSV-GFP to obtain detectable levels of GFP expression. Influenza infected cells were washed for 10 minutes with 0.1% Triton-X in PBS before staining with anti-nucleoprotein-FITC (Argene). rVSV-GFP infected cells were visualized directly. The percentage of FITC or GFP positive cells was determined by flow cytometry.

2.11 Plaque assays

MDCK cells were cultured in 1X Minimal Essential Media (MEM) supplemented with 10% FBS, sodium bicarbonate, PSF (Streptomycin, Penicillin, Amphotericin B), MEM vitamins, and L-glutamine (Gibco). Infection media for MDCK cells is the same as growth media, but replacing 10% FBS with 0.3% BSA and addition of 1 ug/mL of L-(tosylamido-2-phenyl) ethyl chloromethyl ketone-treated trypsin (Worthington Biochemical). Supernatant from infected DF-1 cells was collected twelve hours post infection, and serially diluted in infection media. Monolayers of MDCK cells grown in 6-well plates were infected with serially diluted supernatants. After one hour, supernatants were removed and cells were washed with 1X PBS. Cells were then overlaid with infection media containing 0.9% agar. After 72 hours cells were stained with 0.1% crystal violet solution to calculate the number of PFUs.

2.12 Cellular localization of IFITMs by confocal microscopy

DF-1 cells were seeded onto coverslips in 6-well plates at (8×10^5 cells) and the cells were transfected with dIFITM constructs. 24 hours after transfection, cells were fixed in ice cold 100% methanol for 20 minutes and blocked in 4% BSA for 1 hour. The cellular location of each duck IFITM was determined by staining with rabbit anti-V5 conjugated to Dylight650 (Abcam). Endosomes were stained using a mouse anti-LEP100 antibody (LEP100 IgG; Developmental Studies Hybridoma Bank) followed by staining with a secondary goat anti-mouse antibody conjugated to Alexafluor488 (Thermo Scientific). The nuclei of cells were stained with Hoechst 33342 (Life Technologies). Images were taken on a Zeiss LSM 510 Confocal Microscope. Colocalization analysis of

the Pearson's coefficient between LAMP1 and each V5-tagged protein was completed using ImageJ (Schindelin et al., 2012).

Table 1. Primer sequences for amplification of duck IFITMs

Gene	Primer	Primer Sequence (5'→3')
<i>IFITM1</i>	Forward	GCCGCTAGCATGGAGAACTACCCGCAGTC
	Reverse	CGCGCGGCCCGCTTAGGGGTGGTGTACTGGTC
	Forward V5	GCCGCTAGCATGGGCAAGCCCATCCCCAACCCCTTGCTTGGCTTGGACTCCACC GAGAACTACCCGCAGTC
<i>IFITM2</i>	Forward	GCCGCTAGCATGAAGCCCCAGCGGGAGGAG
	Reverse	CGCGCGGCCCGCTCAGGTGATGACAGCCACGAAGAC
	Forward V5	GCCGCTAGCATGGGCAAGCCCATCCCCAACCCCTTGCTTGGCTTGGACTCCACC AAGCCCCAGCGGGAGGAG
<i>IFITM3</i>	Forward	GCCGCTAGCATGGAGCGGACCCGAGCTCC
	Reverse	CGCGCGGCCCGCTATGTGGGGCCGTAGAAGG
	Forward V5	GCCGCTAGCATGGGCAAGCCCATCCCCAACCCCTTGCTTGGCTTGGACTCCACC GAGCGGACCCGAGCTCC
<i>IFITM5</i>	Forward	GCCGCTAGCATGGACACGTCCTACCCCGG
	Reverse	CGCGCGGCCCGCTTCACTTGTCTCATCGTCG
	Forward V5	GCCGCTAGCATGGGCAAGCCCATCCCCAACCCCTTGCTTGGCTTGGACTCCACC GACACGTCCTACCCCGG

Table 2. Primer sequences for sequencing of duck IFITMs

Vector	Primer	Primer Sequence (5'→3')
pCR2.1-TOPO	M13F-20	GTAAAACGACGGCCAG
	M13R	CAGGAAACAGCTATGAC
pcDNA3.1/Hygro+	T7-pgem	TAATACGACTCACTATAGGG
	BGHR	TAGAAGGCACAGTCGAGG

Table 3. Primer and probe sequences for qPCR analysis of duck IFITM gene expression

Gene	Element	Primer or probe Sequence (5'→3')
<i>GAPDH</i>	Forward Primer	AAATTGTCAGCAATGCCTCTTG
	Reverse Primer	TGGCATGGACAGTGGTCATAA
	Probe	/56-FAM/ACCACCAAC/ZEN/TGCCTGGCGCC/3IABkFQ/
<i>IFITM1</i>	Forward Primer	CTTTGTGCTCTGGTCTTTC
	Reverse Primer	GTTCCGCCAGTGCCTATC
	Probe	/56-FAM/TCTGCTTCC/ZEN/CCGCGCTCAT/3IABkFQ/
<i>IFITM2</i>	Forward Primer	TTCAACGTCCTGATCGGTTAC
	Reverse Primer	GATGTTCAACACCTTGGCC
	Probe	/56-FAM/TCTGCTTCC/ZEN/CCGCGCTCAT/3IABkFQ/
<i>IFITM3</i>	Forward Primer	CACCGCCAAGTACCTGAACA
	Reverse Primer	CGATCAGGGCGATGATGAG
	Probe	/56-FAM/CACGGCCCT/ZEN/GCTGCTCAACATCT/3IABkFQ/
<i>IFITM5</i>	Forward Primer	TCCACCTCTCCAAGCTC
	Reverse Primer	GCTTGTGTTGAACTGGTAG
	Probe	/56-FAM/CCAGGACTC/ZEN/CGTGGCCTTTTCA/3IABkFQ/

Table 4. Primer sequences for generation of chimeric IFITM and mutant dIFITM3 proteins

Primer	Primer Sequence (5'→3')
O.E.IFITM1.rv.3CD225	GAAGAAAGACCAGAGCACGTGGTCGCGGG
O.E.IFITM3.rv.1CD225	GCACAGCGACCAAGCCAGAAAGTCCTTGGGTGGC
O.E.IFITM1.fw.3NTD	CCGCCACCCAAGGACTTTCTGGCTTGGTCGCTGTGC
O.E.IFITM3.fw.1NTD	GCTCCCCCCCCGCGACCACGTGCTCTGGTCTTTCTTCAACG
IFITM3-Y14F.fw	TCGCGCTGCCACCCCTTCGAGCCTCTGGTGGAGGGTTTGGACATGG
IFITM3-Y14F.rv	CCACCAGAGGCTCGAAGGGTGGCAGCGGAGTCCCGGAGCTC
IFITM3-Y56F.fw	CTGTGCTCCACGCTGTTTCAGCAATGTCTGCTGCCTCGGCTTCC
IFITM3-Y56F.rv	AGACATTGCTGAACAGCGTGGAGCACAGCGACCAAGCCAGG
IFITM3-Y82F.fw	GTCCTCGGCGACTTCAGCGGGGCGCTCAGCTACGGCTC
IFITM3-Y82F.rv	CGCCCCGCTGAAGTCGCCGAGGACTTTGCGATCCCTGG
IFITM3-Y94F.fw	CTCCACCGCCAAGTTCCTGAACATCACGGCCCTGCTGCTC
IFITM3-Y94F.rv	CGTGATGTTTCAGGAACTTGGCGGTGGAGCCGTAGCTGAGC

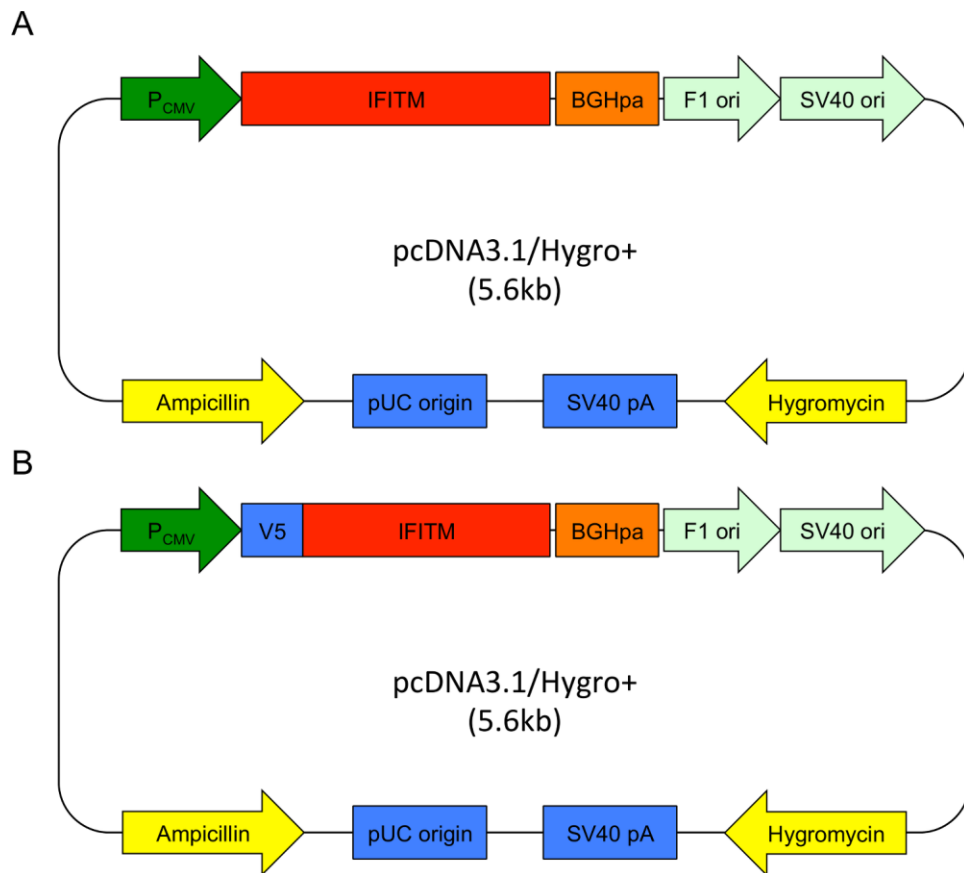


Figure 3. Vector map of pcDNA3.1/Hygro+ with duck IFITM and N-terminal V5 epitope tagged duck IFITM inserts. Non-tagged (A) and V5 epitope tagged (B) IFITM1, -2, -3, and -5 were directionally cloned into pcDNA3.1/Hygro+ using NheI and NotI restriction sites.

Chapter 3. Results

3.1 Characterization of the duck IFITM repertoire

Previously, using subtractive suppressive hybridization a duck IFITM gene was identified as an innate immune gene expressed early in duck lung tissue in response to infection with highly pathogenic influenza A virus (Vandervan et al., 2012). The potential involvement of IFITMs in duck lung tissue in the response to IAV led me to characterize the duck *IFITM* gene repertoire. Analysis of the putative duck *IFITM* locus on scaffold 2493 revealed two predicted *IFITM* genes and the two flanking genes, *B4GALNT4* and *ATHL1*. Using gene synteny from the chicken *IFITM* locus (Smith et al., 2013), and transcripts from RNAseq (Huang et al., 2013) I identified the corresponding duck homologues *dIFITM5*, *dIFITM2*, *dIFITM1*, and *dIFITM3* (Fig. 4). A partial transcript for *dIFITM10* was also identified, but due to its absence from the *IFITM* locus and predicted non-immune function it was not included for further analysis. *dIFITM1*, *dIFITM2*, *dIFITM3*, and *dIFITM5* are all encoded by two exons and contain a CD225 domain, which is characteristic of *IFITM* genes. Transcripts corresponding to each gene were amplified from cDNA and amino acid sequences aligned with their avian and mammalian homologues (Fig. 5A). The immune related duck IFITMs, *dIFITM1*, *dIFITM2* and *dIFITM3*, have 41%, 68% and 76% amino acid identity with the chicken orthologs respectively, whereas the predicted non-immune *dIFITM5* has 91% identity.

Significant divergence between avian and human IFITM1 and IFITM2 suggests they may not be direct orthologs, while avian and human IFITM3 and IFITM5 share critical residues and greater conservation. Duck and chicken *IFITM2* are missing an N-

terminal YXX θ endocytosis motif in the N-terminal domain that is present in human and mouse *IFITM2*. Although this YXX θ motif has not been experimentally shown to function in *IFITM2*, it is functional in *IFITM3* and important for endocytic localization. Phylogenetic analysis of the relationship between duck, chicken, human, and mouse *IFITM* proteins reveals that duck *IFITMs* group most closely to their respective chicken orthologs (Fig. 5B). The orthology to human genes is uncertain because the mammalian *IFITM1*, -2 and -3 homologues segregate to the same clade. Furthermore, the murine and human *IFITM1* and *IFITM2* genes are in different transcriptional orientation compared to duck or chicken (Smith et al., 2013; Zhang et al., 2012). Therefore, I have identified four duck *IFITM* genes in the same order and orientation as the chicken orthologs. Duck *IFITM1* has a unique insertion in exon 1, not seen in chicken *IFITM1*. The presence of this element was confirmed in multiple PCRs and in more than one animal (Fig. 6). The CD225 domain is the most highly conserved region of *IFITMs* as the CD225 domain of d*IFITM3* has 96% and 63% identity with the CD225 of chicken and human *IFITM3* respectively. Additionally, residues shown to be important for antiviral function of human *IFITM3* orthologs are conserved in ducks, including Y20, C72, and Y99 (John et al., 2013).

3.2 Duck *IFITMs* are upregulated in response to influenza A virus infection

Previously, analysis of the duck transcriptome showed transcripts of *IFITM3*, *IFITM5*, and *IFITM10* were increased in duck lung tissue after infection with two different H5N1 strains (A/duck/Hubei/49/05) and A/goose/Hubei/65/05 (Huang et al., 2013). To determine the extent of upregulation of each duck *IFITMs* in response to

infection with IAV, I examined their relative expression using qPCR on cDNA from lung tissue from ducks treated with PBS (mock), or infected with low pathogenic avian H5N2 strain A/British Columbia 500/05 (BC500), or highly pathogenic H5N1 strain A/Vietnam1203/04 (VN1203) (Fig. 7). *dIFITM1* was massively upregulated 370-fold at 1 dpi and remained upregulated 406-fold at 3 dpi with VN1203 (Fig. 7A). *dIFITM1* also was upregulated 43-fold and 11-fold at 1 dpi and 3 dpi with BC500, respectively (Fig. 7A). In contrast, *dIFITM2* and *dIFITM3* were upregulated at 1 dpi with VN1203 24-fold and 28-fold, respectively. Expression of both *dIFITM2* and *dIFITM3* were only modestly upregulated 4-fold at 3 dpi with VN1203 and 2-fold and 3-fold at 1dpi with BC500, respectively (Fig. 7B and C). Interestingly, *dIFITM5*, which has been characterized as a bone-specific gene in mammalian species, was upregulated 5-fold 1dpi with VN1203 (Fig. 7D).

Expression of duck IFITM1, IFITM3 and IFITM5 was also examined in intestinal tissue one day post infection with BC500. I observed upregulation of *dIFITM1* approximately 2-fold, and no upregulation of *dIFITM3*, and *dIFITM5* in intestinal tissue at 1 dpi with BC500 (Fig. 8A, B, and C). I noted higher basal expression of *dIFITM1* in intestine than in lung from mock-infected animals, as previously observed in chicken (Smith et al., 2013). Thus, expression of *IFITM1*, *IFITM2* and *IFITM3* were upregulated in the lung, site of infection with the highly pathogenic VN1203, but only *IFITM1* was upregulated in the intestine, the replication site for low pathogenic strain BC500.

VN1203 replicates efficiently in duck lung tissue, whereas BC500 replicates primarily in intestinal tissue. Tracheal swabs from VN1203 infected ducks were of 10^2 to 10^4 EID₅₀ and cloacal swabs from BC500 infected ducks ranged from 10^5 to 10^7 EID₅₀ (Vanderven et al., 2012). Tracheal swabs were negative for BC500 infected ducks, and cloacal swabs were negative for VN1203 infected ducks. Despite replication of BC500 to higher titres in intestinal tissue in comparison to VN1203 in lung tissue, there is dramatic upregulation of *dIFITMs* in lung tissue, and only slight upregulation of *dIFITM1* in intestinal tissue. This trend is also observed with other ISGs including *ISG12* and *IFIT* (Vanderven et al., 2012).

Specificity of *IFITM1*, *IFITM3* and *IFITM5* qPCR probe and primer sets were validated by running qPCR reactions with *IFITM1*, *IFITM3* and *IFITM5* in pcDNA3.1/Hygro as template. Amplification of each respective *IFITM* gene only occurred when the appropriate probe and primer set was present (Fig. 9). This experiment did not include *IFITM2*, as the presence of this gene was not get identified in the duck *IFITM* locus, but the qPCR probe and primer set is expected to be specific to *IFITM2*, as there is no identical regions in either the primers or probe in *IFITM1*, *IFITM3*, or *IFITM5*.

3.3 Duck *IFITM3* restricts influenza A viruses

Given the antiviral function of orthologous *IFITMs* I examined whether duck *IFITMs* could inhibit IAV replication in DF-1 cells. I performed an initial screen of the antiviral properties of three duck *IFITMs* using transient transfection of constructs

expressing N-terminal V5 tagged IFITM proteins in DF-1 chicken embryonic fibroblast cells. Due to availability of IAV strains in our laboratory, IAV challenge assays were limited to use of H6N2, H11N9, and PR8 (H1N1). DF-1 cells were used as they are easily cultured, and are susceptible to infection with IAV. I challenged DF-1 cells overexpressing dIFITMs with either H6N2 or H11N9 at an MOI=1 or MOI=5, and counted the percentage of infected cells expressing influenza NP protein by high content fluorescent microscopy. Overexpression of dIFITM3 reduced the percentage of H6N2 infected cells by 44% at an MOI=1 and by 38.6% at an MOI=5 in comparison to vector only transfected DF-1 cells (Fig. 10A). A similar restriction of H11N9 by dIFITM3 was seen with a 30% and 36% reduction at an MOI=1 and MOI=5 respectively (Fig. 10B). Additionally, to examine whether dIFITM1 and dIFITM3 could co-operate in restriction of IAV, I co-expressed both proteins in DF-1 cells. Co-expression of dIFITM1 and dIFITM3 resulted in a similar restriction of both H6N2 and H11N9 as dIFITM3 alone (Fig. 10A and B). No reduction in the percentage of infected cells was observed with DF-1 cells transfected with dIFITM1 or dIFITM5 despite high expression levels in comparison to vector only (Fig. 10C). The restriction is obvious in the background of DF-1 cells, which express chicken IFITM3 (Smith et al., 2013). Both epitope-tagged and untagged versions of each dIFITM had similar viral restriction capability, with untagged IFITM3 reducing the % infection of H6N2 and H11N9 in DF-1 cells by 33.6% and 44% at an MOI=1, respectively (Fig. 11). Transfection efficiency for each construct was approximately 60% (Fig. 12). Infection of DF-1 cells was optimized by infecting DF-1 cells with H6N2 at an MOI=1, 5, and 10, and determining the percentage of infected cells as previously described (Fig. 13)

3.4 Duck IFITMs localize to distinct cellular compartments

To determine which of the duck IFITMs were expressed in the endosomal compartment, I examined the colocalization of each of the duck IFITM proteins with LAMP1, a late endosomal marker. DF-1 cells expressing the different V5 tagged dIFITM proteins were stained with anti-V5 and anti-LAMP1 antibodies to examine colocalization using confocal microscopy (Fig. 14). Similar to mammalian IFITM1, dIFITM1 was present at the cell surface. dIFITM2 co-localizes partially with LAMP1 containing lysosomes, but presumably resides in earlier endocytic compartments. dIFITM3 has strong colocalization with endocytic compartments containing LAMP1, consistent with its ability to restrict IAV and previous reports of mammalian and chicken IFITM3 localization. Interestingly, dIFITM5 also colocalizes partially with LAMP1 containing compartments. Thus, IFITM1 localizes to the cell membrane, while IFITM3 is expressed in the endosome, like their mammalian counterparts.

3.5 Duck IFITM3 inhibits influenza, but does not inhibit vesicular stomatitis virus

As a general trend, I observed DF-1 cells transiently transfected with exogenous DNA have a lower percentage of IAV infected cells than non-transfected DF-1 cells. To further, and more accurately, examine the antiviral properties of duck IFITMs, I generated DF-1 clones stably expressing V5 tagged duck IFITMs and challenged them with avian or mammalian viruses and determined the percentage of infected cells by high content fluorescent microscopy or flow cytometry. Two different methods of quantification were used to confirm the results. Generation of stable cell lines expressing

IFITM2, and to a lesser extent IFITM1, at a high level was not achievable. Isolation of multiple clones of IFITM1 from an unsorted stably expressing population consistently produced low level expressing clones. Generation of stably expressing cells was also completed with both linearized and intact circular plasmid DNA, with no significant difference detected in the expression of cell lines generated between linearized or circular plasmid DNA (Fig. 15).

DF1-dIFITM3 cells had 47% fewer H6N2 infected cells, while there was no reduction in the percentage of H6N2 infected DF-1 cells stably overexpressing dIFITM1, dIFITM2, or dIFITM5 (Fig. 16A). Additionally, there was no reduction in the percentage of VSV-GFP infected cells when any of the dIFITMs were overexpressed (Fig. 16B). Instead I noted a slight increase in the percentage of infected cells upon overexpression of each dIFITM. To further examine the range of IAV strains restricted by dIFITM3, I challenged DF1-dIFITM3 or vector-only cells with H6N2 and H11N9, PR8, and VSV at an MOI=1. H6N2 and H11N9 are of avian origin, whereas PR8 is an IAV of mammalian origin. DF1-dIFITM3 cells had reduced percentages of H6N2, H11N9, and PR8 infected cells by 62%, 59%, and 57% respectively than vector only cells (Fig. 16C). I confirmed the decrease in percentage of H6N2 infected DF1-dIFITM3 cells also corresponded to a decrease in viral titer by plaque assay (Fig. 16D). All stable clones expressed IFITM proteins, albeit expression of IFITM2 was low (Fig. 16E). Therefore, duck IFITM3 restricts entry of the three influenza strains tested, including avian strains, but does not restrict VSV viral replication.

3.6 The N-terminal domain of dIFITM3 is not essential for antiviral activity or endosomal localization

In domain swapping experiments a chimera of human IFITM3 containing the N-terminal domain of IFITM1 loses association with endosomal compartments and loses its ability to restrict the IAV (John et al., 2013). The N-terminal domain of human IFITM3 is sufficient to cause localization of human IFITM1 to endocytic compartments but does not result in increased antiviral activity (John et al., 2013). To explore whether the N-terminal domain of dIFITM3 functions similarly to the human ortholog, I generated two chimeric proteins to swap the N-terminal domain of dIFITM1 and dIFITM3 and subsequently generated stably expressing DF-1 clones of each chimera (Fig. 17A). DF-1 clones stably expressing dIFITMs or the chimeric proteins were challenged with H6N2 or VSV at an MOI=1. In contrast to the human chimera, DF-1 cells stably expressing the dIFITM3 chimera containing the N-terminal domain of dIFITM1 (1NTD-3CD225) retained an ability to restrict IAV, and reduced the percentage of H6N2 infected cells by 61% (Fig. 17B). This restriction is comparable to the reduction observed in DF1-dIFITM3 cells. Similar to DF1-dIFITM3 cells, this chimeric protein does not reduce the percentage of VSV infected cells (Fig. 17C). In fact, there was an observed increase in the percentage of VSV infected cells that is comparable to the slight increase in DF1-dIFITM3 VSV infected cells (Fig. 17C). The dIFITM1 chimera containing the N-terminal domain of dIFITM3 (3NTD-1CD225) gained significant antiviral function, and reduces the percentage of H6N2 infected cells by 41%, but does not restrict VSV (Fig. 17B and C). Each protein was expressed at high levels (Fig. 17D). In addition, changing the N-terminal domain of dIFITM3 to that of dIFITM1 results in a partial loss of co-

localization with LAMP1 containing endosomes (Fig. 17E). This is in contrast with a similar human chimera, which dramatically loses association with endosomes, and resembles the staining pattern of IFITM1 (John et al., 2013). Furthermore, the dIFITM1 chimera containing the N-terminal domain of dIFITM3 results in an increased association with endosomes (Fig. 17E). I quantified the degree of localization of each duck IFITM protein or chimeric protein with LAMP1. Neither dIFITM1 nor dIFITM2 displayed significant co-localization with LAMP1, whereas dIFITM3 and dIFITM5 had significant co-localization with LAMP1 (Fig 17F). Replacing the N-terminal domain of dIFITM3 with dIFITM1 resulted in decreased association with LAMP1, but not a complete loss of association analogous to dIFITM1 (Fig 17F). Exchanging the N-terminal domain of dIFITM1 with dIFITM3 increased the association with LAMP1 containing compartments, but this association was not as strong as wild type dIFITM3 (Fig 17F). Therefore, the N-terminal domain of IFITM3 is not essential for localization to endosomes, yet can confer endosomal localization and antiviral activity on IFITM1.

3.7 N-terminal YXX θ endocytic signal sequence of dIFITM3 is not essential for correct cellular localization

The lack of complete mislocalization of the duck IFITM3 chimera containing the N-terminal domain of dIFITM1 away from endosomes led me to further investigate the residues required for dIFITM3 function. Previously, a YXX θ endocytic signal sequence was identified in the N-terminal domain of IFITM3 that is required for correct cellular localization and antiviral function (Jia et al., 2014). Mutation of the critical tyrosine within this residue is sufficient to achieve loss of association with endosomes, and loss of

antiviral function. To explore whether this conserved sequence was necessary for dIFITM3 function, and if other YXX θ motifs were functional within the protein, I mutated four residues of dIFITM3 that appeared to be in YXX θ endocytosis signal sequences (Fig. 18A), and subsequently generated stably expressing DF1 clones of each mutant. All four mutants co-localized strongly with LAMP1 containing endosomes (Fig. 18B). Duck Y14 is equivalent to human and mouse Y20. dIFITM3-Y14F does not co-localize as strongly as wild-type dIFITM3, however there is not the dramatic re-localization of IFITM3 to the cell surface as is seen with mammalian IFITM3 (Jia et al., 2014). Quantification of the co-localization of dIFITM3 or mutant proteins with LAMP1 was completed. Only the Y14F mutant shows a slight decrease in co-localization compared with wild type dIFITM3 (Fig 18C). Of the four dIFITM3 point mutants generated, only Y56F showed a decreased capacity to restrict IAV (Fig 18D). However, given its endosomal location, it is unclear if this is due to reduced function or lower expression level in comparison to the others (Fig 18E). Collectively, these results suggest dIFITM3 has critical residues outside of the N-terminal domain that are required for correct cellular localization and antiviral function.

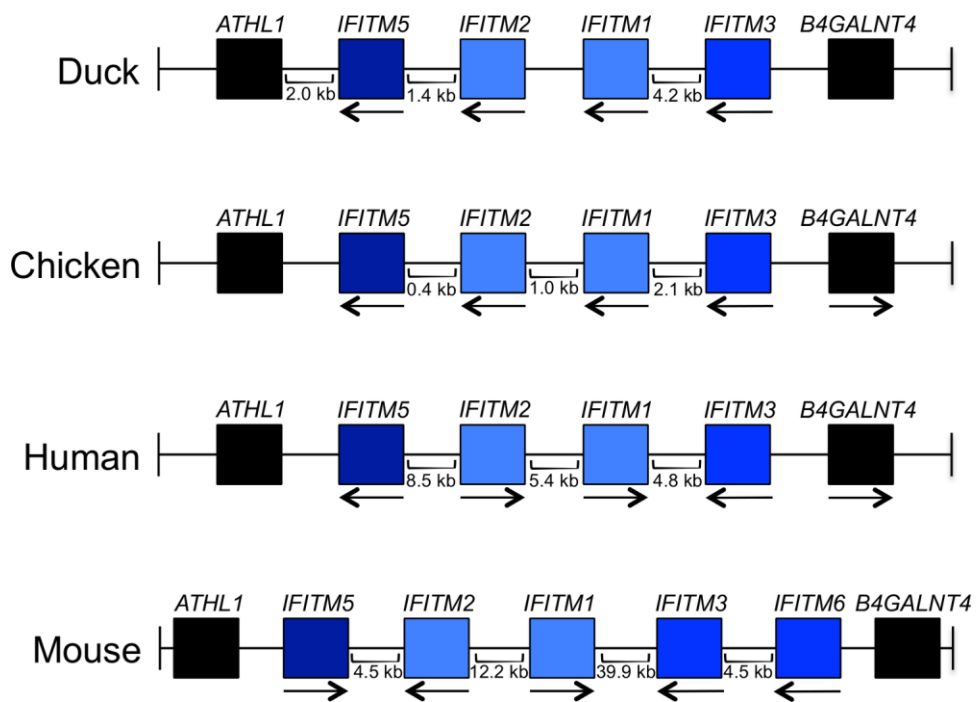


Figure 4. Organization of IFITM locus in duck, chicken, human and mouse. Flanking genes *ATHL1* and *B4GALNT4* are shown with each *IFITM* gene. Direction of transcription is shown with distance between genes shown when possible.

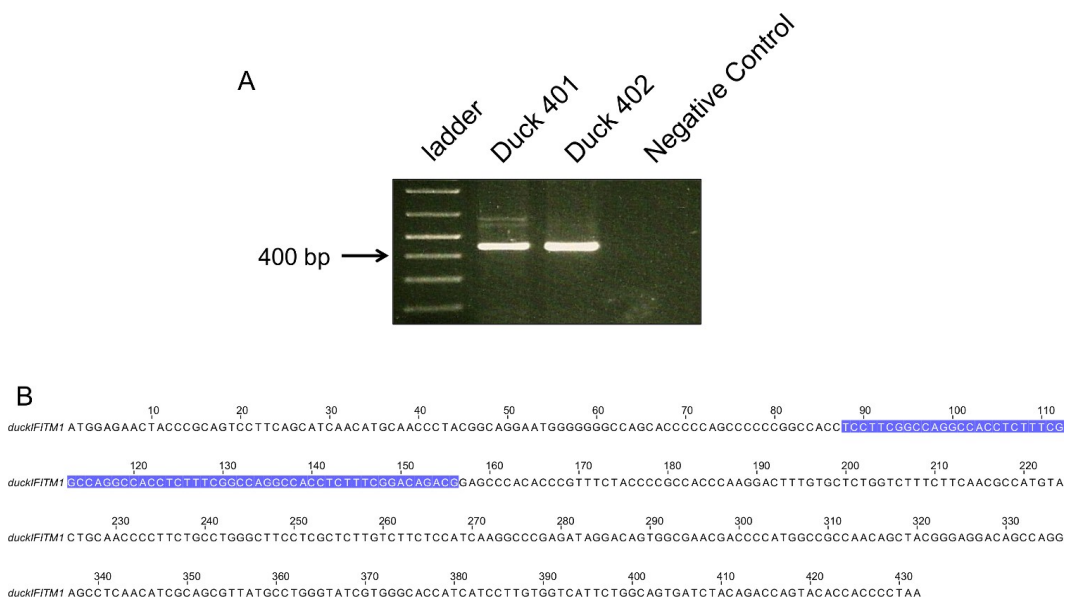


Figure 6. The N-terminal repetitive region of IFITM1 is present in two individual ducks. PCR amplification of duck IFITM1 was performed on cDNA from two different ducks (A). Amplification bands of 432 bp indicate the presence of the N-terminal repetitive region. Absence of the repetitive region in the N-terminal region of duck IFITM1 would yield a PCR product of 363 bp. Nucleotide sequence of duck IFITM1 is shown with the repetitive element shaded (B).

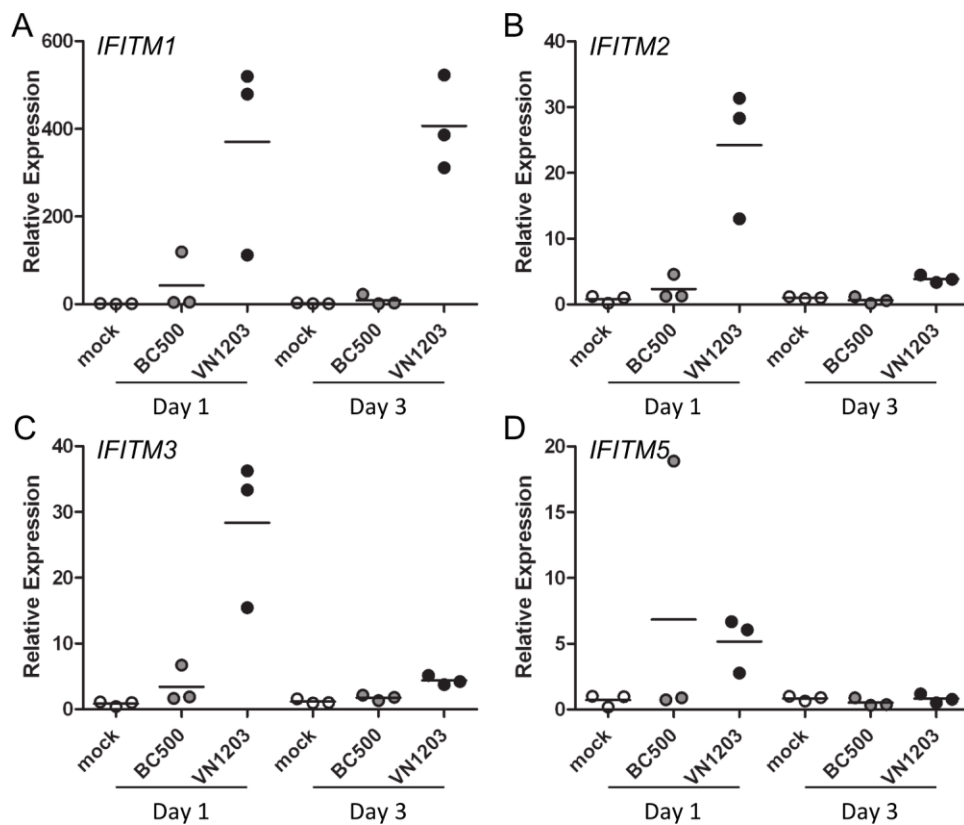


Figure 7. Duck IFITMs are upregulated in lung tissue in response to highly pathogenic IAV infection. Total RNA was isolated from duck lung tissue 1 dpi and 3 dpi with PBS (mock), BC500 (low pathogenic IAV) or VN1203 (highly pathogenic IAV). IFITM1 (A), IFITM2 (B), IFITM3 (C), and IFITM5 (D) expression was measured using qPCR compared with the mock infected group.

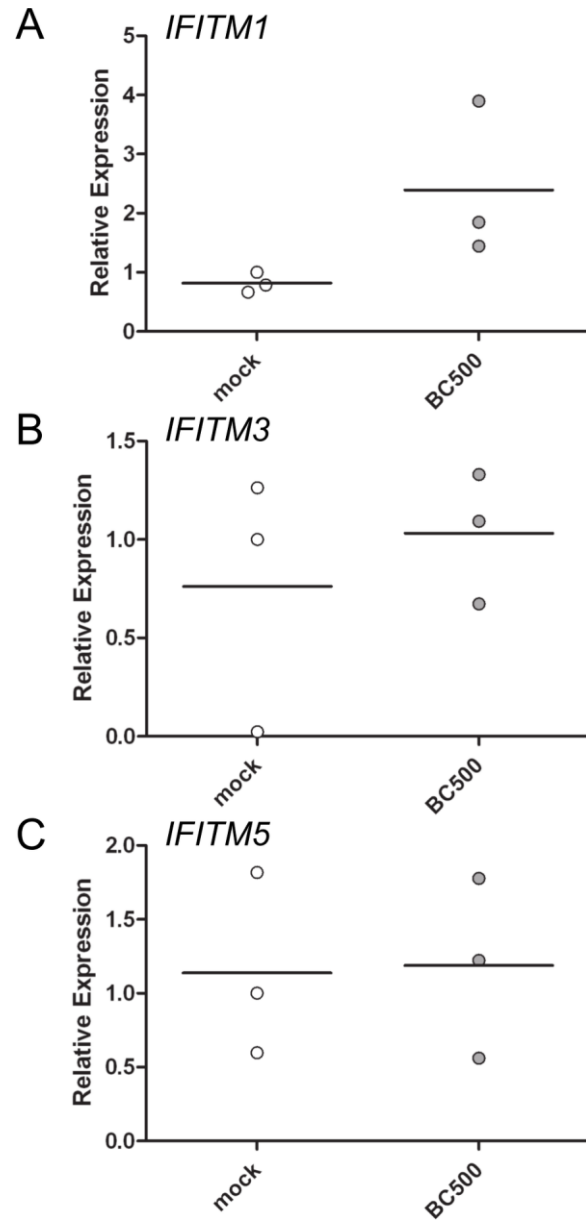


Figure 8. Duck IFITM1 is upregulated in intestinal tissue in response to low pathogenic IAV infection. Total RNA was isolated from duck intestine tissue 1 dpi with PBS (mock), or BC500 (low pathogenic IAV). IFITM1 (A), IFITM3 (B), and IFITM5 (C) expression was measured using qPCR compared with the mock infected group.

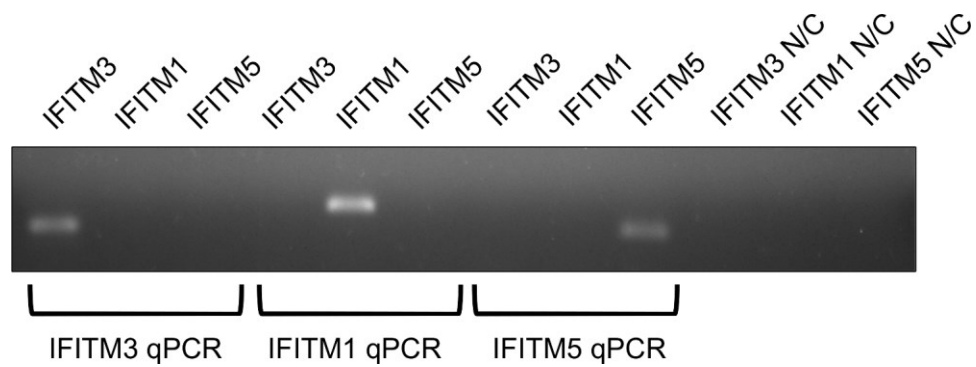


Figure 9. Duck IFITM qPCR probe and primers are specific to their respective IFITMs. PCR amplification of each duck IFITM was completed using qPCR probe and primer sets using purified duck IFITM1/3/5 in pcDNA3.1 as template. Amplification of each respective IFITM is only observed with the appropriate qPCR probe and primer set.

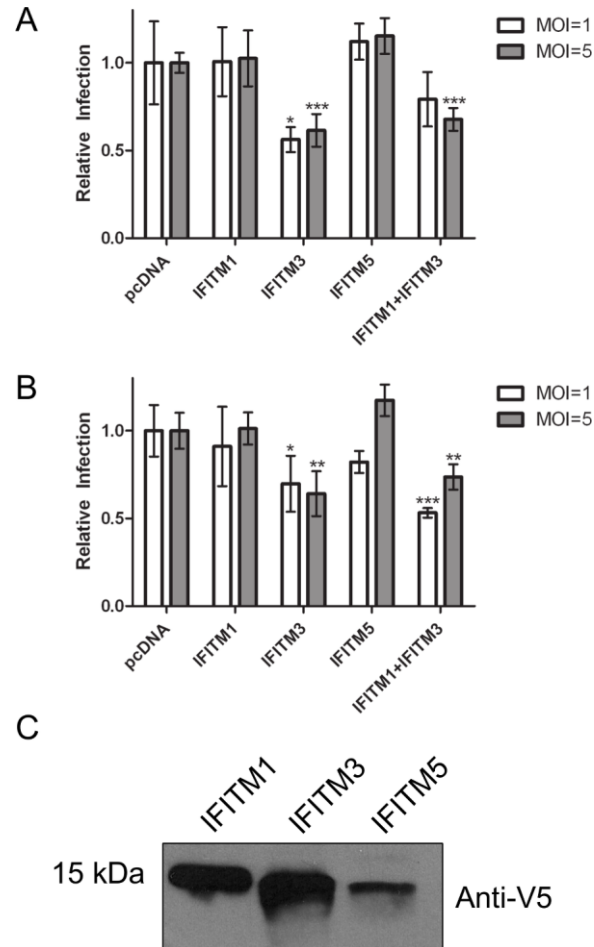


Figure 10. Duck IFITM3 restricts replication of low pathogenic IAV. DF-1 cells transiently overexpressing N-terminal V5 epitope tagged duck IFITMs or empty vector were challenged with H6N2 (A), or H11N9 (B) at an MOI=1 or MOI=5. Six hours after infection cells were fixed, stained for IAV nucleoprotein, and percentage of infected cells was determined. Percentage of infected cells is expressed relative to the vector control. Statistical significance in comparison to vector control cells was analyzed using an unpaired two-tailed Student's t-test (n=4 *, $P \leq 0.05$; **, $P \leq 0.01$; ***, $P \leq 0.001$). Expression level of each duck IFITM was determined by Western blot (C). Representative experiment of three replicates is shown.

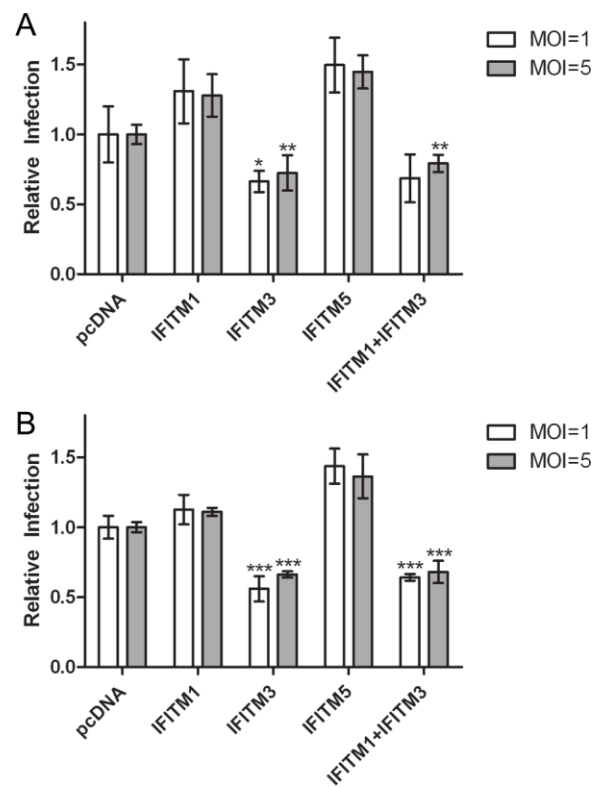


Figure 11. Non-epitope tagged duck IFITM3 restricts replication of low pathogenic IAV. DF-1 cells transiently overexpressing non-epitope tagged duck IFITMs or empty vector were challenged with H6N2 (A), or H11N9 (B) at an MOI=1 or MOI=5. Six hours after infection cells were fixed, stained for IAV nucleoprotein, and percentage of infected cells was determined. Percentage of infected cells is expressed relative to the vector control. Statistical significance in comparison to vector control cells was analyzed using an unpaired two-tailed Student's t-test (n=4, *, $P \leq 0.05$; **, $P \leq 0.01$; ***, $P \leq 0.001$). Representative experiment of three replicates is shown.

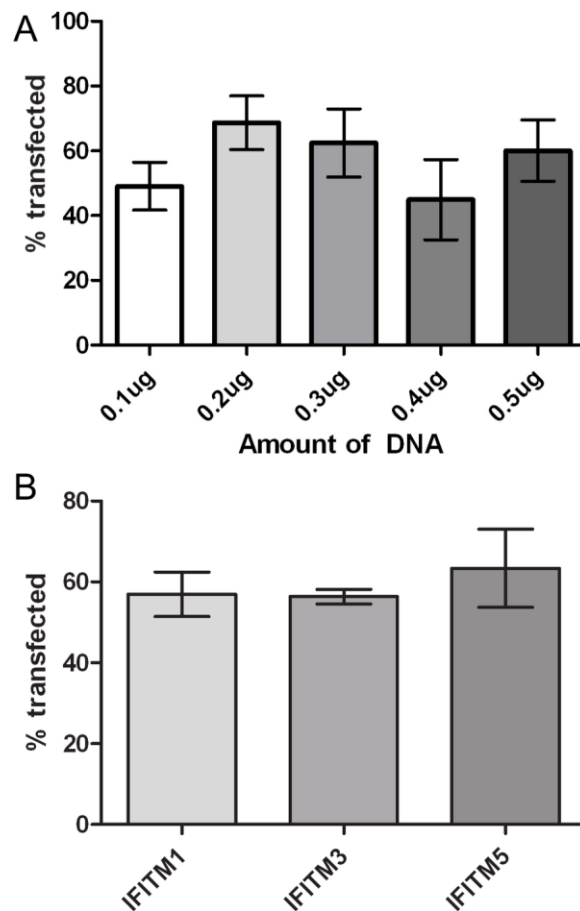


Figure 12. Optimization of transfection of duck IFITMs into DF-1 chicken fibroblast cells. Optimal amounts of DNA for transfection of DF-1 cells was determined using increasing concentration of pDsRED plasmid DNA with 0.5 μ L of lipofectamine in 96 well plates (A). Percent transfection was determined by counting cells expressing red fluorescent protein. Duck IFITMs have similar transfection efficiency (B). DF-1 cells were transfected with 0.2 μ g of V5 epitope tagged duck IFITMs, fixed, stained for V5 positive cells, and percentage of V5 positive cells determined.

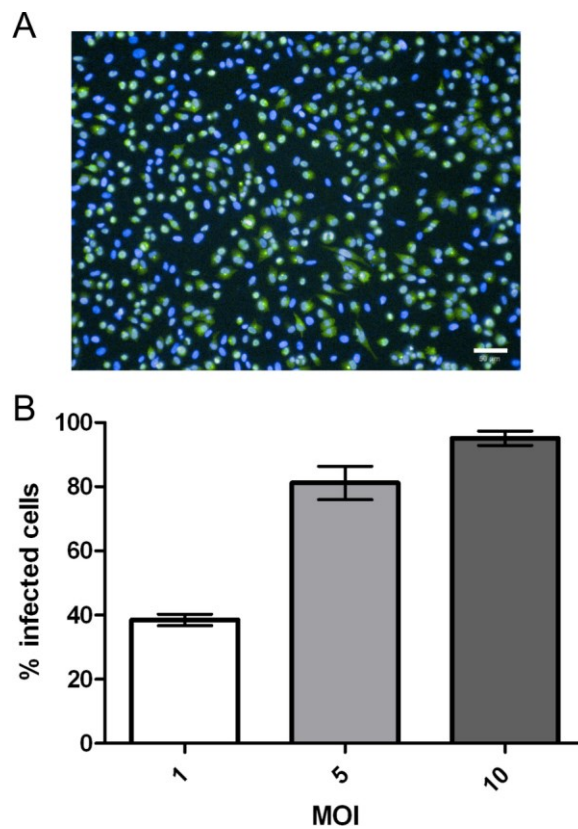


Figure 13. Optimization of IAV infection in DF-1 chicken fibroblast cells. DF-1 cells were infected with H6N2 at an MOI=1. Six hours post infection cells were fixed and stained with anti-nucleoprotein-FITC antibody (green) and Hoechst 33342 (blue) (A). Scale bar indicated 50 μ M. DF-1 cells were infected with H6N2 at various MOIs, and percentage of infected cells determined by counting the percentage of nucleoprotein positive cells (B).

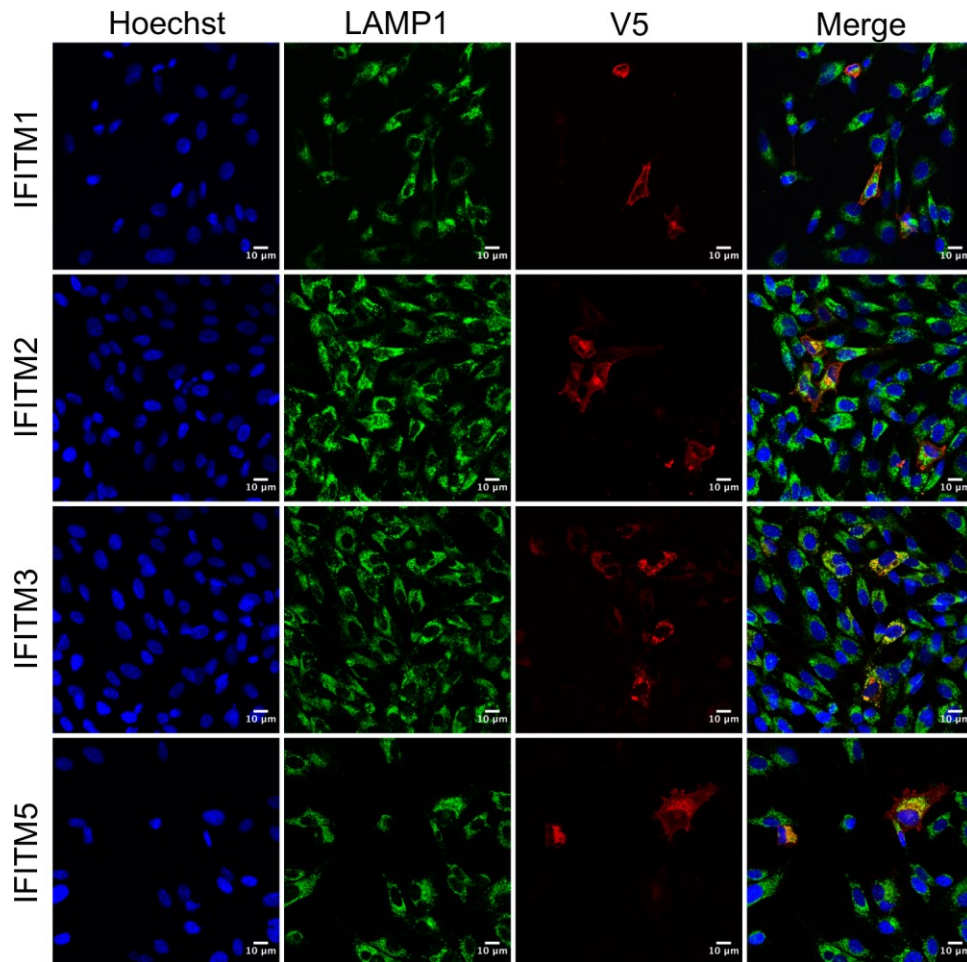


Figure 14. Duck IFITMs localize to different cellular compartments. DF-1 cells overexpressing dIFITM1, dIFITM2, dIFITM3, or dIFITM5 were fixed, stained, and imaged using confocal microscopy. Panels show staining for nuclei using Hoechst 33324 (blue), LAMP1 containing endosomes (green), V5-epitope tagged dIFITM (red), and a merged image.

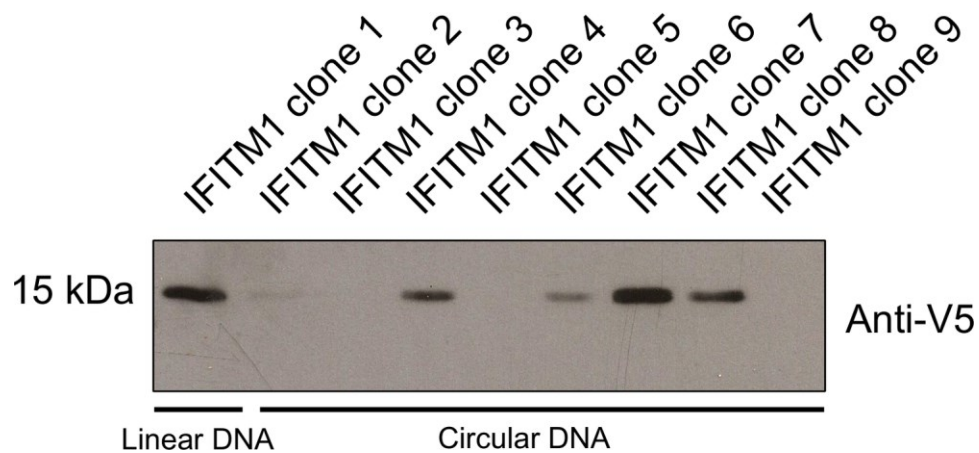


Figure 15. Generation of DF-1 cells stably overexpressing duck IFITM1. DF-1 cells were transfected with either linear or circular duck IFITM1 cloned into pcDNA3.1/Hygro. Stably expressing cells were selected using hygromycin, and individual clones isolated and expanded. Expression levels of each clone was determined by Western blot.

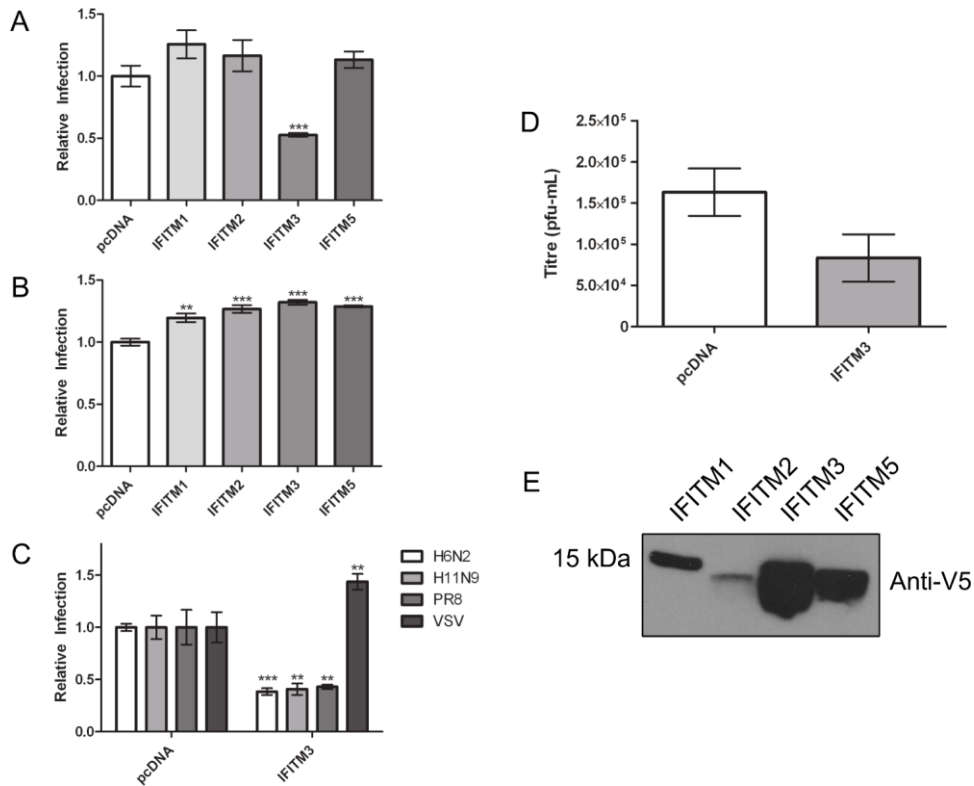


Figure 16. Duck IFITM3 restricts low pathogenic IAV, but not VSV. DF-1 cells stably expressing all dIFITMs were challenged with H6N2 (A) or VSV (B) at an MOI=1. DF-1 cells expressing dIFITM3 were challenged with H6N2, H11N9, PR8, or VSV at an MOI=1 (C). Percentage of infected cells was determined using fluorescent microscopy (A) or flow cytometry (B and C). Statistical significance in comparison to vector control cells was analyzed using an unpaired two-tailed Student's t-test ($n \geq 3$, *, $P \leq 0.05$; **, $P \leq 0.01$; ***, $P \leq 0.001$). Supernatants of DF-1 cells stably expressing empty vector or dIFITM3 were collected 12 hours post infection with H6N2 and viral titre was determined using plaque assay (D). Level of dIFITM protein expression of each stably expressing DF-1 cell line was determined by Western blot (E). Representative experiment of three replicates is shown.

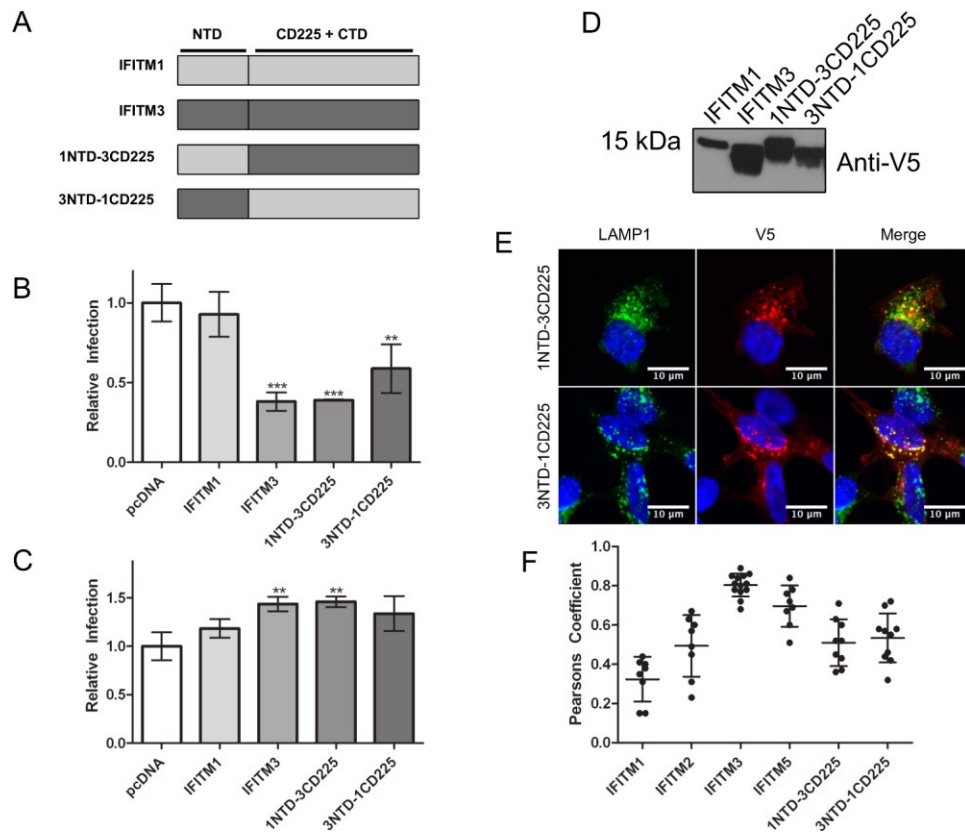


Figure 17. The N-terminal domain of dIFITM3 is not necessary for antiviral activity. Chimeric proteins of dIFITM1 and dIFITM3 were generated (A). DF-1 cells stably overexpressing dIFITM1, dIFITM3, or the chimeric proteins were challenged with H6N2 (B) or VSV (C) at an MOI=1, and percentage of infected cells determined relative to empty vector transduced cells using fluorescent microscopy (B) or flow cytometry (C). Statistical significance in comparison to vector control cells was analyzed using an unpaired two-tailed Student's t-test ($n \geq 3$, *, $P \leq 0.05$; **, $P \leq 0.01$; ***, $P \leq 0.001$). Expression of each dIFITM or mutant protein was determined using Western blot (D). Confocal microscopy images of DF1 cells overexpressing 1NTD-3CD225 and 3NTD-1CD225 stained for nuclei (blue), LAMP1 (green) or chimeric protein (red) with a merged image shown (E). Representative experiment of three replicates is shown. Colocalization of each dIFITM or chimeric protein with LAMP1 was completed using the Pearson's correlation coefficient (F). Bars show mean value of at least 8 analyzed cells.

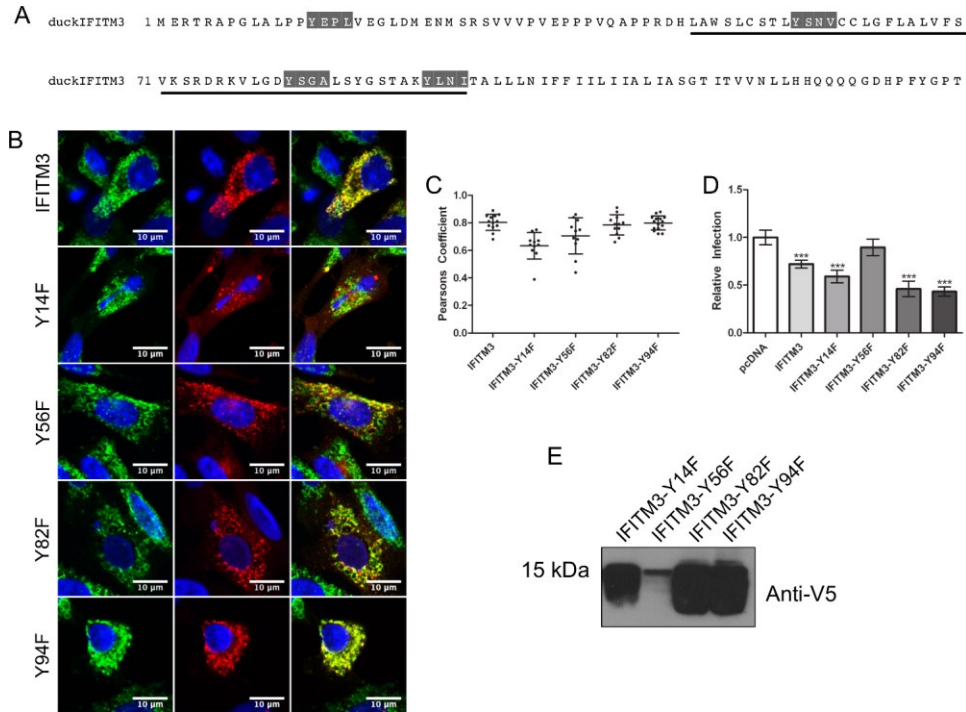


Figure 18. The N-terminal YXX θ endocytic signal sequence of dIFITM3 is not necessary for endosomal localization or antiviral activity. Amino acid sequence of duck IFITM3 with regions targeted for mutagenesis shown in shaded regions, and CD225 domain underlined (A). Confocal microscopy images of DF-1 cells overexpressing IFITM3, IFITM3-Y14F, IFITM3-Y56F, IFITM3-Y82F or IFITM3-Y94F (B). Cells were stained for nuclei (blue), LAMP1 (green) or dIFITM3 protein or mutant protein (red) with a merged image shown. Colocalization analysis of dIFITM3 or mutant protein with LAMP1 was completed using the Pearson's correlation coefficient (C). Bars show mean value of at least 8 analyzed cells. DF-1 cells stably expressing dIFITM3 or point mutants were challenged with H6N2 at an MOI=1 and percentage of infected cells was determined relative to vector only transduced cells by fluorescent microscopy (D). Statistical significance in comparison to vector control cells was analyzed using an unpaired two-tailed Student's t-test ($n \geq 3$, *, $P \leq 0.05$; **, $P \leq 0.01$; ***, $P \leq 0.001$). Level of dIFITM3 protein expression of each stably expressing DF-1 cell line was determined by Western blot (E). Representative experiment of three replicates is shown.

Chapter 4. Discussion

IFITMs have received recent attention for their ability to restrict the replication of a broad range of viruses. Here, I have functionally characterized the duck IFITM gene family and investigated their upregulation in response to influenza. I cloned and expressed each IFITM, and show IFITM3 localizes to endosomes and has antiviral function against influenza viruses, including two avian strains and one mammalian strain. I provide evidence of different signals for endosomal localization of duck IFITM3 than that of mammalian IFITM3. Where mammalian IFITM3 contains an N-terminal endocytic signal sequence that is indispensable for correct cellular localization and antiviral function (Jia et al., 2014), domain swapping or mutation of the N-terminal YXX θ motif of duck IFITM3 does not significantly alter endosomal localization or antiviral function. Nonetheless, the N-terminal domain of IFITM3 is sufficient to localize IFITM1 to the endosomal compartment, where it then gains antiviral activity against influenza.

4.1 Ducks possess a conserved IFITM locus

I used gene synteny and the recently characterized chicken IFITM locus (Smith et al., 2013) in my annotation of the duck IFITM locus, with genes in the order *IFITM5*, *IFITM2*, *IFITM1*, *IFITM3* between flanking genes *ATHL1* and *B4GALNT4*. In a phylogenetic tree, duck IFITMs segregate most closely with their chicken orthologs. Interestingly, duck and chicken *IFITM2* most closely segregate with *IFITM5*. This likely reflects the low sequence identity between orthologous IFITM proteins, in particular avian *IFITM2*. Low sequence identity and gene duplication events of immune-related

IFITMs make assignment of orthologous genes difficult. To reflect the gene synteny with chicken and the function demonstrated herein, I have re-named the previously identified duck *IFITM1* gene as *IFITM3* (Vandervan et al., 2012). There is low sequence identity between mammalian and avian IFITM orthologs, with the exception of IFITM5. The divergence of immune-related IFITMs may be due to selective pressure from viral pathogens specific to each species, whereas IFITM5 possesses a conserved non-immune role and is under less selective pressure. IFITM10 is located at a different locus than the immune-related IFITMs and IFITM5, and has unknown function.

Mammalian IFITM2 and IFITM3 contain an N-terminal YXX θ endocytosis motif. While this element is conserved in both chicken and duck IFITM3, it is absent in chicken and duck IFITM2. Other residues that are important for antiviral activity in human IFITM3 are conserved in duck IFITM3 such as Y20, C72, and F99 affirming the annotation of duck IFITM3. IFITMs have been functionally characterized in human (Brass et al., 2009), mouse (Huang et al., 2011), chicken (I.-C. Huang et al., 2011; Smith et al., 2013), swine (Xu et al., 2014) and flounder (Zhu et al., 2013), although characterization of IFITMs from swine and flounder also are ambiguous in the gene assignment, and it is uncertain if the characterization of orthologous IFITMs is correct. Functional characterization of IFITMs from other species will help determine if My assignment of IFITM nomenclature is correct, or requires recharacterization.

The presence of *IFITM5* transcripts and upregulation after viral infection is intriguing, given IFITM5 is a bone specific protein in mammals (Moffatt et al., 2008). In

fish and chicken, *IFITM5* transcripts are apparently absent in bone tissue, and highly abundant in other tissues (Hickford et al., 2012). The expression of *IFITM5* in non-bone tissue suggests a differential function for non-mammalian IFITM5. High sequence identity of orthologous IFITM5, and grouping of IFITM5 genes in phylogenetic analysis suggests that they have conserved function, however upregulation of duck *IFITM5* in response to viral infection suggests it may be involved in the innate immune response. Overexpression of murine IFITM5 in MC3T3 cells lead to increased expression of other known ISGs including *interferon inducible protein 1 (Irgm)*, and *interferon inducible with tetratricopeptide repeats 3 (ifit3)* (Hanagata and Li, 2011). However, IFITM5 expression was not induced by type-I IFN itself. Interestingly, microarray analysis of DF-1 cells expressing duck RIG-I show 14-fold upregulation of *IFITM5* 15 hours post infection with VN1203 (Barber et al., 2013), further suggesting a potential innate immune function.

4.2 Duck IFITM3 localizes to endosomes, the entry site of IAV

Confocal microscopy reveals that duck IFITM1 is expressed primarily on the cell surface, IFITM2 has partial colocalization with endocytic compartments, and IFITM3 and IFITM5 are localized to LAMP1 containing compartments. Duck IFITM2 is still able to at least partially colocalize to late endosomes, despite lacking the N-terminal YXX θ endocytosis signal motif that is functional in mammalian IFITM3. Presence of duck IFITM2 is also observed at the plasma membrane. Interestingly, the cellular localization of duck IFITM1 most closely resembles that of chicken IFITM2, and the localization of duck IFITM2 closely resembles the cellular localization of chicken IFITM1 (Smith et al.,

2013). The different cellular localization might be explained by the relatively low sequence identity between the orthologous duck and chicken IFITMs.

4.3 Duck IFITM3 has conserved antiviral function against IAV

Crucially, overexpression of dIFITM3, but not dIFITM1, dIFITM2, or dIFITM5 reduces the percentage of IAV infected DF-1 cells *in vitro*. I show this restriction with IAV strains of both mammalian and avian origin, suggesting dIFITM3 is able to broadly restrict a wide range of IAV strains. In addition, dIFITM3 localizes to endosomes, the entry site of IAV. Notably, dIFITM3 possesses residues that are associated with antiviral activity against influenza in mIFITM3, including R87 and Y99 (John et al., 2013). IFITMs have previously been described as being able to restrict IAV in a strain independent manner (Brass et al., 2009; Huang et al., 2011).

Duck IFITM3, as well as orthologous IFITM3 do not display complete protection against IAV *in vitro*. IFITMs may be unable to restrict the entry of a small number of virions entering a single host cell, but large numbers of invading virions may be able to overcome restriction by IFITMs. Additionally, IFITMs have been proposed to alter host membrane characteristics, in order to provide an unfavorable environment for the fusion of viral and host membranes. An unfavorable environment does not translate to a complete inhibition of the fusion of viral and host membranes. Therefore, while IFITMs prevent the entry of invading virions into a host cell, the protection is not complete.

In mammalian species IFITM3 has the most antiviral activity against IAV, while IFITM1 and IFITM2 can restrict IAV replication to a lesser magnitude (Brass et al., 2009; Huang et al., 2011). I were unable to demonstrate antiviral activity of dIFITM2, however, this could be due to low expression levels. Interestingly, IFITM1 appears to be non-functional in ducks. dIFITM1 has a longer N-terminal domain with the insertion of a unique repetitive region that appears to have disrupted the gene. It is interesting that while *dIFITM1* has the highest upregulation after highly pathogenic IAV infection, I could detect no antiviral activity *in vitro*. However, the protein possesses antiviral activity if localized to the endosome by the IFITM3 N-terminal domain. Interestingly, the avian homologue is highly expressed in bursa, ileum and intestinal tissues (Smith et al., 2013). It is perhaps significant that dIFITM1 is non-functional in the tissues where low pathogenic avian influenza replicates (Webster et al., 1978). Meanwhile, dIFITM3 expressed in lung tissue likely contributes to the protection of the duck against highly pathogenic H5N1 avian influenza that replicates to in the respiratory tract, as indicated by high viral titre in pharyngeal swabs (Vandervan et al., 2012).

Several residues that have been characterized as being important for human IFITM3 function are conserved in duck IFITM3 (Fig. 19). The N-terminal domain contains an apparent conserved YXX θ motif that is important for mammalian IFITM3 endosomal localization (Jia et al., 2014). C72 is also conserved in duck IFITM3. C72 is palmitoylated, and mutation of this residue significantly decreases antiviral function (Yount et al., 2012). Residues R85, Y99, and K105 are also important for restriction of IAV (John et al., 2013), and all are conserved in duck. F75 and F78 facilitate interactions

between IFITM2/3 proteins, hypothesized to form a network on the cytosolic leaflet of endosomal membranes (John et al., 2013). F75 is conserved in avian and mammalian IFITM3 orthologs, whereas F78 is not conserved in duck, chicken, or mouse IFITM3. As several important residues are conserved between human and duck IFITM3, is it not surprising that antiviral function is conserved.

While I detected no antiviral activity of dIFITM1, replacement of the N-terminal domain with that of dIFITM3 increased antiviral function. This is interesting given the repetitive region in the N-terminal domain of dIFITM1. Replacement of the N-terminal domain of dIFITM3 with that of dIFITM1 slightly altered cellular localization and did not alter antiviral function. This suggests that the residues within the N-terminal domain of dIFITM3 function in regulation of cellular localization, but have no effect on antiviral activity. Replacement of the N-terminal domain of dIFITM1 with that of dIFITM3 should therefore alter cellular localization, but no additional antiviral activity should be given. The antiviral activity in the 3NTD-1CD225 chimera is likely due to residues within the CD225 and C-terminal tail of dIFITM1. Perhaps the repetitive region within the N-terminal domain of dIFITM1 has disrupted its function. Given a different cellular localization via the N-terminal domain of dIFITM3, dIFITM1 antiviral activity is demonstrated. It would be interesting to further examine duck IFITM1, especially given the repetitive region in the N-terminal domain and the massive and prolonged upregulation. Removal of the repetitive region within the N-terminal region of dIFITM1 may alter cellular localization and increase antiviral function. Studies of the regulation of

antiviral activity of IFITM1 are lacking as the majority of attention has focused on IFITM3, given its association with restriction of IAV.

Interestingly, duck IFITM3 does not reduce the percentage of rVSV-GFP infected DF-1 cells *in vitro*. This is in contrast to mammalian IFITM3, which can restrict VSV replication (Amini-Bavil-Olyaei et al., 2014; Brass et al., 2009; Jia et al., 2012, 2014; Weidner et al., 2010). IAV requires a pH of approximately 5.0-5.7 for membrane fusion whereas VSV requires a less acidic pH of 6 (Clague et al., 1990; Galloway et al., 2013; Gaudin, 1999; Roche and Gaudin, 2004). The sites of fusion of viral and host membranes for IAV and VSV correspond to late endosomes/lysosomes and early endosomes respectively. Additionally, VSV has a two step mechanism of entry where it fuses with intra-vesicular bodies before back fusing with the endosomal membrane to facilitate viral release (Le Blanc et al., 2005). dIFITM3 may have a slightly different cellular localization than its mammalian ortholog, and therefore be unable to restrict viruses that enter in early endocytic compartments. Alternatively, dIFITM3 may not be able to inhibit the fusion of viral membranes with intravesicular bodies, or the fusion of intravesicular bodies with the membrane of endosomes. The differences in the entry mechanism between IAV and VSV, and sequence differences between mammalian and duck IFITM3 likely account for the differential antiviral activity of dIFITM3 against each virus.

I also did not detect any ability of duck IFITM2 to restrict VSV, whereas mammalian IFITM2 efficiently restricts VSV replication (Brass et al., 2009; Li et al., 2013). The apparent inability of duck IFITM2 to restrict the percentage of VSV infected

DF-1 cells may be due to low expression levels. In addition, VSV typically enters host cells from early endosomes. While duck IFITM2 exhibits partial localization with LAMP1 containing endosomes, I did not show localization with any other cellular structures. Further examination of duck IFITM2 cellular localization, and determination if there is association with early endocytic compartments will help our understanding of duck IFITM restriction of VSV. Orthologous IFITM2 restricts multiple viral pathogens that enter host cells through the endocytic pathway (Brass et al., 2009; Huang et al., 2011) so it is likely that duck IFITM2 is also associated with endosomal compartments. It is also possible that VSV has mechanisms that allow evasion of restriction by duck IFITMs, but is unable to evade restriction by mammalian IFITMs.

The functional experiments performed were completed in DF-1 cells. DF-1 cells express endogenous IFITMs, and in particular, knockdown of chicken IFITM3 expression in DF-1 cells results in increased susceptibility to IAV infection (Smith et al., 2013). It is therefore important to interpret my results in the context of background expression of chicken IFITM. Background expression of chicken IFITM3 likely diminishes the observed effect of duck IFITM3 antiviral function. Additionally, IFITMs are known to form homo- and heterodimers (John et al., 2013) which are important for antiviral function. The possibility exists that chicken and duck IFITMs can interact, potentially skewing antiviral function and cellular localization of duck IFITMs. However, IFITMs are expressed at low levels in the absence of type-I IFN, and chicken IFITMs would be expressed to a much lower amount than the overexpressed duck IFITMs. Antibody reagents for avian IFITMs are currently not commercially available, making the

detection of endogenous chicken IFITM in DF-1 cells difficult. Due to the massive overexpression of duck IFITM in comparison to endogenous chicken IFITM expression, it is not expected that chicken IFITMs will significantly influence duck IFITM function.

4.4 N-terminal domain of duck IFITM3 partially regulates cellular localization

The N-terminal domain of mammalian IFITM3 has previously been identified as a region that is important for regulation of cellular localization. A minor allele of IFITM3 (rs12252-C) was identified in patients hospitalized with IAV infections that introduces a splice adaptor site that results in a truncated protein missing the first 21 amino acids (Everitt et al., 2012). This truncated protein was unable to restrict IAV replication *in vitro*. Truncation of the N-terminal domain resulted in mislocalization of IFITM3 away from endosomes to the cell periphery (Jia et al., 2012). Subsequent work showed IFITM3 contained an N-terminal YXX θ endocytic signal sequence, and mutation of the critical tyrosine within this sequence was sufficient to achieve loss of association with endosomes and loss of antiviral function (Jia et al., 2014). Additionally, generation of a chimeric protein replacing the N-terminal domain of IFITM1 with the N-terminal domain of IFITM3 resulted in mislocalization of IFITM1 away from the cell surface towards endosomes with a staining pattern that was similar to wild type IFITM3, suggesting the N-terminal domain is sufficient to regulate cellular localization of IFITMs (John et al., 2013). Further, this chimera gained antiviral function, which was observed with the similar duck chimera. Importantly, replacement of the N-terminal domain of IFITM3 with that of IFITM1 resulted in localization to the cellular periphery and severely impaired antiviral function. This is in contrast with the similar duck chimera, which does

not have altered antiviral function and has only a slight alteration of cellular localization. Additionally, mutation of the conserved tyrosine residue in the N-terminal domain of dIFITM3, part of a YXX θ endocytosis signal sequence in mammalian IFITM3, results in only partial loss with endocytic compartments and a slight reduction in antiviral function. This is consistent with my results of chimeric dIFITM proteins that suggest while the N-terminal domain may contribute to endosomal localization, there are clearly other residues that are outside of the N-terminal domain required for endosomal localization.

Consistent with my results, a recent demonstration of antiviral function in the rs12252-C allele suggests that the N-terminal domain of IFITM3 may not be as important for cellular localization and antiviral function as previously thought. Neither deletion of the N-terminal 21 amino acids of IFITM3 or mutation of Y20 resulted in a loss of antiviral function (Williams et al., 2014). These authors suggest that the use of certain epitope tags, and insufficient control of protein levels in *in vitro* experiments have lead to the previous characterization of the N-terminal domain of IFITM3 as a vital regulator of cellular localization. I observed no effect of the addition of an N-terminal V5 tag on the antiviral activity of duck IFITM3. Additionally, early work with IFITM3 function in murine germ cell homing demonstrated that chimeric IFITM1 expressing the N-terminal domain of IFITM3 maintained expression at the cell surface, suggesting the N-terminal domain is not sufficient to cause localization to endosomes (Tanaka et al., 2005).

In an attempt to screen dIFITM3 for other tyrosine based endocytosis motifs that contribute to endosomal localization outside of the N-terminal domain, I identified three

potential motifs and mutated the critical tyrosine residue to examine the effect on both cellular localization and antiviral function. Mutation of Y14, the N-terminal motif, or Y56, Y82 or Y94 has no effect on cellular localization. dIFITM3-Y56F shows a decreased antiviral function against IAV, but this is likely due to lower expression levels. Y56, Y82, and Y94 are conserved in duck and chicken IFITM3, but not human or mouse IFITM3 (Fig. 19). Interestingly, duck Y94 corresponds to C105 in human IFITM3, which is known to be a site of palmitoylation (Yount et al., 2012). Collectively, these results suggest that while the N-terminal domain of dIFITM3 is a contributor to the localization to late endosomes, other signals outside of this region are also responsible for targeting to endosomal compartments. It is possible that dIFITM3 requires multiple tyrosine based endocytosis signal sequences for complete endosomal localization, and complete loss would only be seen when all of the motifs are mutated. In addition there may be other unidentified non-tyrosine motifs that contribute to endosomal localization. The C-terminus of dIFITM3 contains residues that closely resemble di-leucine based motifs (reviewed by Bonifacino and Traub, 2003) that may be important for proper cellular localization. Interestingly, human IFITM1 has the potential to associate with endosomal compartments, and requires a C-terminal KRXX dibasic sequence to regulate endosomal localization (Li et al., 2014). This motif is not conserved in mouse, chicken or duck IFITM1.

My results demonstrate duck IFITMs are important mediators in the innate immune response of the natural host of IAV. I show evidence that duck IFITM3 localizes to endosomal compartments, where it likely inhibits the entry of IAV. The cellular

localization of duck IFITMs is associated with an ability to restrict IAV infection *in vitro*. Duck IFITM1 is localized to the cell surface where it is unable to restrict IAV replication, whereas IFITM3 is localized to the site of IAV entry (Fig. 20). Increased association of duck IFITM1 with endosomal membranes was associated with increased antiviral function. Duck IFITM5 also localizes to endosomal compartments, suggesting that cellular localization alone is not sufficient to restrict viral replication.

IFITMs have previously been shown to display altered cellular localization depending on the cell type (Bailey et al., 2013). The functional data presented above may be a result of overexpression in DF-1 cells. Duck IFITMs may display differential cellular localization, or differential regulation of endosomal localization if overexpressed in a different cell type. DF-1 cells were used, as they are an avian cell line that is susceptible to infection with influenza viruses. The availability of avian cell lines, in particular duck cells lines are limited. In addition, reagents for use with avian cell lines are also limited. Overexpression of duck IFITMs in more widely used human or mouse cells lines may not be as accurate as overexpression in avian cell lines. Regardless, investigation of the function of mammalian IFITMs in avian cell lines, or duck IFITM function in mammalian cell lines may reveal important information on IFITM regulation.

4.5 Post-translational modifications of IFITMs

Post-translational modification of IFITM, including palmitoylation, phosphorylation and ubiquitination also contributes to cellular localization. While post-translational modifications of mammalian IFITM3 have been extensively studied, little is

known about post-translational modifications of avian IFITM3. I observe in my Western blot analysis of dIFITM3 the presence of higher molecular mass species, which are likely ubiquitinated forms of the protein due to an appropriate size shift (Fig. 21). Human IFITM3 is K48 ubiquitinated at K24, K83, and K88 residues, but this ubiquitination is most prevalent at K24 (Yount et al., 2012). IFITM3 is also K63 ubiquitinated at K24. Ubiquitination of IFITM3 has been suggested to increase its degradation by the proteasome, and therefore act as a negative regulator. Interestingly, K24 is not conserved in dIFITM3 whereas K83 and K88 are (Fig. 19). Chicken IFITM3 has an N-terminal K25, which is absent in dIFITM3. Y20 of the conserved endocytic signal sequence of mammalian IFITM3 can be phosphorylated which can decrease its function as an endocytic signal sequence, resulting in accumulation at the cell surface and decreased antiviral activity (Jia et al., 2012). Phosphorylation of Y20 can negatively regulate ubiquitination of IFITM3, indicating there may be cross-talk between the regulation of post-translational modifications of IFITM3 (Chesarino et al., 2014). Additionally, there is a single report of lysine methylation at K88, which is also a site of ubiquitination (Shan et al., 2013). In summary, IFITM3 undergoes at least 4 different post-translational modifications that tightly regulate cellular localization, membrane association, and antiviral activity.

In my Western blots, dIFITM3 appears as a doublet (Fig. 21). There are several possibilities for the presence of this doublet. The addition of post-translational modifications such as phosphorylation or palmitoylation could be responsible. Alternatively, the exposure of the C-terminal tail of duck IFITM3 to the lumen of

endosomal compartments could result in cleavage of the tail. I note that the cysteine residues equivalent to C71 and C72 of human IFITM3 are conserved in duck and chicken IFITM3, whereas C105 is not (Fig. 19). These conserved membrane proximal C71, C72 and C105 residues are palmitoylated and removal of these palmitoylated cysteine residues (especially C72) reduces membrane clustering and reduces antiviral function (Yount et al., 2010, 2012). Further analysis must be completed in order to determine the origin of the higher molecular mass species of duck IFITM3.

4.6 Future directions

Several questions remain regarding duck IFITM function. While duck IFITM3 was able to potently restrict IAV replication, I was unable to detect any antiviral activity of duck IFITM1, IFITM2, or IFITM5 against IAV or VSV. It would be interesting to examine the range of viruses inhibited by duck IFITM3 and identify viruses that are restricted by IFITM1 and IFITM2. Importantly, it would be interesting to examine if the repetitive element in the N-terminal domain of duck IFITM1 disrupts its antiviral function. My domain swapping experiments suggest duck IFITM1 has antiviral potential, although this gene has been disrupted.

Several viruses are either able to evade restriction by human IFITMs, or use IFITMs to promote their own infection. Intriguingly, these are human adapted viruses in human hosts, suggesting mechanisms to evade IFITM function arise in the natural host. Although I detected no ability of avian IAV to evade restriction by duck IFITM3. The antiviral capabilities of duck IFITMs against these viruses would be an attractive area of

future research, and may identify important differences between avian and mammalian IFITMs.

While duck IFITM3 is able to restrict low pathogenic IAV of both avian and mammalian origin, it is unresolved if duck IFITM3 is able to restrict the replication of highly pathogenic IAV. Key differences exist between the entry of highly pathogenic and low pathogenic IAV including introduction of multiple basic residues into the cleavage site of IAV HA. It is also noted that HA from highly pathogenic strains have a higher pH at which membrane fusion occurs in comparison to low pathogenic strains (DuBois et al., 2011; Galloway et al., 2013; Reed et al., 2010). As highly pathogenic strains often result in systemic infection in the natural host, and have differences in their entry mechanism in comparison to low pathogenic strains, it would be interesting to determine if duck IFITM3 is capable of restricting highly pathogenic strains. Duck IFITM3 is upregulated in duck lung tissue in response to highly pathogenic IAV, suggesting it may be protective.

IFITM5 is described as a bone-restricted protein in mammalian species. The expression of *IFITM5* in non-bone tissue in avian and fish species suggests a different function than mammalian species. The upregulation of duck IFITM5 in response to highly pathogenic IAV indicates it may have immune function. However, the relatively high sequence identity observed suggests a conserved function. Examining the function of duck IFITM5, and examining if it has immune function is an interesting area of future research. It is possible that duck IFITM5 does not function in direct inhibition of viral

entry, but instead functions in the induction of ISGs as reported by (Hanagata and Li, 2011).

Perhaps the most interesting area of future research is the regulation of cellular localization of duck IFITM3. I have shown that the N-terminal domain, in particular the YXX θ motif, is only a partial regulator of cellular localization. There are residues outside of the N-terminal domain that contribute to endosomal localization. Previously, it has been shown that the N-terminal domain of duck IFITM3 is the major contributor to endosomal localization. However, a recent study suggests that the N-terminal domain of IFITM3 may not be as important for cellular localization as previously believed (Williams et al., 2014). The contrasting results likely originate from the use of epitope tags, which can influence cellular localization. Regardless, it is clear the signals necessary for endosomal localization need to be further examined for avian and mammalian IFITM3. Further mutational analysis of duck IFITM3 will reveal the signals required for endosomal localization, and determine the effect of post-translational modifications on antiviral activity and cellular localization. Additionally, analysis of the membrane topology of avian IFITMs is interesting, given the high sequence variation in comparison to orthologous proteins.

More broadly, the characterization of the antiviral activity of other duck ISGs against IAV replication will help our understanding of the innate immune response of the natural host of IAV. It is important to remember that IFITMs represent only a small number of the hundreds of ISGs that are upregulated by type-I IFN. Other candidate duck

ISGs have been previously identified including IFIT5, ISG15, and OASL (Vandervan et al., 2012).

4.7 Conclusions

Here, I have provided evidence of the presence of an intact conserved IFITM locus in the natural host of the influenza A virus. I show the upregulation of duck IFITMs in lung tissue in response to highly pathogenic IAV infection. Significantly, I show duck IFITM3 is able to restrict IAV replication, but is unable to restrict VSV replication *in vitro*. The ability of duck IFITM3 to restrict IAV replication *in vitro*, and the upregulation at the site of replication of highly pathogenic IAV suggests IFITM3 likely plays a protective role against highly pathogenic strains. Additionally, duck IFITM3 localizes to endosomal compartments, the entry site of IAV. Mutation of the N-terminal domain of duck IFITM3 did not disrupt its antiviral function. While there was a noted shift in cellular localization, mutant proteins still had a significant portion of proteins associated with endosomes suggesting the N-terminal domain of duck IFITM3 is not required for antiviral activity or endosomal localization. My results suggest that the N-terminal YXX θ of duck IFITM3 is one of multiple signals required for endosomal localization.

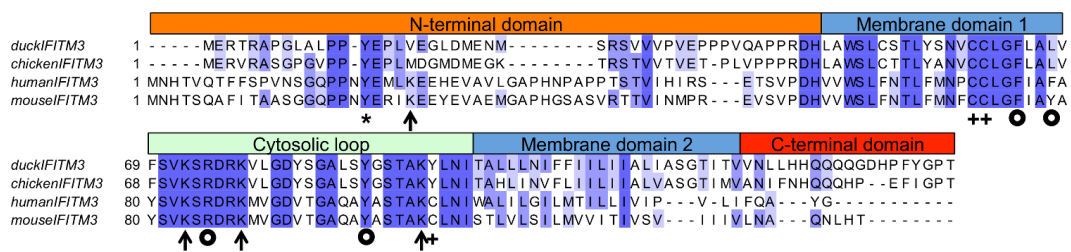


Figure 19. Multiple residues important for antiviral function are conserved in duck IFITM3. IFITM3 sequences from duck, chicken, human and mouse were aligned using T-COFFEE. Residues that are post-translationally modified in mammalian IFITM3 are indicated by a * (phosphorylation), arrow (ubiquitination), and + (palmitoylation). Additional residues important for antiviral function against IAV are marked with ○.

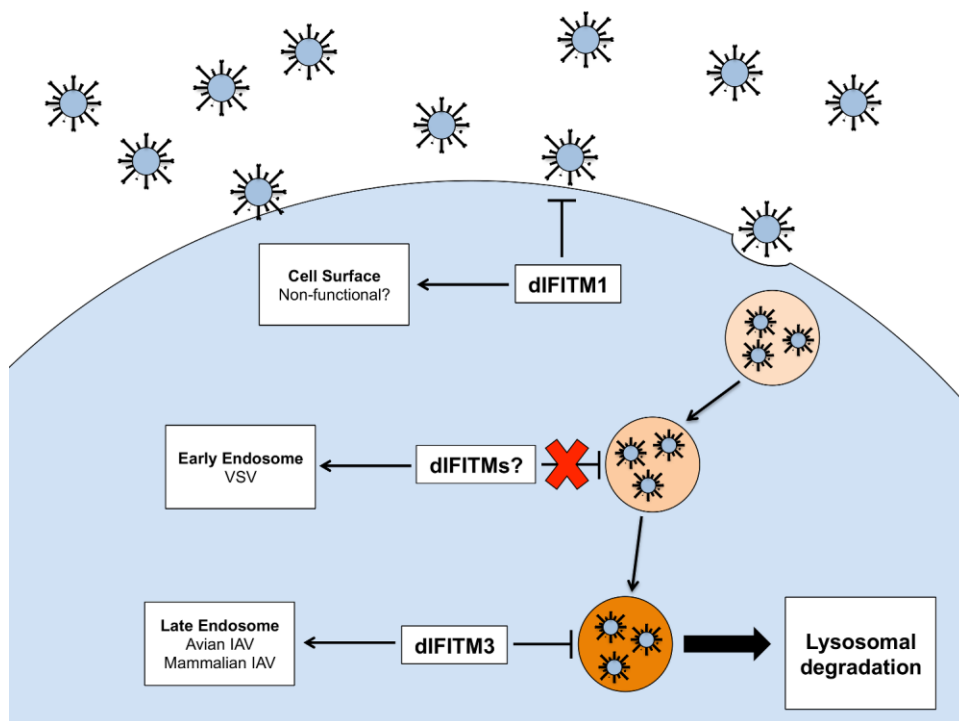


Figure 20. Summary of duck IFITM localization and function. Duck IFITMs localize to distinct cellular compartments. Duck IFITM1 resides primarily at the cell surface, whereas duck IFITM3 resides in late endosomal compartments where it restricts the replication of both IAV of mammalian and avian origin. Duck IFITMs are unable to restrict VSV replication, which enters host cells at early endosomes. Duck IFITM1 may be non-functional due to the insertion of a repetitive element in the N-terminal domain.

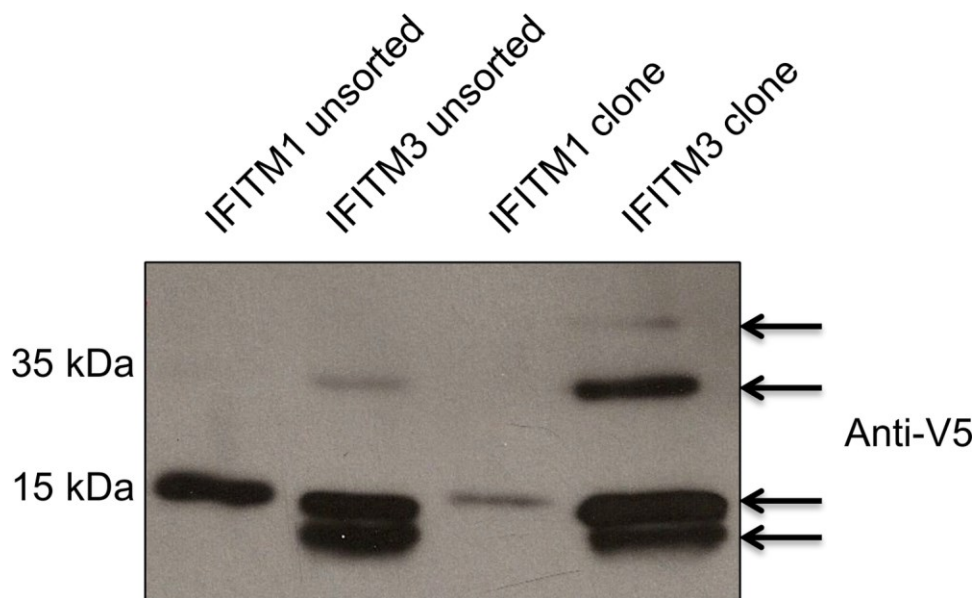


Figure 21. Duck IFITM3 likely undergoes post-translational modification. Western blot of DF-1 cells stably expressing N-terminal V5 epitope tagged duck IFITM1 or IFITM3 from an unsorted population, and a selected clone. Overexposure of the membrane reveals higher molecular mass species. Presence of a double band is also observed. Arrows identify bands corresponding to likely post-translationally modified duck IFITM3.

References

- Akarsu, H., Burmeister, W. P., Petosa, C., Petit, I., Mu, C. W., & Ruigrok, R. W. H. (2003). Crystal structure of the M1 protein-binding domain of the influenza A virus nuclear export protein (NEP / NS2). *EMBO Journal*, 22(18), 4646–4655.
- Alber, D., & Staeheli, P. (1996). Patrial Inhibition of Vesicular Stomatitis Virus by the Interferon-Induced Human 9-27 Protein. *Journal of Interferon and Cytokine Research*, 16, 375–380.
- Alexander, D. J., Parsons, G., & Manvell, R. J. (1986). Experimental assessment of the pathogenicity of eight avian influenza A viruses of H5 subtype for chickens, turkeys, ducks and quail. *Avian Pathology*, 15, 647–662. doi:10.1080/03079458608436328
- Allen, H., McCauley, J., Waterfield, M., & Gething, M.-J. (1980). Influenza virus RNA segment 7 has the coding capacity for two polypeptides. *Virology*, 107, 548–551.
- Almén, M. S., Bringeland, N., Fredriksson, R., & Schiöth, H. B. (2012). The dispanins: a novel gene family of ancient origin that contains 14 human members. *PloS One*, 7(2), e31961. doi:10.1371/journal.pone.0031961
- Amini-Bavil-Olyaei, S., Choi, Y. J., Lee, J. H., Shi, M., Huang, I.-C., Farzan, M., & Jung, J. U. (2014). The antiviral effector IFITM3 disrupts intracellular cholesterol homeostasis to block viral entry. *Cell Host Microbe*, 13(4), 452–464. doi:10.1016/j.chom.2013.03.006.

- Anafu, A. A., Bowen, C. H., Chin, C. R., Brass, A. L., & Holm, G. H. (2013). Interferon-inducible transmembrane protein 3 (IFITM3) restricts reovirus cell entry. *The Journal of Biological Chemistry*, 288(24), 17261–71. doi:10.1074/jbc.M112.438515
- Bailey, C. C., Huang, I.-C., Kam, C., & Farzan, M. (2012). Ifitm3 limits the severity of acute influenza in mice. *PLoS Pathogens*, 8(9), e1002909. doi:10.1371/journal.ppat.1002909
- Bailey, C. C., Kondur, H. R., Huang, I.-C., & Farzan, M. (2013). Interferon-induced Transmembrane Protein 3 Is a Type II Transmembrane Protein. *The Journal of Biological Chemistry*, 288(45), 32184–93. doi:10.1074/jbc.M113.514356
- Bailey, C. C., Zhong, G., Huang, I.-C., & Farzan, M. (2014). IFITM-Family Proteins: The Cell's First Line of Antiviral Defense. *Annual Review of Virology*, 1, 261–283. doi:10.1016/j.biotechadv.2011.08.021.
- Barber, M. R. W., Aldridge, J. R., Fleming-Canepa, X., Wang, Y.-D., Webster, R. G., & Magor, K. E. (2013). Identification of avian RIG-I responsive genes during influenza infection. *Molecular Immunology*, 54(1), 89–97. doi:10.1016/j.molimm.2012.10.038
- Barber, M. R. W., Aldridge, J. R., Webster, R. G., & Magor, K. E. (2010). Association of RIG-I with innate immunity of ducks to influenza. *Proceedings of the National Academy of Sciences*, 107(13), 5913–8. doi:10.1073/pnas.1001755107

- Bevins, S. N., Pedersen, K., Lutman, M. W., Baroch, J. A., Schmit, B. S., Kohler, D., Gidlewski, K., Nolte, D. L., Swafford, S. R., & DeLiberto, T. J. (2014). Large-scale avian influenza surveillance in wild birds throughout the United States. *PLoS ONE*, 9(8), 1–8. doi:10.1371/journal.pone.0104360
- Bonifacino, J. S., & Traub, L. M. (2003). Signals for sorting of transmembrane proteins to endosomes and lysosomes. *Annual Review of Biochemistry*, 72, 395–447. doi:10.1146/annurev.biochem.72.121801.161800
- Bonafous, P., & Stegmann, T. (2000). Membrane perturbation and fusion pore formation in influenza hemagglutinin-mediated membrane fusion. A new model for fusion. *Journal of Biological Chemistry*, 275(9), 6160–6166. doi:10.1074/jbc.275.9.6160
- Bourmakina, S. V., & García-Sastre, A. (2003). Reverse genetics studies on the filamentous morphology of influenza A virus. *Journal of General Virology*, 84, 517–527. doi:10.1099/vir.0.18803-0
- Bouvier, N. M., & Palese, P. (2008). The biology of influenza viruses. *Vaccine*, 12(26), D49–D53. doi:10.1016/j.vaccine.2008.07.039
- Bradbury, L. E., Kansas, G. S., Levy, S., Evans, R. L., & Tedder, T. F. (1992). The CD19/CD21 signal transducing complex of human B lymphocytes includes the target of antiproliferative antibody-1 and Leu-13 molecules. *Journal of Immunology*, 149(9), 2841–2850.

- Brass, A. L., Huang, I.-C., Benita, Y., John, S. P., Krishnan, M. N., Feeley, E. M., ... Elledge, S. J. (2009). The IFITM proteins mediate cellular resistance to influenza A H1N1 virus, West Nile virus, and dengue virus. *Cell*, *139*(7), 1243–54. doi:10.1016/j.cell.2009.12.017
- Brubaker, S. W., Bonham, K. S., Zanoni, I., & Kagan, J. C. (2015). Innate Immune Pattern Recognition : A Cell Biological Perspective. *Annual Review of Immunology*, (33), 10.1–10.34. doi:10.1146/annurev-immunol-032414-112240
- Burleigh, L. M., Calder, L. J., Skehel, J. J., & Steinhauer, D. A. (2005). Influenza a viruses with mutations in the m1 helix six domain display a wide variety of morphological phenotypes. *Journal of Virology*, *79*(2), 1262–1270. doi:10.1128/JVI.79.2.1262-1270.2005
- Chan, Y. K., Huang, I.-C., & Farzan, M. (2012). IFITM proteins restrict antibody-dependent enhancement of dengue virus infection. *PloS One*, *7*(3), e34508. doi:10.1371/journal.pone.0034508
- Chen, H., Li, Y., Li, Z., Shi, J., Shinya, K., Deng, G., Qi, Q., Tian, G., Fan, S., Zhao, H., Sun, Y., & Kawaoka, Y. (2006). Properties and dissemination of H5N1 viruses isolated during an influenza outbreak in migratory waterfowl in western China. *Journal of Virology*, *80*(12), 5976–5983. doi:10.1128/JVI.00110-06
- Chen, H., Smith, G. J. D., Zhang, S. Y., Qin, K., Want, J., Li, K. S., Webster, R. G., Peiris, J. S. M., & Guan, Y. (2005). H5N1 virus outbreak in migratory waterfowl. *Nature*, *436*(14), 192. doi:10.1038/436192a

- Chen, W., Calvo, P. A., Malide, D., Gibbs, J., Schubert, U., Bacik, I., Basta, S., O'Neill, R., Schickli, J., Palese, P., Hanklein P., Bennink, J. R., & Yewdell, J. W. (2001). A novel influenza A virus mitochondrial protein that induces cell death. *Nature Medicine*, 7(12), 1306–1312. doi:10.1038/nm1201-1306
- Chen, Y. X., Welte, K., Gebhard, D. H., & Evans, R. L. (1984). Induction of T cell aggregation by antibody to a 16kd human leukocyte surface antigen. *Journal of Immunology*, 133(5), 2496–2501.
- Chesarino, N. M., McMichael, T. M., Hach, J. C., & Yount, J. S. (2014). Phosphorylation of the antiviral protein interferon-inducible transmembrane protein 3 (IFITM3) dually regulates its endocytosis and ubiquitination. *The Journal of Biological Chemistry*, 289(17), 11986–92. doi:10.1074/jbc.M114.557694
- Choppin, P. W., Murphy, J. S., & Tamm, I. (1960). Studies of two kinds of virus particles which comprise influenza A2 virus strains. III. Morphological characteristics: independence to morphological and functional traits. *The Journal of Experimental Medicine*, 112(18), 945–952. doi:10.1084/jem.112.5.945
- Clague, M., Schoch, C., Zech, L., & Blumenthal, R. (1990). kinetics of pH-activated membrane fusion of vesicular stomatitis virus with cells: stopped-flow measurements by dequenching of octadecylrhodamine fluorescence. *Biochemistry*, 29, 1303–1308.
- Colman, P. M., Varghese, J. N., & W G, L. (1983). Structure of the catalytic and antigenic sites in influenza virus neuraminidase. *Nature*, 303, 41–44.

- Connor, R. J., Kawaoka, Y., Webster, R. G., & Paulson, J. C. (1994). Receptor specificity in human, avian, and equine H2 and H3 influenza virus isolates. *Virology*. doi:10.1006/viro.1994.1615
- Cooley, A. J., Van Campen, H., Philpott, M. S., Easterday, B. C., & Hinshaw, V. S. (1989). Pathological lesions in the lungs of ducks infected with influenza A viruses. *Veterinary Pathology*, 26(1989), 1–5. doi:10.1177/030098588902600101
- Cross, K. J., Langley, W. A., Russell, R. J., Skehel, J. J., & Steinhauer, D. A. (2009). Composition and functions of the influenza fusion peptide. *Protein and Peptide Letters*, 16, 766–778. doi:10.2174/092986609788681715
- Daly, J. M., Lai, A. C. K., Binns, M. M., Chambers, T. M., Barrandeguy, M., & Mumford, J. A. (1996). Antigenic and genetic evolution of equine H3N8 influenza A viruses. *Journal of General Virology*, 77, 661–671. doi:10.1099/0022-1317-77-4-661
- Damjanovic, D., Small, C. L., Jeyanthan, M., McCormick, S., & Xing, Z. (2012). Immunopathology in influenza virus infection: Uncoupling the friend from foe. *Clinical Immunology*, 144(1), 57–69. doi:10.1016/j.clim.2012.05.005
- Dereeper, A., Guignon, V., Blanc, G., Audic, S., Buffet, S., Chevenet, F., Dufayard, D.-F., Guindon, S., Lefort, V., Lescot, M., Claverie, J.-M., & Gascuel, O. (2008). Phylogeny.fr: robust phylogenetic analysis for the non-specialist. *Nucleic Acids Research*, 36, W465–9. doi:10.1093/nar/gkn180

- Desai, T. M., Marin, M., Chin, C. R., Savidis, G., Brass, A. L., & Melikyan, G. B. (2014). IFITM3 restricts influenza A virus entry by blocking the formation of fusion pores following virus-endosome hemifusion. *PLoS Pathogens*, *10*(4), e1004048. doi:10.1371/journal.ppat.1004048
- Dias, A., Bouvier, D., Crépin, T., McCarthy, A. A., Hart, D. J., Baudin, F., Cusack, S., & Ruigrok, R. W. H. (2009). The cap-snatching endonuclease of influenza virus polymerase resides in the PA subunit. *Nature*, *458*(April), 914–918. doi:10.1038/nature07745
- Diebold, S. S., Kaisho, T., Hemmi, H., Akira, S., & Reis E Sousa, C. (2004). Innate antiviral responses by means of TLR7-mediated recognition of single-stranded RNA. *Science*, *303*(2000), 1529–1531. doi:10.1126/science.1093616
- DuBois, R. M., Zaraket, H., Reddivari, M., Heath, R. J., White, S. W., & Russell, C. J. (2011). Acid stability of the hemagglutinin protein regulates H5N1 influenza virus pathogenicity. *PLoS Pathogens*, *7*(12), 1–11. doi:10.1371/journal.ppat.1002398
- Egorov, A., Brandt, S., Sereinig, S., Romanova, J., Ferko, B., Katinger, D., Grassauer, A., Alexandrova, G., Katinger, H., & Muster, T. (1998). Transfectant influenza A viruses with long deletions in the NS1 protein grow efficiently in Vero cells. *Journal of Virology*, *72*(8), 6437–6441.
- Ellis, T. M., Bousfield, R. B., Bissett, L. A., Dyrting, K. C., Luk, G. S. M., Tsim, S. T., Sturm-Ramirez, K., Webster, R. G., Guan, Y., & Malik Peiris, J. S. (2004). Investigation of outbreaks of highly pathogenic H5N1 avian influenza in waterfowl

and wild birds in Hong Kong in late 2002. *Avian Pathology*, 33(5), 492–505.

doi:10.1080/03079450400003601

Evans, S. S., Lee, D. B., Han, T., Tomasi, T. B., & Evans, R. L. (1990). Monoclonal antibody to the interferon-inducible protein Leu-13 triggers aggregation and inhibits proliferation of leukemic B cells. *Blood*, 76, 2583–2593.

Everitt, A. R., Clare, S., McDonald, J. U., Kane, L., Harcourt, K., Ahras, M., Lall, A., Hale, C., Rodgers, A., Young, D. B., Haque, A., Billker, O., Tregoning, J. S., Dougan, G., & Kellam, P. (2013). Defining the range of pathogens susceptible to ifitm3 restriction using a knockout mouse model. *PloS One*, 8(11), e80723.

doi:10.1371/journal.pone.0080723

Everitt, A. R., Clare, S., Pertel, T., John, S. P., Wash, R. S., Smith, S. E., Chin, C. R., Feeley, E. M., Sims, J. S., Adams, D. J., Wise, H. M., Kane, L., Goulding, D., Digard, P., Anttila, V., Kenneth Baillie, J., Walsh, T. S., Hume, D. A., Palotie, A., Xue, Y., Vincenza, C., Tyler-Smith, C., Dunning, J., Gordon, S. B., The GenISIS Investigators, The MOSAIC Investigators, Smyth, R. L., Openshaw, P. J., Dougan, G., Brass, A. L., & Kellam, P. (2012). IFITM3 restricts the morbidity and mortality associated with influenza. *Nature*, 484(7395), 519–23. doi:10.1038/nature10921

Fechter, P., Mingay, L., Sharps, J., Chambers, A., Fodor, E., & Brownlee, G. G. (2003). Two aromatic residues in the PB2 subunit of influenza A RNA polymerase are crucial for cap binding. *Journal of Biological Chemistry*, 278(22), 20381–20388. doi:10.1074/jbc.M300130200

- Feeley, E. M., Sims, J. S., John, S. P., Chin, C. R., Pertel, T., Chen, L.-M., Gaiha, G. D., Ryan, B. J., Donis, R. O., Elledge, S. J., & Brass, A. L. (2011). IFITM3 inhibits influenza A virus infection by preventing cytosolic entry. *PLoS Pathogens*, 7(10), e1002337. doi:10.1371/journal.ppat.1002337
- Friedman, R. L., Manly, S. P., McMahon, M., Kerr, I. M., & Stark, G. R. (1984). Transcriptional and posttranscriptional regulation of interferon-induced gene expression in human cells. *Cell*, 38(3), 745–55.
- Fujiyoshi, Y., Kume, N. P., Sakata, K., & Sato, S. B. (1994). Fine structure of influenza A virus observed by electron cryo-microscopy. *The EMBO Journal*, 13(2), 318–326. doi:10.1093/embo-reports/kve234
- Gack, M. U., Shin, Y. C., Joo, C.-H., Urano, T., Liang, C., Sun, L., Takeuchi, O., Akira, S., Chen, Z., Inoue, S., & Jung, J. U. (2007). TRIM25 RING-finger E3 ubiquitin ligase is essential for RIG-I-mediated antiviral activity. *Nature*, 446, 916–920. doi:10.1038/nature05732
- Galloway, S. E., Reed, M. L., Russell, C. J., & Steinhauer, D. A. (2013). Influenza HA subtypes demonstrate divergent phenotypes for cleavage activation and pH of fusion: implications for host range and adaptation. *PLoS Pathogens*, 9(2), e1003151. doi:10.1371/journal.ppat.1003151
- García-Sastre, A., Egorov, A., Matassov, D., Brandt, S., Levy, D. E., Durbin, J. E., Palese, P., & Muster, T. (1998). Influenza A virus lacking the NS1 gene replicates in interferon-deficient systems. *Virology*, 252, 324–330. doi:10.1006/viro.1998.9508

- Gaudin, Y. (1999). Mutations in the glycoprotein of viral haemorrhagic septicaemia virus that affect virulence for fish and the pH threshold for membrane fusion. *Journal of General Virology*, 80, 1221–1229.
- Hanagata, N., & Li, X. (2011). Biochemical and Biophysical Research Communications
Osteoblast-enriched membrane protein IFITM5 regulates the association of CD9 with an FKBP11 – CD81 – FPRP complex and stimulates expression of interferon-induced genes. *Biochemical and Biophysical Research Communications*, 409(3), 378–384. doi:10.1016/j.bbrc.2011.04.136
- Hanagata, N., Li, X., Morita, H., Takemura, T., Li, J., & Minowa, T. (2011). Characterization of the osteoblast-specific transmembrane protein IFITM5 and analysis of IFITM5-deficient mice. *Journal of Bone and Mineral Metabolism*, 29(3), 279–90. doi:10.1007/s00774-010-0221-0
- Health, W. H. O. for A. (2014). Terrestrial Animal Health Code 10.4, Infection with Avian Influenza Viruses. *World Health Organization for Animal Health*, 3–8.
- Hickford, D., Frankenberg, S., Shaw, G., & Renfree, M. B. (2012). Evolution of vertebrate interferon inducible transmembrane proteins. *BMC Genomics*, 13, 155. doi:10.1186/1471-2164-13-155
- Hinshaw, V. S., Webster, R. G., & Turner, B. (1980). The perpetuation of orthomyxoviruses and paramyxoviruses in Canadian waterfowl. *Canadian Journal of Microbiology*, 26, 622–629. doi:10.1139/m80-108

- Honda, K., Yanai, H., Negishi, H., Asagiri, M., Sato, M., Mizutani, T., Shimada, N., Ohba, O., Takaoka, A., Yoshida, N., & Taniguchi, T. (2005). IRF-7 is the master regulator of type-I interferon-dependent immune responses. *Nature*, *434*, 772–777. doi:10.1038/nature03419.1.
- Horimoto, T., & Kawaoka, Y. (1994). Reverse genetics provides direct evidence for a correlation of hemagglutinin cleavability and virulence of an avian influenza A virus. *Journal of Virology*, *68*(5), 3120–3128. doi:0022-538X/94/04.00+0
- Horimoto, T., & Kawaoka, Y. (1995). The hemagglutinin cleavability of a virulent avian influenza virus by subtilisin-like endoproteases is influenced by the amino acid immediately downstream of the cleavage site. *Virology*, *210*, 466–470. doi:10.1006/viro.1995.1363
- Hornung, V., Kato, H., Poeck, H., Akira, S., Conzelmann, K., & Schlee, M. (2010). 5'-Triphosphate RNA Is the Ligand for RIG-I. *Science*, *314*, 994–997. doi:10.1126/science.1132505
- Huang, I.-C., Bailey, C. C., Weyer, J. L., Radoshitzky, S. R., Becker, M. M., Chiang, J. J., Brass, A. L., Ahmed, A. >, Chi, X., Dong, L., Longobardi, L. E., Boltz, D., Kuhn, J. H., Elledge, S. J., Bavari, S., Denison, M. R., Choe, H., & Farzan, M. (2011). Distinct patterns of IFITM-mediated restriction of filoviruses, SARS coronavirus, and influenza A virus. *PLoS Pathogens*, *7*(1), e1001258. doi:10.1371/journal.ppat.1001258

Huang, Y., Li, Y., Burt, D. W., Chen, H., Zhang, Y., Qian, W., Kim, H., Gan, S., Zhao, Y., Li, J., Yi, K., Feng, H., Zhu, P., Li, B., Liu, Q., Fairley, S., Magor, K. E., Du, Z., Hu, X., Goodman, L., Tafer, H., Vignal, A., Lee, T., Kim, K.-W., Sheng, Z., An, Y., Searle, S., Herrero, J., Groenen, M. A. M., Crooijmans, R. P. M. A., Faraut, T., Cai, Q., Webster, R. G., Aldridge, J. R., Warren, W. C., Bartschat, S., Kehr, S., Marz, M., Stadler, P. F., Smith, J., Kraus, R. H. S., Zhao, Y., Ren, L., Fei, J., Marisson, M., Kaiser, P., Griffin, D. K., Rao, M., Pitel, F., Wang, J., & Li, N. (2013). The duck genome and transcriptome provide insight into an avian influenza virus reservoir species. *Nature Genetics*, *45*(7), 776–83. doi:10.1038/ng.2657

Hulse-Post, D. J., Sturm-Ramirez, K. M., Humberd, J., Seiler, P., Govorkova, E. A., Krauss, S., Scholtissek, C., Puthavathana, P., Buranathai, C., Nguyen, T. D., Long, H. T., Naipospos, T. S. P., Chen, H., Ellis, T. M., Guan, Y., Peiris, J. S. M., & Webster, R. G. (2005). Role of domestic ducks in the propagation and biological evolution of highly pathogenic H5N1 influenza viruses in Asia. *Proceedings of the National Academy of Sciences*, *102*, 10682–10687. doi:10.1073/pnas.0504662102

Ikasaki, A., & Pillai, P. S. (2014). Innate immunity to influenza virus infection. *Nature Reviews Immunology*, *14*(5), 315–328. doi:10.1016/j.biotechadv.2011.08.021.

Jagger, B. W., Wise, H. M., Kash, J. C., Walters, K. A., Wills, N. M., Xiao, Y.-L., Dunfee, R. L., Schwartzman, L. M., Ozinsky, A., Bell, G. L., Dalton, R. M., Lo, A., Efstathiou, S., Atkins, J. F., Firth, A. E., Taubenberger, J. K., & Digard, P. (2012). An Overlapping Protein-Coding Region in Influenza A Virus Segment 3 Modulates the Host Response. *Science*, *337*, 199–204.

- Jensen, S., & Thomsen, A. R. (2012). Sensing of RNA Viruses: a Review of Innate Immune Receptors Involved in Recognizing RNA Virus Invasion. *Journal of Virology*, *86*, 2900–2910. doi:10.1128/JVI.05738-11
- Jia, R., Pan, Q., Ding, S., Rong, L., Liu, S.-L., Geng, Y., Qiao, W., & Liang, C. (2012). The N-terminal region of IFITM3 modulates its antiviral activity by regulating IFITM3 cellular localization. *Journal of Virology*, *86*(24), 13697–707. doi:10.1128/JVI.01828-12
- Jia, R., Xu, F., Qian, J., Yao, Y., Miao, C., Zheng, Y. M., Liu, S. L., Guo, F., Geng, Y., Qiao, W., & Liang, C. (2014). Identification of an endocytic signal essential for the antiviral action of IFITM3. *Cellular Microbiology*, *16*(7), 1080–1093. doi:10.1111/cmi.12262
- Jiang, D., Weidner, J. M., Qing, M., Pan, X.-B., Guo, H., Xu, C., Zhang, X., Birk, A., Chang, J., Shi, P.-Y., Block, T. M., & Guo, J.-T. (2010). Identification of five interferon-induced cellular proteins that inhibit west nile virus and dengue virus infections. *Journal of Virology*, *84*(16), 8332–41. doi:10.1128/JVI.02199-09
- John, S. P., Chin, C. R., Perreira, J. M., Feeley, E. M., Aker, A. M., Savidis, G., Smith, S. E., Elia, A. E. H., Everitt, A. R., Vora, M., Pertel, T., Elledge, S. J., Kellam, P., & Brass, A. L. (2013). The CD225 domain of IFITM3 is required for both IFITM protein association and inhibition of influenza A virus and dengue virus replication. *Journal of Virology*, *87*(14), 7837–52. doi:10.1128/JVI.00481-13

- Jourdain, E., Gunnarsson, G., Wahlgren, J., Latorre-Margalef, N., Bröjer, C., Sahlin, S., Svensson, L., Waldenstrom, J., Lundkvist, A., & Olsen, B. (2010). Influenza virus in a natural host, the mallard: Experimental infection data. *PLoS ONE*, *5*(1). doi:10.1371/journal.pone.0008935
- Kato, H., Takeuchi, O., Mikamo-Satoh, E., Hirai, R., Kawai, T., Matsushita, K., Hiiragi, A., Dermody, T. S., Fujita, T., & Akira, S. (2008). Length-dependent recognition of double-stranded ribonucleic acids by retinoic acid-inducible gene-I and melanoma differentiation-associated gene 5. *The Journal of Experimental Medicine*, *205*(7), 1601–1610. doi:10.1084/jem.20080091
- Kato, H., Takeuchi, O., Sato, S., Yoneyama, M., Yamamoto, M., Matsui, K., Uematsu, S., Jung, A., Kawai, T., Ishii, K. J., Yamaguchi, O., Otsu, K., Tsujimura, Y., Koh, C.-S., Reis e Sousa, C., Matsuura, Y., Fujita, T., & Akira, S. (2006). Differential roles of MDA5 and RIG-I helicases in the recognition of RNA viruses. *Nature*, *441*, 101–105. doi:10.1038/nature04734
- Kawai, T., Takahashi, K., Sato, S., Coban, C., Kumar, H., Kato, H., Ishii, J., J., Takeuchi, O., & Akira, S. (2005). IPS-1, an adaptor triggering RIG-I- and Mda5-mediated type I interferon induction. *Nature Immunology*, *6*(10), 981–988. doi:10.1038/ni1243
- Kida, H., Yanagawa, R., & Matsuoka, Y. (1980). Duck influenza lacking evidence of disease signs and immune response. *Infection and Immunity*, *30*(2), 547–553.

- Kim, J., & Negovetich, N. (2009). Ducks: The “Trojan Horses” of H5N1 influenza. *Influenza and Other Respiratory Viruses*, 3(4), 121–128. doi:10.1111/j.1750-2659.2009.00084.x.Ducks
- Klenk, H. D., Rott, R., Orlich, M., & Blödorn, J. (1975). Activation of influenza A viruses by trypsin treatment. *Virology*, 68, 426–439. doi:10.1016/0042-6822(75)90284-6
- Koerner, I., Kochs, G., Kalinke, U., Weiss, S., & Staeheli, P. (2007). Protective role of beta interferon in host defense against influenza A virus. *Journal of Virology*, 81(4), 2025–2030. doi:10.1128/JVI.01718-06
- Lamb, R. A., Choppin, P. W., Chanock, R. M., & Lai, C. J. (1980). Mapping of the two overlapping genes for polypeptides NS1 and NS2 on RNA segment 8 of influenza virus genome. *Proceedings of the National Academy of Sciences*, 77(4), 1857–1861. doi:10.1073/pnas.77.4.1857
- Lange, U. C., Adams, D. J., Lee, C., Barton, S., Schneider, R., Bradley, A., & Surani, M. A. (2008). Normal germ line establishment in mice carrying a deletion of the Ifitm/Fragilis gene family cluster. *Molecular and Cellular Biology*, 28(15), 4688–96. doi:10.1128/MCB.00272-08
- Laver, W. G., & Valentine, R. C. (1969). Morphology of the isolated hemagglutinin and neuraminidase subunits of influenza virus. *Virology*, 38, 105–119. doi:10.1016/0042-6822(69)90132-9

Lazarus, S., Moffatt, P., Duncan, E. L., & Thomas, G. P. (2013). A brilliant breakthrough in OI type V. *Osteoporosis International : A Journal Established as Result of Cooperation between the European Foundation for Osteoporosis and the National Osteoporosis Foundation of the USA*. doi:10.1007/s00198-013-2465-8

Le Blanc, I., Luyet, P.-P., Pons, V., Ferguson, C., Emans, N., Petiot, A., Mayran, N., Demaurex, N., Faure, J., Sadoul, R., Parton, R. G., & Gruenberg, J. (2005). Endosome-to-cytosol transport of viral nucleocapsids. *Nature Cell Biology*, 7(7), 653–64. doi:10.1038/ncb1269

Lewin, A. R., Reid, L. E., McMahon, M., Stark, G. R., & Kerr, I. M. (1991). Molecular analysis of a human interferon-inducible gene family. *European Journal of Biochemistry / FEBS*, 199(2), 417–23.

Li, K., Jia, R., Li, M., Zheng, Y., Miao, C., Yao, Y., Geng, Y., Qiao, W., Albritton, L. M., Liang, C., & Liu, S. (2014). A sorting signal suppresses IFITM1 restriction of viral entry. *The Journal of Biological Chemistry*, 10.1074/jbc. doi:10.1074/jbc.M114.630780

Li, K., Markosyan, R. M., Zheng, Y.-M., Golfetto, O., Bungart, B., Li, M., Ding, S., He, Y., Liang, C., Lee, J. C., Gratton, E., Cohen, F. S., & Liu, S.-L. (2013). IFITM proteins restrict viral membrane hemifusion. *PLoS Pathogens*, 9(1), e1003124. doi:10.1371/journal.ppat.1003124

Lin, S.-C., Lo, Y.-C., & Wu, H. (2010). Helical assembly in the MyD88-IRAK4-IRAK2 complex in TLR/IL-1R signalling. *Nature*, *465*(7300), 885–890.

doi:10.1038/nature09121

Lin, T.-Y., Chin, C. R., Everitt, A. R., Clare, S., Perreira, J. M., Savidis, G., Aker, A. M., John, S. P., Sarlah, D., Carreira, E. M., Elledge, S. J., Kellam, P., & Brass, A. L.

(2013). Amphotericin B Increases Influenza A Virus Infection by Preventing IFITM3-Mediated Restriction. *Cell Reports*, *5*(4), 895–908.

doi:10.1016/j.celrep.2013.10.033

Liniger, M., Summerfield, A., Zimmer, G., McCullough, K. C., & Ruggli, N. (2012).

Chicken Cells Sense Influenza A Virus Infection through MDA5 and CARDIF Signaling Involving LGP2. *Journal of Virology*, *86*(Ivi), 705–717.

doi:10.1128/JVI.00742-11

Liu, S., Chen, J., Cai, X., Wu, J., Chen, X., Wu, Y. T., Sun, L., & Chen, Z. J. (2013).

MAVS recruits multiple ubiquitin E3 ligases to activate antiviral signaling cascades.

eLife, *2013*, 1–24. doi:10.7554/eLife.00785.001

Lu, J., Pan, Q., Rong, L., He, W., Liu, S.-L., & Liang, C. (2011). The IFITM proteins inhibit HIV-1 infection. *Journal of Virology*, *85*(5), 2126–37.

doi:10.1128/JVI.01531-10

Lund, J. M., Alexopoulou, L., Sato, A., Karow, M., Adams, N. C., Gale, N. W., Iwasaki, A., & Flavell, R. A. (2004). Recognition of single-stranded RNA viruses by Toll-

like receptor 7. *Proceedings of the National Academy of Sciences*, *101*, 5598–5603.
doi:10.1073/pnas.0400937101

MacDonald, M. R. W., Xia, J., Smith, A. L., & Magor, K. E. (2008). The duck toll like receptor 7: genomic organization, expression and function. *Molecular Immunology*, *45*, 2055–2061. doi:10.1016/j.molimm.2007.10.018

Magor, K. E. (2011). Immunoglobulin genetics and antibody responses to influenza in ducks. *Developmental and Comparative Immunology*, *35*(9), 1008–1016.
doi:10.1016/j.dci.2011.02.011

Magor, K. E., Higgins, D. A., Middleton, D. L., & Warr, G. W. (1994). One gene encodes the heavy chains for three different forms of IgY in the duck. *Journal of Immunology*, *153*, 5549–5555.

Magor, K. E., Miranzo Navarro, D., Barber, M. R. W., Petkau, K., Fleming-Canepa, X., Blyth, G. A. D., & Blaine, A. H. (2013). Defense genes missing from the flight division. *Developmental and Comparative Immunology*, *41*(3), 377–88.
doi:10.1016/j.dci.2013.04.010

Magor, K. E., Warr, G. W., Middleton, D., Wilson, M. R., & Higgins, D. A. (1992). Structural relationship between the two IgY of the duck, *Anas platyrhynchos*: molecular genetic evidence. *Journal of Immunology*, *149*, 2627–2633.

- Marshall, N., Priyamvada, L., Ende, Z., Steel, J., & Lowen, A. C. (2013). Influenza Virus Reassortment Occurs with High Frequency in the Absence of Segment Mismatch. *PLoS Pathogens*, *9*(6), 1–11. doi:10.1371/journal.ppat.1003421
- Martin, K., & Helenius, A. (1991). Nuclear transport of influenza virus ribonucleoproteins: The viral matrix protein (M1) promotes export and inhibits import. *Cell*, *67*, 117–130. doi:10.1016/0092-8674(91)90576-K
- Matlin, K. S., Reggio, H., Helenius, A., & Simons, K. (1981). Infectious Entry Pathway of Influenza-Virus in A Canine Kidney-Cell Line. *Journal of Cell Biology*, *91*(17), 601–613.
- Matsumoto, A. K., Martin, D. R., Carter, R. H., Klickstein, L. B., Ahearn, S. J. M., & Fearon, D. T. (1993). Functional Dissection of the CD21/CD19/TAPA-1/Leu13 Complex of B Lymphocytes. *The Journal of Experimental Medicine*, *178*, 1407–1417.
- Miranzo-Navarro, D., & Magor, K. E. (2014). Activation of duck RIG-I by TRIM25 is independent of anchored ubiquitin. *PLoS ONE*, *9*(1), 1–12. doi:10.1371/journal.pone.0086968
- Moffatt, P., Gaumond, M., Salois, P., Sellin, K., Bessette, M., Godin, É., Oliveira, P. T. D., Atkins, G. J., Nanci, A., & Thomas, G. (2008). Bril : A Novel Bone-Specific Modulator of Mineralization. *Journal of Bone and Mineral Research*, *23*(9), 1497–1508. doi:10.1359/JBMR.080412

- Motshwene, P. G., Moncrieffe, M. C., Grossmann, J. G., Kao, C., Ayaluru, M., Sandercock, A. M., Robinson, C. V., Latz, E., & Gay, N. J. (2009). An Oligomeric Signaling Platform formed by the toll-like receptor signal transducers MyD88 and IRAK-4. *Journal of Biological Chemistry*, *284*(37), 25404–25411. doi:10.1074/jbc.M109.022392
- Mudhasani, R., Tran, J. P., Retterer, C., Radoshitzky, S. R., Kota, K. P., Altamura, L. A., Smith, J. M., Packard, B. Z., Kuhn, J. H., Costantino, J., Garrison, A. R., Schmaljohn, C. S., Huang, I.-C., Farzon, M., & Bavari, S. (2013). IFITM-2 and IFITM-3 but not IFITM-1 restrict Rift Valley fever virus. *Journal of Virology*, *87*(15), 8451–64. doi:10.1128/JVI.03382-12
- Müller, M., Briscoe, J., Laxton, C., Guschin, D., Ziemiecki, A., Silvennoinen, O., Harpur, A. G., Barbieri, G., Witthuhn, B. A., Schinder, C., Pellegrini, S., Wilks, A. F., Ihle, J. N., Stark, G. R., & Kerr, I. M. (1993). The protein tyrosine kinase JAK1 complements defects in interferon-alpha/beta and -gamma signal transduction. *Nature*, *363*.
- Munster, V. J., Baas, C., Lexmond, P., Waldenström, J., Wallensten, A., Fransson, T., Rimmelzwan, G. F., Beyer, W. E. P., Schutten, M., Olsen, B., Osterhaus, A. D. M. E., & Fouchier, R. A. M. (2007). Spatial, temporal, and species variation in prevalence of influenza A viruses in wild migratory birds. *PLoS Pathogens*, *3*(5), 0630–0638. doi:10.1371/journal.ppat.0030061

- Muramoto, Y., Noda, T., Kawakami, E., Akkina, R., & Kawaoka, Y. (2013). Identification of novel influenza A virus proteins translated from PA mRNA. *Journal of Virology*, *87*(5), 2455–62. doi:10.1128/JVI.02656-12
- Noton, S. L., Medcalf, E., Fisher, D., Mullin, A. E., Elton, D., & Digard, P. (2007). Identification of the domains of the influenza A virus M1 matrix protein required for NP binding, oligomerization and incorporation into virions. *Journal of General Virology*, *88*, 2280–2290. doi:10.1099/vir.0.82809-0
- O’Neill, R. E., Jaskunas, R., Blobel, G., Palese, P., & Moroianu, J. (1995). Nuclear Import of Influenza Virus RNA Can Be Mediated by Viral Nucleoprotein and for Protein Import. *The Journal of Biological Chemistry*, *270*, 22701–22704.
- Palese, P., Ritchey, M. B., & Schulman, J. L. (1977). Mapping of the influenza virus genome. II. Identification of the P1, P2, and P3 genes. *Virology*, *76*, 114–121. doi:10.1016/0042-6822(77)90288-4
- Palese, P., & Schulman, J. L. (1976). Mapping of the influenza virus genome: identification of the hemagglutinin and the neuraminidase genes. *Proceedings of the National Academy of Sciences*, *73*(6), 2142–2146. doi:10.1073/pnas.73.6.2142
- Palese, P., Tobita, K., Ueda, M., & Compans, R. W. (1974). Characterization of temperature sensitive influenza virus mutants defective in neuraminidase. *Virology*, *61*, 397–410. doi:10.1016/0042-6822(74)90276-1

- Parvin, J. D., Moscona, a, Pan, W. T., Leider, J. M., & Palese, P. (1986). Measurement of the mutation rates of animal viruses: influenza A virus and poliovirus type 1. *Journal of Virology*, *59*(2), 377–383.
- Perdue, M. L., García, M., Senne, D., & Fraire, M. (1997). Virulence-associated sequence duplication at the hemagglutinin cleavage site of avian influenza viruses. *Virus Research*, *49*, 173–186. doi:10.1016/S0168-1702(97)01468-8
- Philbin, V. J., Iqbal, M., Boyd, Y., Goodchild, M. J., Beal, R. K., Bumstead, N., Young, J., & Smith, A. L. (2005). Identification and characterization of a functional, alternatively spliced Toll-like receptor 7 (TLR7) and genomic disruption of TLR8 in chickens. *Immunology*, *114*, 507–521. doi:10.1111/j.1365-2567.2005.02125.x
- Pichlmair, A., Schulz, O., Tan, C. P., Naslund, T. I., Liljestrom, P., Weber, F., & Sousa, C. R. E. (2006). RIG-I–Mediated Antiviral Responses to Single-Stranded RNA Bearing 5′-Phosphates. *Science*, *314*, 997–1002.
- Pinto, L. H., Holsinger, L. J., & Lamb, R. A. (1992). Influenza virus M2 protein has ion channel activity. *Cell*, *69*, 517–528. doi:10.1016/0092-8674(92)90452-I
- Reed, M. L., Bridges, O. A., Seiler, P., Kim, J.-K., Yen, H.-L., Salomon, R., Govorkova, E. A., Webster, R. G., & Russell, C. J. (2010). The pH of activation of the hemagglutinin protein regulates H5N1 influenza virus pathogenicity and transmissibility in ducks. *Journal of Virology*, *84*(3), 1527–1535. doi:10.1128/JVI.02069-09

- Reikine, S., Nguyen, J. B., & Modis, Y. (2014). Pattern recognition and signaling mechanisms of RIG-I and MDA5. *Frontiers in Immunology*, 5(July), 1–7.
doi:10.3389/fimmu.2014.00342
- Ritchey, M. B., Palese, P., & Schulman, J. L. (1976). Mapping of the influenza virus genome. III. Identification of genes coding for nucleoprotein, membrane protein, and nonstructural protein. *Journal of Virology*, 20(1), 307–313.
- Roche, S., & Gaudin, Y. (2004). Evidence that rabies virus forms different kinds of fusion machines with different pH thresholds for fusion. *Journal of Virology*, 78(16), 8746–52. doi:10.1128/JVI.78.16.8746-8752.2004
- Rojek, J. M., & Kunz, S. (2008). Cell entry by human pathogenic arenaviruses. *Cellular Microbiology*, 10, 828–835. doi:10.1111/j.1462-5822.2007.01113.x
- Rott, R., Klenk, H. D., Nagai, Y., & Tashiro, M. (1995). Influenza viruses, cell enzymes, and pathogenicity. *American Journal of Respiratory and Critical Care Medicine*, 152. doi:10.1164/ajrccm/152.4_Pt_2.S16
- Schindelin, J., Arganda-Carreras, I., Frise, E., Kaynig, V., Longair, M., Pietzsch, T., Preibish, S., Ruden, C., Saalfeld, S., Schmid, B., Tinevez, J.-Y., White, D. J., Hartenstein, V., Eliceiri, K., Tomancak, P., & Cardona, A. (2012). Fiji: an open-source platform for biological-image analysis. *Nature Methods*, 9(7), 676–82.
doi:10.1038/nmeth.2019

- Schneider, W. M., Chevillotte, M. D., & Rice, C. M. (2014). Interferon-stimulated genes: a complex web of host defenses. *Annual Review of Immunology*, *32*, 513–45. doi:10.1146/annurev-immunol-032713-120231
- Schoggins, J. W. (2014). Interferon-stimulated genes: Roles in viral pathogenesis. *Current Opinion in Virology*, *6*, 40–46. doi:10.1016/j.coviro.2014.03.006
- Schoggins, J. W., Wilson, S. J., Panis, M., Murphy, M. Y., Jones, C. T., Bieniasz, P., & Rice, C. M. (2011). A diverse range of gene products are effectors of the type I interferon antiviral response. *Nature*, *472*(7344), 481–485. doi:10.1038/nature09907
- Scholtissek, C., Rohde, W., Von Hoyningen, V., & Rott, R. (1978). On the origin of the human influenza virus subtypes H2N2 and H3N2. *Virology*, *87*, 13–20. doi:10.1016/0042-6822(78)90153-8
- Selman, M., Dankar, S. K., Forbes, N. E., Jia, J.-J., & Brown, E. G. (2012). Adaptive mutation in influenza A virus non-structural gene is linked to host switching and induces a novel protein by alternative splicing. *Emerging Microbes & Infections*, *1*(000), e42. doi:10.1038/emi.2012.38
- Senne, D. A., Panigrahy, B., Kawaoka, Y., Pearson, J. E., Süß, J., Lipkind, M., Kida, H., & Webster, R. G. (1996). Survey of the hemagglutinin (HA) cleavage site sequence of H5 and H7 avian influenza viruses: amino acid sequence at the HA cleavage site as a marker of pathogenicity potential. *Avian Diseases*, *40*(2), 425–437.

- Shan, Z., Han, Q., Nie, J., Cao, X., Chen, Z., Yin, S., Gao, Y., Lin, F., Zhou, X., Xu, K., Fan, H., Qian, Z., Sun, B., Zhong, J., Li, B., & Tsun, A. (2013). Negative regulation of interferon-induced transmembrane protein 3 by SET7-mediated lysine monomethylation. *Journal of Biological Chemistry*, 288(49), 35093–35103. doi:10.1074/jbc.M113.511949
- Shortridge, K. F., Zhou, N. N., Guan, Y., Gao, P., Ito, T., Kawaoka, Y., Kodihalli, S., Krauss, S., Markwell, D., Murti, K. G., Norwood, M., Senne, D., Sims, L., Takada, A., & Webster, R. G. (1998). Characterization of avian H5N1 influenza viruses from poultry in Hong Kong. *Virology*, 252(December 1997), 331–342. doi:10.1006/viro.1998.9488
- Sieczkarski, S. B., & Whittaker, G. R. (2002). Influenza Virus Can Enter and Infect Cells in the Absence of Clathrin-Mediated Endocytosis Influenza Virus Can Enter and Infect Cells in the Absence of Clathrin-Mediated Endocytosis. *Journal of Virology*, 76(20), 10455–10464. doi:10.1128/JVI.76.20.10455
- Skehel, J. J., & Wiley, D. C. (2000). Receptor binding and membrane fusion in virus entry: The influenza hemagglutinin. *Annual Review of Biochemistry*, 69, 531–569.
- Smith, R. A., Young, J., Weis, J. J., & Weis, J. H. (2006). Expression of the mouse fragilis gene products in immune cells and association with receptor signaling complexes. *Genes and Immunity*, 7, 113–121. doi:10.1038/sj.gene.6364278
- Smith, S. E., Gibson, M. S., Wash, R. S., Ferrara, F., Wright, E., Temperton, N., Kellam, P., & Fife, M. (2013). Chicken interferon-inducible transmembrane protein 3

restricts influenza viruses and lyssaviruses in vitro. *Journal of Virology*, 87(23), 12957–66. doi:10.1128/JVI.01443-13

Songserm, T., Jam-on, R., Sae-heng, N., Meemak, N., Hulse-post, D. J., Sturm-Ramirez, K. M., & Webster, R. G. (2006). Domestic Ducks and H5NI Influenza Epidemic, Thailand. *Emerging Infectious Diseases*, 12(4), 575–581.

Stallknecht, D. E., Shane, S. M., Kearney, M. T., & Zwank, P. J. (1990). Persistence of avian influenza viruses in water. *Avian Diseases*, 34(2), 406–411.

Stallknecht, D. E., Shane, S. M., Zwank, P. J., Senne, D. A., & Kearney, M. T. (1990). Avian influenza viruses from migratory and resident ducks of coastal Louisiana. *Avian Diseases*, 34(2), 398–405.

Stark, G. R., & Darnell, J. E. (2012). The JAK-STAT Pathway at Twenty. *Immunity*, 36(4), 503–514. doi:10.1016/j.immuni.2012.03.013

Sturm-Ramirez, K. M., Ellis, T., Bousfield, B., Bissett, L., Dyrting, K., Rehg, J. E., Poon, L., Guan, Y., Peiris, M., & Webster, R. G. (2004). Reemerging H5N1 Influenza Viruses in Hong Kong in 2002 Are Highly Pathogenic to Ducks. *Journal of Virology*, 78(9), 4892–4901. doi:10.1128/JVI.78.9.4892

Sturm-Ramirez, K. M., Hulse-Post, D. J., Govorkova, E. A., Humberd, J., Seiler, P., Puthavathana, P., Buranathai, C., Nguyen, T. D., Chaisingh, A., Long, H. T., Naipospos, T. S. P., Chen, H., Ellis, T. M., Guan, Y., Peiris, J. S. M., & Webster, R. G. (2005). Are Ducks Contributing to the Endemicity of Highly Pathogenic H5N1

Influenza Virus in Asia? *Journal of Virology*, 79(17), 11269–11279.

doi:10.1128/JVI.79.17.11269

Tanaka, S. S., & Matsui, Y. (2002). Developmentally regulated expression of mil-1 and mil-2, mouse interferon-induced transmembrane protein like genes, during formation and differentiation of primordial germ cells. *Mechanisms of Development*, 119S(2002), S261–7.

Tanaka, S. S., Yamaguchi, Y. L., Tsoi, B., Lickert, H., & Tam, P. P. L. (2005).

IFITM/Mil/fragilis family proteins IFITM1 and IFITM3 play distinct roles in mouse primordial germ cell homing and repulsion. *Developmental Cell*, 9(6), 745–56.

doi:10.1016/j.devcel.2005.10.010

Tang, E. D., & Wang, C.-Y. (2009). MAVS self-association mediates antiviral innate immune signaling. *Journal of Virology*, 83(8), 3420–3428. doi:10.1128/JVI.02623-08

Tong, S., Zhu, X., Li, Y., Shi, M., Zhang, J., Bourgeois, M., Yang, H., Chen, X., Recuenco, S., Gomez, J., Chen, L.-M., Johnson, A., Tao, Y., Dreyfus, C., Yu, W., McBride, R., Carney, P. J., Gilbert, A. T., Chang, J., Guo, Z., Davis, C. T., Paulson, J. C., Stevens, J., Rupprecht, C. E., Holmes, E. C., Wilson, I. A., & Donis, R. O. (2013). New World Bats Harbor Diverse Influenza A Viruses. *PLoS Pathogens*, 9(10). doi:10.1371/journal.ppat.1003657

Tsurudome, M., Glück, R., Graf, R., Falchetto, R., Schaller, U., & Brunner, J. (1992).

Lipid interactions of the hemagglutinin HA2 NH2-terminal segment during

influenza virus-induced membrane fusion. *Journal of Biological Chemistry*, 267(28), 20225–20232. doi:VL - 267

Vandervan, H. A., Petkau, K., Ryan-Jean, K. E. E., Aldridge, J. R., Webster, R. G., & Magor, K. E. (2012). Avian influenza rapidly induces antiviral genes in duck lung and intestine. *Molecular Immunology*, 51(3-4), 316–24.

doi:10.1016/j.molimm.2012.03.034

Vasin, A. V., Temkina, O. A., Egorov, V. V., Klotchenko, S. A., Plotnikova, M. A., & Kiselev, O. I. (2014). Molecular mechanisms enhancing the proteome of influenza A viruses: an overview of recently discovered proteins. *Virus Research*, 185, 53–63.

doi:10.1016/j.virusres.2014.03.015

Wakim, L. M., Gupta, N., Mintern, J. D., & Villadangos, J. A. (2013). Enhanced survival of lung tissue-resident memory CD8⁺ T cells during infection with influenza virus due to selective expression of IFITM3. *Nature Immunology*, 15(3), 204.

doi:10.1038/ni.2525

Warr, G. W., Magor, K. E., & Higgins, D. A. (1995). IgY: clues to the origins of modern antibodies. *Immunology Today*, 16, 392–398. doi:10.1016/0167-5699(95)80008-5

Warren, C. J., Griffin, L. M., Little, A. S., Huang, I.-C., Farzan, M., & Pyeon, D. (2014). The antiviral restriction factors IFITM1, 2 and 3 do not inhibit infection of human papillomavirus, cytomegalovirus and adenovirus. *PloS One*, 9(5), e96579.

doi:10.1371/journal.pone.0096579

- Waterhouse, A. M., Procter, J. B., Martin, D. M. A., Clamp, M., & Barton, G. J. (2009). Jalview Version 2--a multiple sequence alignment editor and analysis workbench. *Bioinformatics (Oxford, England)*, *25*(9), 1189–91. doi:10.1093/bioinformatics/btp033
- Webster, R. G. (1993). Are equine 1 influenza viruses still present in horses? *Equine Veterinary Journal*, *25*(6), 537–538.
- Webster, R. G., Bean, W., Gorman, O., Chambers, T., & Kawaoka, Y. (1992). Evolution and Ecology of Influenza A Viruses. *Microbiological Reviews*, *56*(1), 152–179.
- Webster, R. G., Peiris, M., Chen, H., & Guan, Y. (2006). H5N1 outbreaks and enzootic influenza. *Emerging Infectious Diseases*, *12*(1), 3–8. doi:10.3201/eid1201.051024
- Webster, R. G., Yakhno, M., Hinshaw, V. S., Bean, W. J., & Murti, K. G. (1978). Intestinal influenza: replication and characterization of influenza viruses in ducks. *Virology*, *84*, 268–278. doi:10.1016/0042-6822(78)90247-7
- Wee, Y. S., Roundy, K. M., Weis, J. J., & Weis, J. H. (2012). Interferon-inducible transmembrane proteins of the innate immune response act as membrane organizers by influencing clathrin and v-ATPase localization and function. *Innate Immunity*, *18*(6), 834–45. doi:10.1177/1753425912443392
- Wei, L., Cui, J., Song, Y., Zhang, S., Han, F., Yuan, R., Gong, L., Jiao, P., & Liao, M. (2014). Duck MDA5 functions in innate immunity against H5N1 highly pathogenic

avian influenza virus infections. *Veterinary Research*, 45(1), 1–13.

doi:10.1186/1297-9716-45-66

Weidner, J. M., Jiang, D., Pan, X.-B., Chang, J., Block, T. M., & Guo, J.-T. (2010).

Interferon-induced cell membrane proteins, IFITM3 and tetherin, inhibit vesicular stomatitis virus infection via distinct mechanisms. *Journal of Virology*, 84(24),

12646–57. doi:10.1128/JVI.01328-10

Weston, S., Czieso, S., White, I. J., Smith, S. E., Kellam, P., & Marsh, M. (2014). A

Membrane Topology Model for Human Interferon Inducible Transmembrane Protein 1. *PloS One*, 9(8), e104341. doi:10.1371/journal.pone.0104341

Wharton, S. A., Belshe, R. B., Skehel, J. J., & Hay, A. J. (1994). Role of virion M2

protein in influenza virus uncoating: Specific reduction in the rate of membrane fusion between virus and liposomes by amantadine. *Journal of General Virology*,

75, 945–948. doi:10.1099/0022-1317-75-4-945

Wilkins, C., Woodward, J., Lau, D. T.-Y., Barnes, A., Joyce, M., McFarlane, N.,

McKeating, J. A., Tyrrell, D. L., & Gale, M. (2013). IFITM1 is a tight junction protein that inhibits hepatitis C virus entry. *Hepatology*, 57(2), 461–9.

doi:10.1002/hep.26066

Williams, D. E. J., Wu, W.-L., Grotefend, C. R., Radic, V., Chung, C., Chung, Y.-H.,

Farzan, M., & Huang, I.-C. (2014). IFITM3 polymorphism rs12252-C restricts

influenza A viruses. *PloS One*, 9(10), e110096. doi:10.1371/journal.pone.0110096

- Wise, H. M., Foeglein, A., Sun, J., Dalton, R. M., Patel, S., Howard, W., Anderson, E. C., Barclay, W. S., & Digard, P. (2009). A complicated message: Identification of a novel PB1-related protein translated from influenza A virus segment 2 mRNA. *Journal of Virology*, *83*(16), 8021–8031. doi:10.1128/JVI.00826-09
- Wise, H. M., Hutchinson, E. C., Jagger, B. W., Stuart, A. D., Kang, Z. H., Robb, N., Schwartzman, L. M., Kash, J. C., Fodor, E., Firth, A. E., Gog, J. R., Taubenberger, J. K., & Digard, P. (2012). Identification of a Novel Splice Variant Form of the Influenza A Virus M2 Ion Channel with an Antigenically Distinct Ectodomain. *PLoS Pathogens*, *8*(11). doi:10.1371/journal.ppat.1002998
- Wrensch, F., Winkler, M., & Pöhlmann, S. (2014). IFITM proteins inhibit entry driven by the MERS-coronavirus spike protein: evidence for cholesterol-independent mechanisms. *Viruses*, *6*(9), 3683–98. doi:10.3390/v6093683
- Wu, B., Peisley, A., Tetrault, D., Li, Z., Egelman, E. H., Magor, K. E., Walz, T., Penczek, P. A., & Hur, S. (2014). Molecular Imprinting as a Signal-Activation Mechanism of the Viral RNA Sensor RIG-I. *Molecular Cell*, *55*(4), 511–523. doi:10.1016/j.molcel.2014.06.010
- Xu, J., Qian, P., Wu, Q., Liu, S., Fan, W., Zhang, K., Wang, R., Zhang, H., Chen, H., & Li, X. (2014). Swine interferon-induced transmembrane protein, sIFITM3, inhibits foot-and-mouth disease virus infection in vitro and in vivo. *Antiviral Research*, *109*, 22–9. doi:10.1016/j.antiviral.2014.06.008

- Xu, Y., Yang, G., & Hu, G. (2009). Binding of IFITM1 enhances the inhibiting effect of caveolin-1 on ERK activation. *Acta Biochimica et Biophysica Sinica*, *41*(6), 488–494. doi:10.1093/abbs/gmp034
- Yoneyama, M., Kikuchi, M., Matsumoto, K., Imaizumi, T., Miyahishi, M., Taira, K., Foy, E., Loo, Y.-M., Gale, M., Akira, S., Yonehara, S., Kato, A., & Fujita, T. (2005). Shared and Unique Functions of the DExD/H-Box Helicases RIG-I, MDA5, and LGP2 in Antiviral Innate Immunity. *Journal of Immunology*, *175*, 2851–2858. doi:10.4049/jimmunol.175.5.2851
- Yoneyama, M., Kikuchi, M., Natsukawa, T., Shinobu, N., Imaizumi, T., Miyagishi, M., Taira, K., Akira, S., & Fujita, T. (2004). The RNA helicase RIG-I has an essential function in double-stranded RNA-induced innate antiviral responses. *Nature Immunology*, *5*(7), 730–737. doi:10.1038/ni1087
- Yoon, S.-W., Webby, R. J., & Webster, R. G. (2014). Evolution and ecology of influenza A viruses. *Current Topics in Microbiology and Immunology*, *385*, 359–375. doi:10.1007/82
- Yount, J. S., Karssemeijer, R. A., & Hang, H. C. (2012). S-palmitoylation and ubiquitination differentially regulate interferon-induced transmembrane protein 3 (IFITM3)-mediated resistance to influenza virus. *The Journal of Biological Chemistry*, *287*(23), 19631–41. doi:10.1074/jbc.M112.362095
- Yount, J. S., Moltedo, B., Yang, Y.-Y., Charron, G., Moran, T. M., López, C. B., & Hang, H. C. (2010). Palmitoylome profiling reveals S-palmitoylation-dependent

antiviral activity of IFITM3. *Nature Chemical Biology*, 6(8), 610–4.

doi:10.1038/nchembio.405

Zhang, Y.-H., Zhao, Y., Li, N., Peng, Y.-C., Giannoulatou, E., Jin, R.-H., Yan, H.-P., Wu, H., Liu, J.H., Lie, N., Wang, D.-Y., Shu, Y.-L., Ho, L.-P., Kellam, P., McMichael, A., & Dong, T. (2013). Interferon-induced transmembrane protein-3 genetic variant rs12252-C is associated with severe influenza in Chinese individuals. *Nature Communications*, 4, 1418. doi:10.1038/ncomms2433

Zhang, Z., Liu, J., Li, M., Yang, H., & Zhang, C. (2012). Evolutionary dynamics of the interferon-induced transmembrane gene family in vertebrates. *PloS One*, 7(11), e49265. doi:10.1371/journal.pone.0049265

Zhao, X., Guo, F., Liu, F., Cuconati, A., Chang, J., Block, T. M., & Guo, J.-T. (2014). Interferon induction of IFITM proteins promotes infection by human coronavirus OC43. *Proceedings of the National Academy of Sciences*, 111(18), 6756–61. doi:10.1073/pnas.1320856111

Zhu, R., Wang, J., Lei, X.-Y., Gui, J.-F., & Zhang, Q.-Y. (2013). Evidence for *Paralichthys olivaceus* IFITM1 antiviral effect by impeding viral entry into target cells. *Fish & Shellfish Immunology*, 35(3), 918–26. doi:10.1016/j.fsi.2013.07.002